SCHOOL OF CIVIL ENGINEERING

JOINT HIGHWAY RESEARCH PROJECT

JHRP-77-6

NONDESTRUCTIVE TESTING AND EVALUATION OF FLEXIBLE HIGHWAY PAVEMENTS

M. E. Harr

G. Y. Baladi

PURDUE UNIVERSITY

INDIANA STATE HIGHWAY COMMISSION

Final Report

NONDESTRUCTIVE TESTING AND EVALUATION OF
FLEXIBLE HIGHWAY PAVEMENTS

TO: J. F. McLaughlin, Director
Joint Highway Research Project

May 16, 1977

Project: C-36-63F

FROM: H. L. Michael, Associate Director
Joint Highway Research Project

File: 9-7-6

The Report attached is the Final Report on the HPR Part II Research Study titled "Predicting Pavement Performance Using Time Dependent Transfer Functions". It is titled "Nondestructive Testing and Evaluation of Flexible Highway Pavements" and has been authored by M. E. Harr and G. Y. Baladi of our staff. The Report is presented for acceptance as fulfillment of the objectives of this research.

The report provides evidence that the time dependent transfer functions obtained do represent the characteristics of flexible pavements. Changes in parameters of these functions reflect changes in pavement performance and conditions.

Additional research in this area on highway pavements to apply the developed energy concept is desirable. In addition a device for rapid measuring of pavement deflections mounted on the vehicle applying the load has been developed in related research and its utilization on highway pavements is possible. A proposal for a new study utilizing the new device and applying the developed energy concept to highway pavements is planned.

This Report after acceptance by the JHRP Board will be forwarded to the ISHC and FHWA for review, comment and acceptance as fulfillment of the objectives of the Study.

Respectfully submitted,

Harold L. Michael

Harold L. Michael
Associate Director

HLM:ms

cc: W. L. Dolch
R. L. Eskew
G. D. Gibson
W. H. Goetz
M. J. Gutzwiller
G. K. Hallock
D. E. Hancher
M. L. Hayes
K. R. Hoover
G. A. Leonards
R. D. Miles
P. L. Owens
G. T. Satterly
C. F. Scholer
M. B. Scott
K. C. Sinha
L. E. Wood
E. J. Yoder
S. R. Yoder

Final Report

NONDESTRUCTIVE TESTING AND EVALUATION OF FLEXIBLE HIGHWAY PAVEMENTS

by

M. E. Harr
Research Engineer

and

G. Y. Baladi
Graduate Instructor in Research

Joint Highway Research Project

Project No.: C-36-63F

File No.: 9-7-6

Prepared as Part of an Investigation

Conducted by

Joint Highway Research Project
Engineering Experiment Station
Purdue University

in cooperation with the

Indiana State Highway Commission

and the

U.S. Department of Transportation
Federal Highway Administration

The contents of this report reflect the views of the author who is responsible for the facts and the accuracy of the data presented herein. The contents do not necessary reflect the official views or policies of the Federal Highway Administration. This report does not constitute a standard, specification, or regulation.

Purdue University
West Lafayette, Indiana
May 16, 1977

TECHNICAL REPORT STANDARD TITLE PAGE

1. Report No.	2. Government Accession No.	3. Recipient's Catalog No.
JHRP-77-6		

4. Title and Subtitle	5. Report Date
NONDESTRUCTIVE TESTING AND EVALUATION OF FLEXIBLE HIGHWAY PAVEMENTS	May 16, 1977
	6. Performing Organization Code
7. Author(s)	8. Performing Organization Report No.
M. E. Harr and G. Y. Baladi	JHRP-77-6
9. Performing Organization Name and Address	10. Work Unit No.
Joint Highway Research Project Civil Engineering Building Purdue University W. Lafayette, Indiana 47907	11. Contract or Grant No. HPR-1(14) Part II
12. Sponsoring Agency Name and Address	13. Type of Report and Period Covered
Indiana State Highway Commission State Office Building 100 North Senate Avenue Indianapolis, Indiana 46204	Final Report
	14. Sponsoring Agency Code

15. Supplementary Notes

Conducted in cooperation with the U.S. Dept. of Transportation, Federal Highway Administration, Research Study titled "Predicting Pavement Performance Using Time Dependent Transfer Functions"

16. Abstract

The motion of vehicles over pavements makes the problem of predicting consequent effects time dependent. Present design procedures, however, account for this motion as a sequence of equivalent static conditions reduced to passes or coverages. A solution to this problem was obtained by verifying the following hypothesis:

A pavement system operated upon by a vehicular input produces an output response. Relating the two is a time dependent transfer (TDT) function that contains within it the properties of the system. This function is obtained, in a mathematical sense, using Laplace transformations, without the need to simulate respective material performance or to determine values for preselected descriptors. The TDT functions can be employed to predict a pavement system's response and performance when subjected to an imposed load.

The investigation was carried out by extending transfer function theory in connection with a finite convolution procedure to define the pavement's TDT functions. Full scale dynamic tests (moving trucks and aircraft) were performed in service environments (6 highway and 2 runway cross-sections).

It has been shown that the TDT functions obtained do represent the characteristics of flexible pavements. Changes in parameters of the TDT function reflect changes in pavement performance and conditions.

17. Key Words	18. Distribution Statement
Nondestructive Testing, Evaluation, Flexible Highway Pavements, Parameters	No restrictions. This document is available to the public through the National Technical Information Service, Springfield, Virginia 22161

19. Security Classif. (of this report)	20. Security Classif. (of this page)	21. No. of Pages	22. Price
Unclassified	Unclassified	159	

Form DOT F 1700.7 (8-69)

ACKNOWLEDGEMENTS

The writers are grateful to the Indiana State Highway Commission and the Federal Highway Administration for the support which made this work possible. In particular, they would like to acknowledge the contribution of Mr. R. H. Lowry, who never hesitated with his assistance and was especially helpful during the field investigation phase of this study. In addition, the help of Mr. W. L. DeGroff, Mr. N. T. Ng-A-Qui, Mr. L. A. Holm and Mr. W. R. Bergstrom is gratefully acknowledged.

TABLE OF CONTENTS

TABLE OF CONTENTS (con't)

LIST OF TABLES

LIST OF FIGURES

ABBREVIATIONS AND SYMBOLS

a = Contact Area

a_e = Equivalent Contact Area

$A(0,t)$ = Calculated Deflection at the Edge of a Tire and Time "t" (Signature)

A_p = Calculated Peak Deflection

A_{TDT} = Area under the Transfer Function Curve

B = Parameter

c = System Equivalent Viscosity

$CAL(G_i)$ = Calibration Factor of Gage G_i

CBR = California Bearing Ratio

CBR_D = Dynamic California Bearing Ratio

ce = Equivalent Coverages

DSM = Dynamic Stiffness Modulus

E = Elastic Modulus

$F(t)$ = Equivalent Forcing Function

f_i = Frequency

ft = Feet

G_i = Gage Number

$\overline{G}(s)$ = Reduced Transfer Function (Laplace Domaine)

$G(t)$ = Reduced Transfer Function (Time Domain)

$\overline{g}(s)$ = Transfer Function (Lapalce Domain)

in = inch

$I(s)$ = Lapalce Transform of Input Function, $I(t)$

k = System Equivalent Spring

k_s	= Modulus of Subgrade Reaction
lb	= Pound
$\mathcal{L}$	= Laplace's Operetor
m	= System Equivalent Mass
N	= Parameter
O(s)	= Laplace Transform of Output Function, O(t)
P	= Total Number of Passes
pci	= Pound per cubic inch
P_m	= Pressure on a Material other than Standard
psi	= Pound per square inch
PSI	= Present Serviceability Index
P_s	= Pressure on Standard Material
r	= Radius of Contact Area
$RF(G_i,0)$	= Reference Point of Gage G_i at Time Zero
s	= Complex Variable
sec	= Second
$SI(G_i,t)$	= Digitized Electrical Signal of Gage G_i at Time T
SSV	= Soil Support Value
t	= Time
T	= Total Thickness of a Pavement Section
(t_{IF})	= The Time at the Point of Inflection that were Produced by the Front Tire
(t_{II})	= The Time at the Point of Inflection that were Produced by the Intermediate Tire
(t_{IR})	= The Time at the Point of Inflection that were Produced by The Rear Tire
t_{PFF}	= The Time of Occurence of Peak Force due to the Front Tire

t_{PFI} = The Time of Occurence of Peak Force due to the Intermediate Tire

t_{PFR} = The Time of Occurence of Peak Force due to the Rear Tire

T_s = Surface Thickness of a Pavement Section

$y(G_i,t)$ = Pavement Dflections (inches) of Gage G_i at Time t

$y_{p_{x=R}}$ = Measured Peak Deflection at a Point "R" Lateral Distance from the Edge of the Loading Tire

y = Total Peak Deflection

$y(z)$ = Cumulative Total Peak Deflection

$\ddot{y}(t)$ = System Acceleration

$\dot{y}(t)$ = System Velocity

$Y(t)$ = System Displacement

$y(x,t)$ = Measured Deflection at Lateral Distance "x" from the Edge of Tire at Time "t"

x = Lateral Distance

Δ = One Increment of Time

τ = Time

CHAPTER 1

INTRODUCTION

The major problem which faces the highway engineer today is not how to design and construct new pavements, but rather how to evaluate, maintain and upgrade existing pavement systems to meet today's traffic demand for higher magnitudes of loading and frequencies.

The closing of a highway to permit conventional destructive evaluation methods (test pits, plate test) may have catastrophic consequences. Thus, the need for rapid nondestructive methods of pavement evaluation has been recognized in recent years (48*, 49), and different methods of nondestructive pavement evaluation were developed (50, 51, 52). However, these methods do not simulate actual traffic loading or take cognizance of the complexity of the pavement - subgrade interaction mechanism.

Recognizing the dimensions of the problem, and the need for a rapid nondestructive method of evaluation, research activities were initiated and developed at Purdue University over the last ten years using transfer function theory.

The primary objectives of the present study is to develop, design, and apply a rapid nondestructive technique to measure a pavement's time dependent deflection response function. In addition, this work seeks to develop a methodology that will account for the complexity and variability of pavement - subgrade interactive mechanism. To this end, it was hypothesized (a) that there exists a

* Figures in brackets refer to references in the Bibliography.

relationship between a pavement's deflection response function (output) and a vehicular forcing function (input) in the form of a time dependent transfer function, (b) that the characteristics of this transfer function indicate pavement performance and conditions and the manner in which it attenuates energy induced by the passage of a vehicle, and (c) that this time dependent transfer function can be employed to predict pavement deflection response to a wide range of vehicular loadings.

CHAPTER 2

REVIEW OF LITERATURE

In the early stages of development, design and/or evaluation of a pavement system consisted of rule-of-thumb procedures based on judgement and past experience. In the 1920's, the U. S. Bureau of Public Roads* developed a soil classification system based upon the observed field performance of soils under highway pavements (10)**. This system, in conjunction with the accumulated data, helped the highway engineer to correlate performance with subgrade types.

Beginning in the late 1940's engineers were faced with the need to predict the performance of pavement systems subjected to greater wheel loads and frequencies than they had ever before experienced (11, 12, 23). Thus, a rational design procedure was introduced in the early 1950's (8); however, severe breakup is still a common phenomenon on some highways and runways (7, 11).

An important problem which the highway engineer faces today is that of providing remedial measures to upgrade existing pavements to meet today's traffic loadings and frequencies. This need has led many investigators to develop various measuring devices and models of pavement systems. Excellent reviews of the literature are available (9, 12, 26, 27, 28, 29, 30, 31).

Boyer and Highter (9, 12) reviewed the Winkler hypothesis,

---

* The Bureau of Public Roads is now called Federal Highway Administration (FHWA) (11).

**Figures in brackets refer to references in the Bibliography.

classical elastic solutions, viscoelastic theory, and other mechanistic solutions.

Hall (27), Green and Hall (28), and Yoder and Witczack (11) discussed the use of test pits and plate bearing test, and in-situ tests. They acknowledged that test pits and in-situ tests are destructive, costly, and time consuming methods for pavement evaluation.

A. C. Benkelman, in connection with the Western Association of State Highway Officials (WASHO), used a long pivoted deflection beam, presently known as the "Benkelman beam", and measured deflections at the pavement surface due to a moving load. Later the State of California and the Road Research Laboratory automated the Benkelman beam and renamed it the "California deflectometer". The "La croix deflectometer" is another version of the Benkelman beam that was developed in France (31). A detailed study of the Benkelman beam may be found in reference (30).

Vibratory devices have also found some popularity, such as the "Dynaflect". These induce a vibratory force on the pavement by means of two small metal wheels (11). Deflections are detected by means of sensors spaced at specified distances ahead of the wheels. Applied loads are quite small in comparison to vehicular loadings. Results have been correlated with those of the Benkelman beam.

The U. S. Army Engineer Waterways Experiment Station (WES), in cooperation with the Royal Dutch Shell Laboratory, uses a vibratory testing procedure of pavements as their nondestructive evaluation methodology. The "dynamic stiffness modulus (DSM)" is determined and correlated with pavement performance. Results have been reported by Henkelom and Foster (32), Mawell (33), and by Green and Hall (28). Wave Propogation techniques have been used by WES and the Air Force (31). Green and Hall (28) noted that results of such tests were erratic.

In Table (2.1) is presented a summary of various existing measuring systems (28).

Swami, Goetz, and Harr (6) were the first to apply the "transfer function theory" to study the stress deformation behavior of anisotropic asphaltic mixtures (9). They found that the transfer function was independent of the loading input and was, for their tests, mainly a function of temperature.

Ali (15) applied transfer function theory to flexible pavements. He reported that:

> "Temperature, surface course thickness and spatial location have their respective influences on the transfer function..."

Boyer and Harr (55) extended transfer function theory to an in-service pavement system. He used installed linear variable differential transducer (LVDT) gages in the pavement and conducted field tests at Kirtland Air Force Base, New Mexico. He concluded that the characteristics of flexible pavements could be represented by "time dependent transfer (TDT) functions". He also succeeded in predicting pavement deflections using the calculated TDT functions.

Highter and Harr (56), using energy concepts, concluded that:

> "Performance trends in airfield and highway pavements can be predicted from knowledge of cumulative total peak deflection."

Figure (2.1) shows the effect of surface course thickness on the

TABLE 2.1 SUMMARY OF EXISTING MEASUREMENT SYSTEMS. (AFTER YODER (28)).

CATEGORY	PRINCIPLE OF OPERATION	DEVICE	PROPERTY MEASURED	DATA OUTPUT
A	Bearing Value	Plate	Modulus E	Immediate
B	Deflection	(a) Benkleman Beam	Rebound, Curvature,	Direct Reading
		(b) California Deflectometer	Rebound	Print Out
		(c) La Croix Deflectometer	Rebound	Digital
C	Curvature	So. African	Curvature	Immediate
D	Impact	Washington State	Deflection	
E	Vibratory	Shell	Deflection, Curvature, Modulus E	Deflection Print Out
		Road Rater	Deflection, Curvature, Modulus E	Immediate
		Dynaflect	Deflection, Curvature, Dynamic E	Immediate
F	Wave Propogation	Corps Engineers (Waterways Exp. Station)	Deflection, Curvature, Dynamic E	Automated

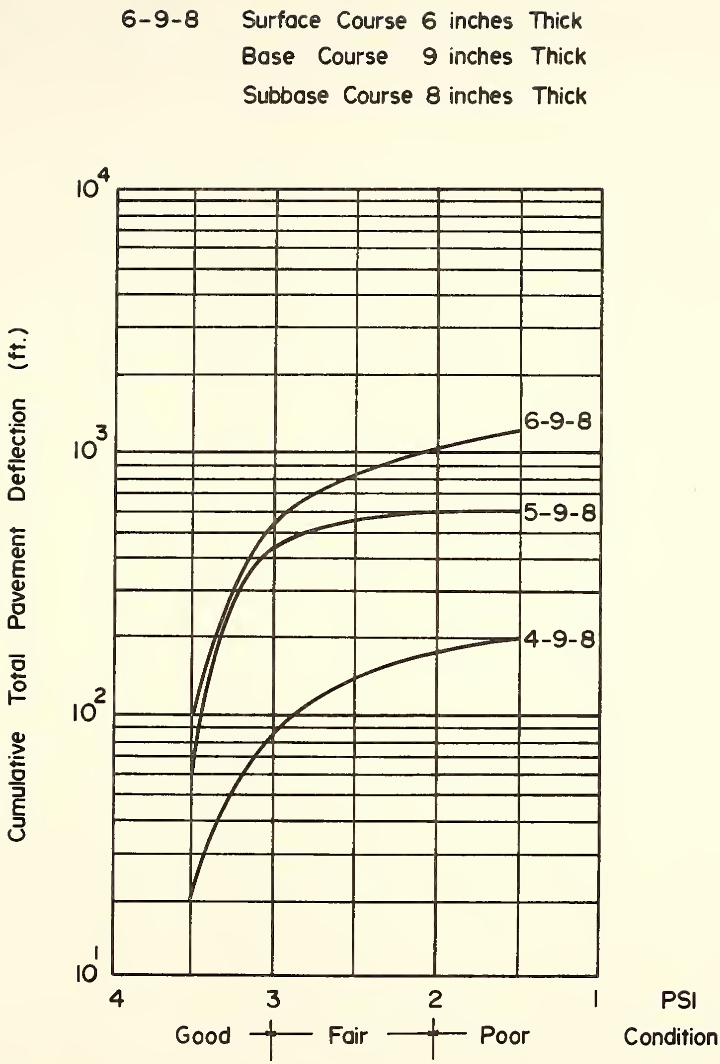

FIGURE 2.1 THE EFFECT OF SURFACE COURSE THICKNESS ON THE CONDITION OF A PAVEMENT AS A FUNCTION OF ITS CUMULATIVE TOTAL DEFLECTION. (12)

condition of a pavement as a function of its cumulative total deflection obtained by Highter and Harr (56).

CHAPTER 3

TRANSFER FUNCTION

I) Introduction

By definition, a transfer function is the ratio of an operational output (expressed as the Laplace transform of the output) to an operational input (Laplace transform of the input) of a time dependent system (1, 2, 3). If a system is subjected to a dynamic input, I(t), and evidences a resulting output O(t), then mathematically, the transfer function is given as

$$\bar{g}(s) = \frac{\bar{O}(s)}{\bar{I}(s)} \tag{3.1}$$

where, s = complex variable

$\bar{G}(s)$ = transfer function

$\bar{I}(s)$ = Laplace transform of input function, I(t)

$\bar{O}(s)$ = Laplace transform of output function, O(t)

Note that the transfer function is the ratio of two Laplace transforms, and hence is a function of the complex variable "s" (5).

The Laplace transform of a function f(t) is defined as the integral

$$\bar{F}(s) = \int_0^{\infty} f(t)e^{-st}dt, \qquad s > 0 \tag{3.2}$$

for those values of the complex variable "s" for which the integral converges.

II) Model

The Kelvin mass-spring-dashpot model shown in Figure (3.1) will be used in this study to simulate the reaction of a pavement under

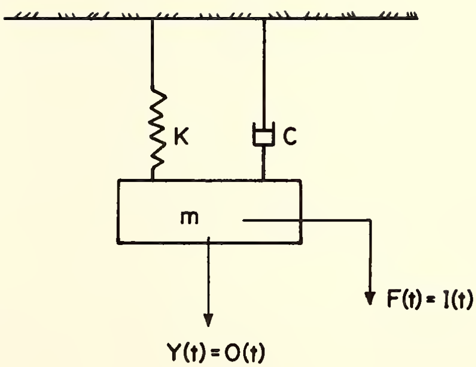

FIGURE 3.1 THE KELVIN MASS-SPRING-DASHPOT MODEL.

loading. This representation has been reported with considerable success by Harr (45) and Boyer and Harr (55). The mass (m), the spring constant (k), and the dashpot constant (c) represent equivalent lumped parameters of an actual pavement system. The governing differential equation of motion may be written as (37)

$$m\ddot{y}(t) + c\dot{y}(t) + ky(t) = F(t) \tag{3.3}$$

where, $\ddot{y}(t)$ = system acceleration

$\dot{y}(t)$ = system velocity

$y(t)$ = system displacement (output)

$F(t)$ = forcing function (input)

m = system equivalent mass

c = system equivalent viscosity

k = system equivalent spring

Taking the Laplace transformation of both sides of equation (3.3) yields

$$\mathcal{L}\left\{m\ddot{y}(t) + c\dot{y}(t) + ky(t)\right\} = \mathcal{L}\left\{F(t)\right\}$$

or (4)

$$(ms^2 + cs + k)\bar{y}(s) - (mc + s)y(0) - m\dot{y}(0) = \bar{F}(s)$$

Assuming that the pavement is at rest before the vehicle arrives; that is, $y(0) = \dot{y}(0) = 0.0$, produces

$$(ms^2 + cs + k)\bar{y}(s) = \bar{F}(s)$$

from which

$$\left[\frac{1}{s^2 + \frac{c}{m}s + \frac{k}{m}}\right] = \frac{m\bar{y}(s)}{\bar{F}(s)} \tag{3.4}$$

The terms in brackets in equation (3.4) will be called the "reduced" transfer function of the system and will be designated as $\bar{G}(s)$, thus

$$\bar{G}(s) = \frac{1}{s^2 + \frac{c}{m}s + \frac{k}{m}} \qquad (3.5)$$

III) Determining Transfer Function

a) Closed form solution

From references (38, 39) the inverse transform of equation (3.5) is found to be

$$G(t) = \frac{e^{-\frac{c}{2m}t}}{\sqrt{\frac{k}{m} - \frac{c^2}{4m^2}}} \sin\sqrt{\frac{k}{m} - \frac{c^2}{4m^2}}\,t, \quad \frac{k}{m} > \frac{c^2}{4m^2} \qquad (3.6)$$

or

$$G(t) = \frac{e^{-\frac{c}{2m}t}}{\sqrt{\frac{c^2}{4m^2} - \frac{k}{m}}} \sinh\sqrt{\frac{c^2}{4m^2} - \frac{k}{m}}\,t, \quad \frac{k}{m} < \frac{c^2}{4m^2} \qquad (3.7)$$

Thus, knowing m, c, and k of a system, or their ratios, $(\frac{c}{m}, \frac{k}{m})$, the reduced transfer function G(t) can be calculated using either equation (3.6) or (3.7).

Rearranging equation (3.6) and substituting

$$w = \sqrt{\frac{k}{m}}, \qquad a = \frac{c}{2\sqrt{mk}} \qquad \text{results in}$$

$$G(t) = \frac{e^{-awt}}{w\sqrt{1-a^2}} \sin\ w\sqrt{1-a^2}\ t \qquad (3.8)$$

Some characteristic plots of $G(t)$ for $a > 1$, and $a < 1$ are shown in Figure (3.2).

b) Convolution technique

Real convolution is defined as

$$O(t) = \int_0^t g(\tau)F(t-\tau)d\tau$$

or from equation (3.4)

$$y(t) = \frac{1}{m}\int_0^t G(\tau)F(t-\tau)d\tau \tag{3.9}$$

where,

$y(t)$ = response function

$G(t)$ = reduced transfer function

$F(t)$ = forcing function

Equation (3.9) may be written in difference form such as

$$y(t_k) = \frac{1}{m}\sum_{n=1}^{k} G(\tau_n)\, F\,(t_k-\tau_{n-1})\,\Delta\tau_n, \quad k = t/\Delta\tau \tag{3.10}$$

The smaller the value of $\Delta\tau$, the better the approximation in equation (3.10). An example of discrete convolution is shown in Figure (3.3), and a detailed study of convolution convergence is presented in Appendix (B).

Taking $\Delta\tau_n$ in equation (3.10) at equal intervals, i.e., $\Delta\tau_1 = \Delta\tau_2 = \ldots = \Delta\tau_n = \Delta$, yields

$$y(t_k) = \frac{\Delta}{m}\sum_{n=1}^{k} G(t_n)F(t_k-t_{n-1})$$

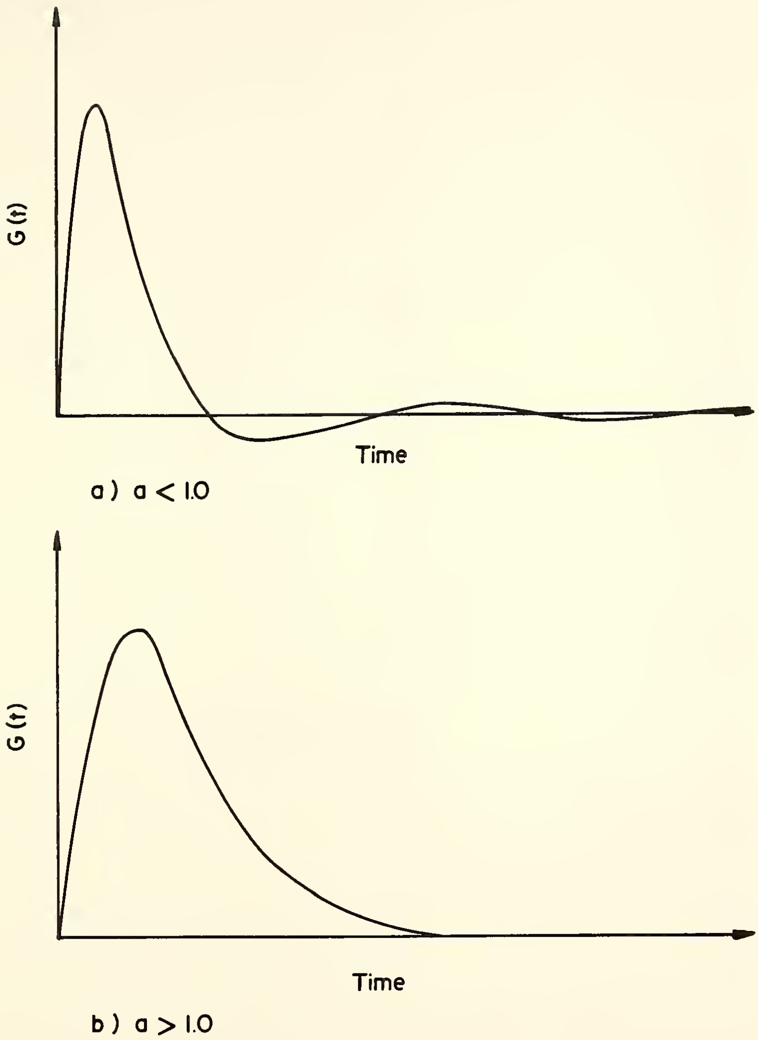

FIGURE 3.2 CHARACTERISTIC PLOTS OF THE REDUCED TRANSFER FUNCTION G (t) .

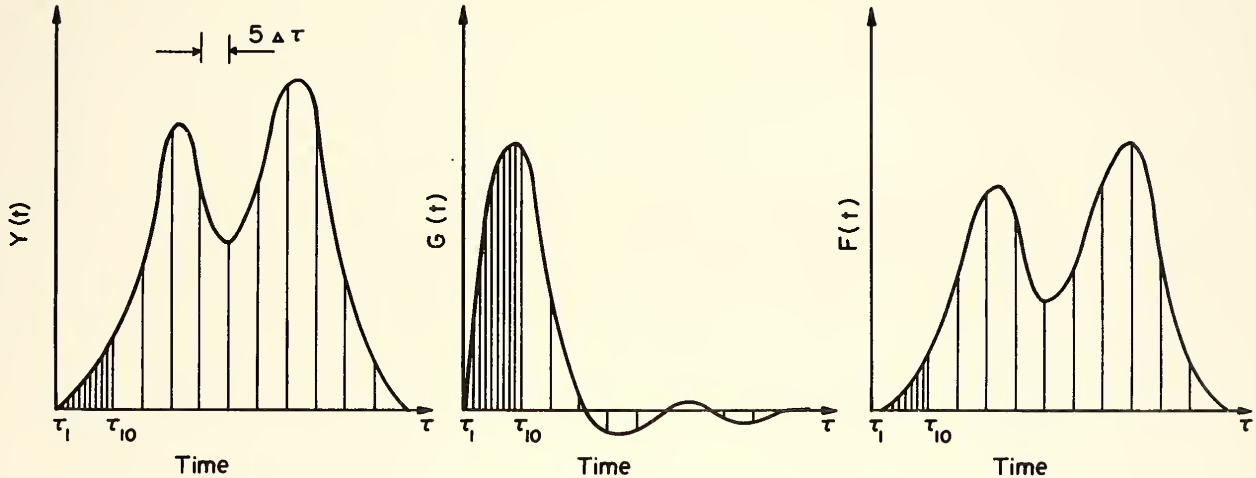

FIGURE 3.3 ILLUSTRATION OF RESPONSE FUNCTION, TRANSFER FUNCTION, AND FORCING FUNCTION Vs. TIME FOR CONVOLUTION PURPOSE.

with $\tau_o = 0$ and realizing that, $F(t_k - t_{n-1}) = F(t_{k+1-n})$, then

$$y(t_k) = \frac{\Delta}{m} \sum_{n=1}^{k} G(t_n) F(t_{k+1-n}) \tag{3.11a}$$

or

$$F(t_k) = m \left[\frac{y(t_k) - \Delta \sum_{n=1}^{k-1} F(t_n) G(t_{k+1-n})}{\Delta\, G(t_1)} \right] \tag{3.11b}$$

or

$$G(t_k) = m \left[\frac{y(t_k) - \Delta \sum_{n=1}^{k-1} G(t_n) F(t_{k+1-n})}{\Delta\, F(t_1)} \right] \tag{3.11c}$$

Equation (3.11a) is called "explicit convolution" whereas equations (3.11b) and (3.11c) are examples of "implicit convolution".

CHAPTER 4

FIELD INVESTIGATION

I) Field Investigation

The field phase of this study had as its objective the development, design, and use of nondestructive techniques for obtaining the data needed to determine:

1. a highway's time dependent transfer (TDT) function,
2. a vehicle's forcing function,
3. the attenuation of energy in highway pavements,

Boyer's work (12) at Kirtland Air Force Base, New Mexico, provided the technical guidance for the early phases of the present investigation. He reported that accurate deflection measurements could be obtained using linear variable differential transducer (LVDT) gages embedded in the pavement system. He also noted that accelerometer gages are inadequate to the task because of their slow response and electrical drift. Based upon Boyer's tests, it was decided to use LVDT's with an accuracy of one one-ten-thousandths (0.0001) of an inch (details of instrumentation are presented in Appendix A).

The initial LVDT installations (see Appendix A) were made on a line perpendicular to the wheel path at a gravel pit road (near the West Lafayette campus of Purdue University). The objectives of these installations were to determine the width of the dynamic deflection basin of a pavement, for a wide variety of trucks that enter the gravel pit plant; and to help in designing and checking the nondestructive measurement system (see Appendix A). Results of this test program indicated that the width of the deflection basin (for deflection less than 0.0001 inches) extends less than four feet laterally from the outside edge of the wheel for highway pavements. The same result was observed to be less than five feet for airfield pavements (47).

The time dependent response functions of the pavements were recorded under varying ambient conditions, using the installed (LVDT) gages at the gravel pit road, and for a wide variety of truck gear configurations.

The analyses of the above mentioned results led this writer to construct a light weight aluminum beam carrying six LVDT (s) which would obviate the need to install gages in subsequent tests. A schematic representation of the LVDT beam is shown in Figure (4.1). It should be emphasized that measurements made with the LVDT beam are "nondestructive".

The LVDT beam was first placed over the installed gages, and pavement deflections were recorded by both systems. Figure (4.2)shows a plot of pavement deflections that were recorded by the LVDT beam versus those recorded by the installed LVDT gages at the same lateral distances from the edge of tire. It is of importance to note that the LVDT beam deflection measurements were also checked with two other sets of installed LVDT gages at Eglin Air Force Base, Florida. In these tests, an F-4 aircraft was used as a loading vehicle (twenty five kips wheel load). Tests were performed on a parking area as well as on an active taxiway. Pavement deflections, at the same lateral distances from the wheel

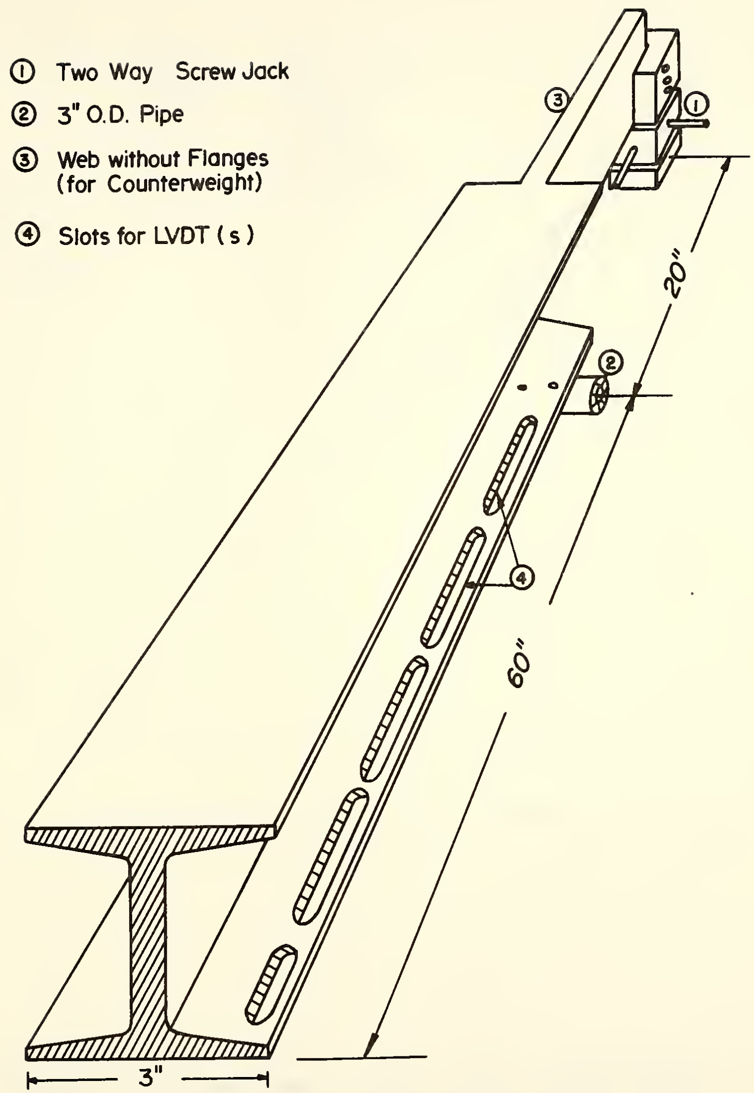

FIGURE 4.1 SCHEMATIC REPRESENTATION OF THE LVDT BEAM.

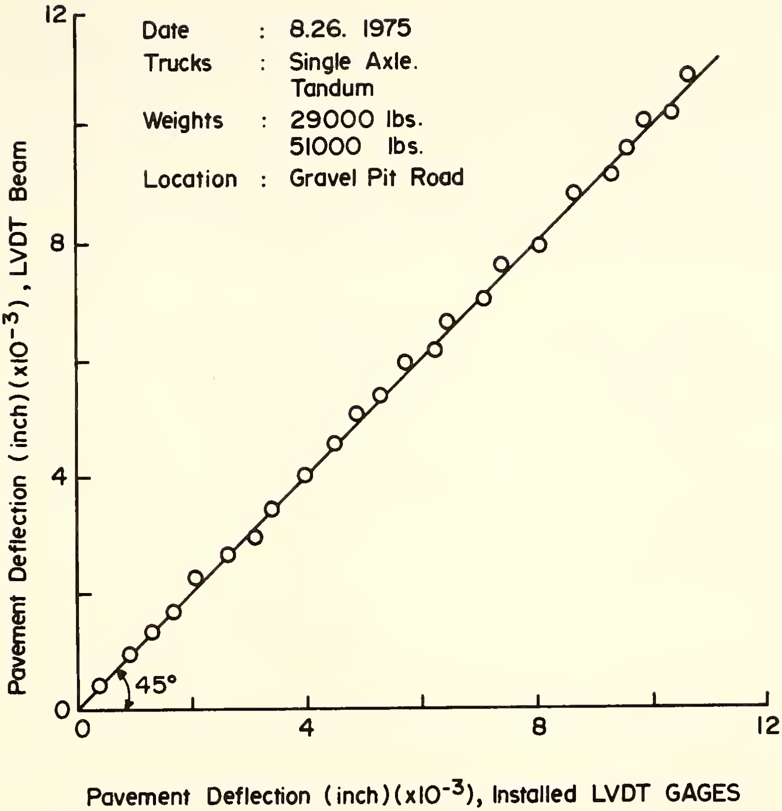

FIGURE 4.2 PAVEMENT DEFLECTION RESPONSES BY LVDT BEAM AND INSTALLED LVDT GAGES.

path, showed the same relative equivalence as was demonstrated by Figure (4.2).

II) Scope of Field Tests

The investigations were conducted at seven sites. Four sites were in the greater Lafayette area. Table (4.1) and Figure (4.3) show their locations and cross-sectional characteristics, respectively. Locations and characteristics of the other three sites are given in Table (4.2) and Figure (4.4).

The investigations were designed and tests were performed to account for certain factors which were thought to influence pavement performance and time dependent transfer (TDT) functions. Listed below are the various factors and the means whereby they were accounted for.

1. Ambient conditions: Table (4.3) provides a list of the ambient conditions encountered at the test sites, at various dates, during the testing program.
2. Gear Configuration: An Indiana State highway truck (tandem) was used as the standard loading vehicle throughout the course of this investigation. Various other trucks with different gear configurations were tested at the gravel pit road. Table (4.4) provides a listing of these vehicles.
3. Load: Load variations were achieved by varying the sand load carried by the standard highway truck.
4. Tire pressure: The tire pressure on the standard highway truck was varied between sixty five and one hundred psi.
5. Load repetitions: Counts of the number of vehicles that

TABLE 4.1 LOCATION OF SITES (1-4).

SITE NUMBER	ROAD	LOCATIONS
1	Gravel Pit Road	West Lafayette, Indiana. Entrance of the gravel plant from South River Road. First right after the railroad bridge. Installed LVDT gages are located fifty yards inside the gate.
2	Happy Hollow Road	West Lafayette, Indiana. From U.S. 52 south about four miles, two hundred yards north of Happy Hollow Park entrance.
3	North 9th Street	Lafayette, Indiana, from the south end of bridge over Wabash River south one mile, at the exit of a small road leading to an old bridge.
4	County Road 200 North	West Lafayette, Indiana, between McCormick Road and the west city limits of West Lafayette, one and a half miles west of the intersection of Northwestern and County Road 200 North.

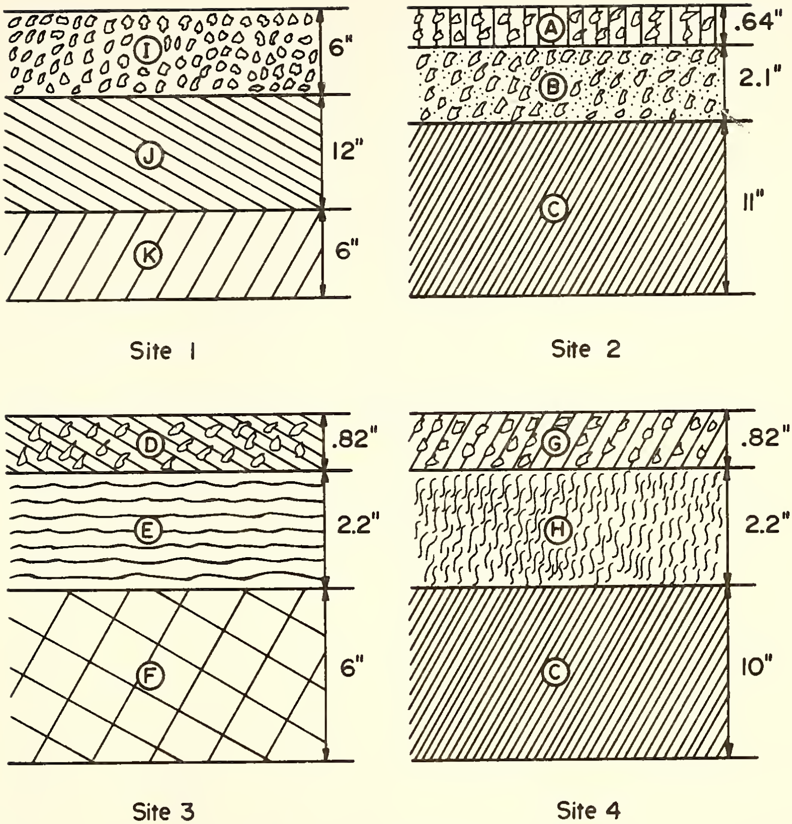

- (A) Bituminous Coated Blended Aggregate Surface
- (B) Bituminous Coated Blended Aggregate Binder
- (C) Compacted Aggregate Base
- (D) Bituminous Surface
- (E) Bituminous Binder # 9
- (F) Bituminous Base
- (G) Hac Surface Type B
- (H) Hac Base
- (I) A C Surface (3 Overlays)
- (J) Bituminous Coated, Compacted Sand Gravel Base
- (K) Compacted Sand and Gravel

FIGURE 4.3 CROSS-SECTIONS OF SITES 1, 2, 3 AND 4.

TABLE 4.2 LOCATION OF SITES (5-7)

SITE NUMBER	ROAD	LOCATIONS
5	State Road 59	Indiana, three miles north of U.S. 40 junction, one hundred yards north of Clay Park County Line. The south traffic lane was tested.
6	Interstate 64	Indiana, junction of U.S. 231 South and I-64 West, one hundred yards west of the ramp's end. Right lane of the west traffic lanes was tested. The section opened to traffic six months prior to testing.
7	Interstate 64	Indiana, junction of U.S. 231 South and I-64 West, four hundred yards east of site 6, approximately one hundred yards west of bridge. The right lane of the west traffic lanes was tested. The section was newly completed but not opened to traffic.

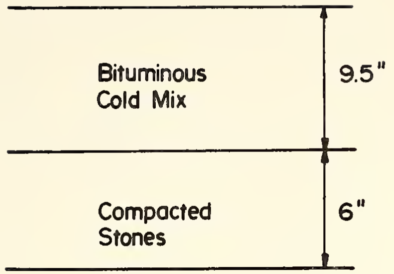

Overlays	Year
1.5" Cold mix	1934
4.0" Cold mix	1938
0.5" Kentucky Asphalt	1953
1.0" Type I	1967†
0.5" Type 4 Sand Mix	
1.5" Type 3	1974

† Widened to 16 Feet

Site 5

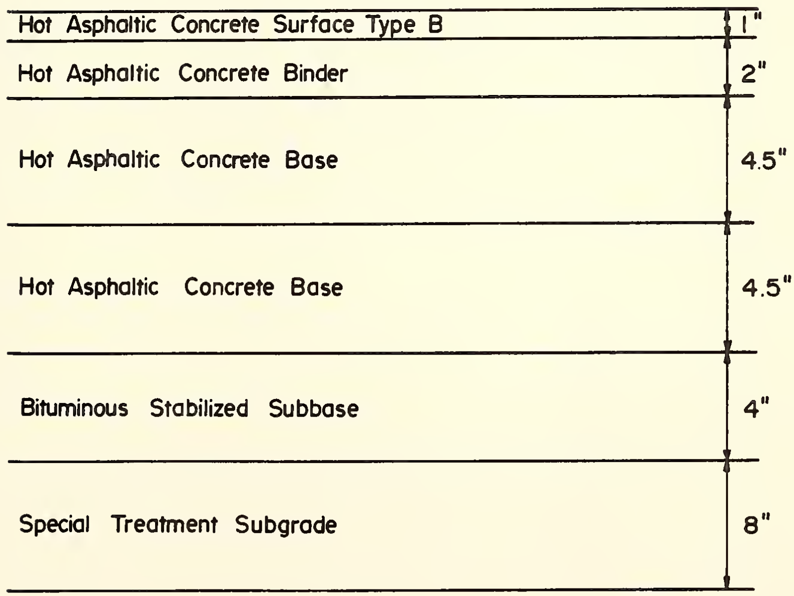

Sites 6,7

FIGURE 4.4 CROSS-SECTIONS OF SITES 5 AND 6 AND 7.

TABLE 4.3 AMBIENT CONDITIONS BEFORE AND DURING THE TEST PERIOD.

DATE	TIME	TEMPERATURE °F	WIND m.p.h.	CLOUDY	RAIN OR SNOW*
3-12-75	9:00 - 13:00	37	North at 10	cloudy	- 1 S
3-13-75	9:00 - 13:00	25	North at 7	cloudy	snowing
4-10-75	9:00 - 14:00	28	Southwest at 10	cloudy	snowing
4-12-75	9:00 - 14:00	40	South at 10	cloudy	- 2 S
8-26-75	9:00 - 15:00	75	Southwest at 10	partial	- 1 R
10-10-75	10:00 - 15:00	45	North at 8	clear	- 3 R
1- 5-76	9:00 - 13:00	- 12	North at 10	clear	- 1 S
1-10-76	9:00 - 11:00	- 10	North at 8	clear	- 1 S
3-17-76	9:00 - 14:00	22	Southeast at 5	clear	- 2 S
5-13-76	9:00 - 13:00	64	Northwest at 10	partial	- 5 R
7-30-76	9:00 - 13:00	78	Southwest at 8	partial	- hours R
8-12-76	9:00 - 16:00	80	South at 8	partial	- 5 R
9-13-76	12:00 - 13:00	80	Southwest at 10	clear	-10 R

* - 1 R = one day after it rained

- 2 S = two days after it snowed

TABLE 4.4 WEIGHT , TIRE PRESSURE AND GEAR CONFIGURATION OF VARIOUS TRUCKS USED AT THE GRAVEL PIT ROAD SITE.

NUMBER	GROSS LOAD lbs		SPEED RANGE m.p.h	GEAR CONFIGURATION	TIRE PRESSURE RANGE psi
	empty	loaded			
1	25000	73000	11 - 25	double tandem	70 - 90
2	20000	50000	6 - 25	tandem	75 - 100
3	8000	20000	10 - 30	single axle	75 - 90
4	4000	4300	4 - 10	car	20 - 25
5	6000	9000	10 - 15	pick-up	25 - 35
6	30000	65000	10 - 20	concrete truck	80 - 100
7	21000	52000	2 - 30	tandem	70 - 95

traveled over each of the test sites were obtained on three different days. Table (4.5) provides the average load repetitions on each site.

6. Cross-section: Figures (4.3) and (4.4) show the cross-sections of the pavement systems that were tested.

III) Signature

The signature of a vehicle will be defined as: the pavement time dependent deflection response function that is measured or calculated at the edge of the tires of the loading vehicle. Symbolically, the signature will be designated as A(0,t) or y(0,t).

The overhang of the LVDT beam prevented the direct measurment of the signature. However, pavement deflections could be and were measured at different lateral distances from the edge of tire. A study of the deflection basin at the embedded LVDT gages directed that the deflection will follow the expression.

$$y(x,t) = A(0,t)e^{-\frac{1}{B}x^{N}} \qquad (4.1)$$

where, y(x,t) = Measured deflection at lateral distance "x" from the tire edge at time "t"

A(o,t) = Calculated deflection (signature) at the edge of tire and time "t"

x = Lateral distance from the edge of tire to the LVDT gage at which y(x,t) was measured

B,N = Parameters of the equation.

TABLE 4.5 AVERAGE COUNT OF LOAD REPETITION ON SITES (1-4).

SITE NUMBER	ROAD	AVERAGE LOAD REPETITION[1] per year	VEHICLE TYPE	DAYS OF COUNTING
1	Gravel Pit Road	200,000	90% trucks[2] 10% cars	Monday, Wednesday, Friday[3]
2	Happy Hollow Road	250,000	5% trucks 95% cars	Monday, Wednesday, Saturday
3	North 9th Street	300,000	10% trucks 20% pick up 70% cars	Monday, Wednesday, Saturday
4	County Road 200 North	200,000	5% trucks 15% pick up 80% cars	Monday, Wednesday, Saturday

1 - Load repetition per car = the number of wheels that passed over one point in the pavement
2 - Checked with the Gravel Road Plant bookkeeper at the scale
3 - Plant closes over the weekends

IV) <u>Measured and Calculated Peak Deflections</u>

Throughout the course of this study, calculated peak deflections will be defined as the largest deflection values of the signature during the pass of a loading wheel; symbolically, it will be designated as A_p. On the other hand, measured peak deflections will be defined as the largest deflection values recorded by an LVDT gage at the various lateral distances from the tire edge. Symbolically, they will be designated as ${y_P}_{x=R}$; where, "R" is the lateral distance. For examples, a truck having a single axle gear configuration will produce two calculated peak deflections, one caused by the front tire and the other by the rear tire. On the other hand, a truck having a tandem gear configuration, will produce three calculated peak deflections: the front, intermediate, and rear tires. Figure (4.5) shows a calculated signature, measured deflections and peak deflections resulting from the passage of a tandum gear truck.

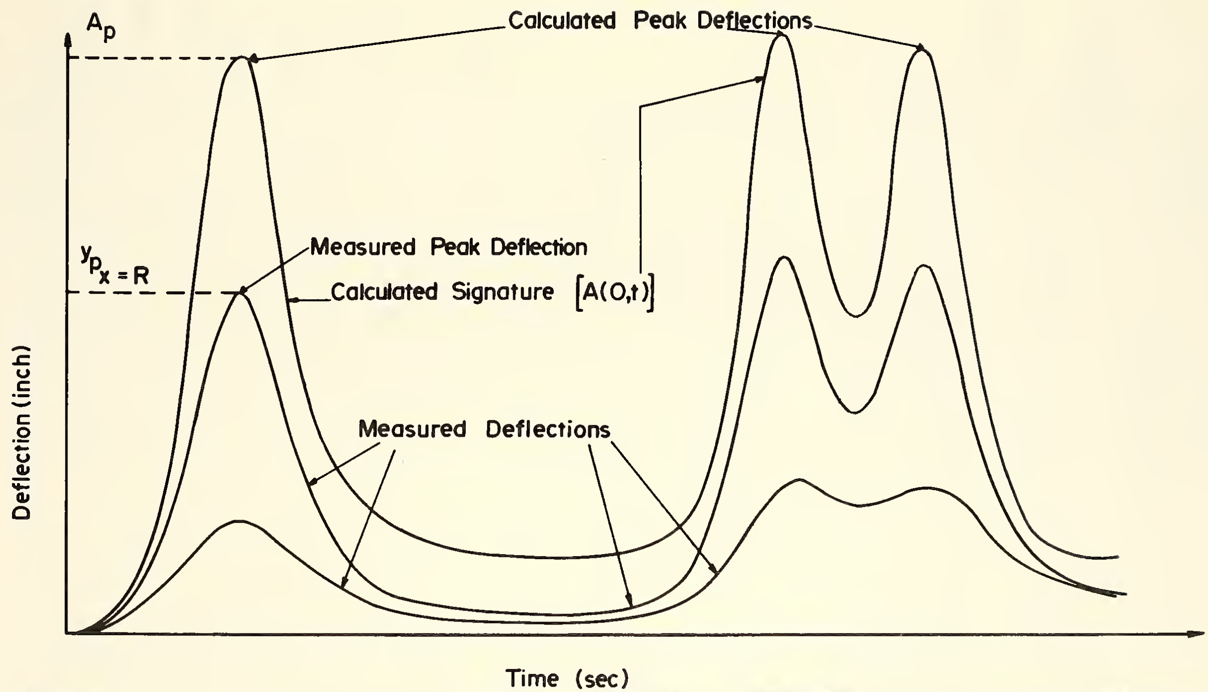

FIGURE 4.5 TYPICAL DEFLECTION Vs. TIME PLOT SHOWING SIGNATURE AND MEASURED AND CALCULATED PEAK DEFLECTION.

CHAPTER 5

DATA ANALYSIS

I) Hypothesis

The general hypothesis which serves as the basis of this research effort is:

> There exists a relationship between a pavement's deflection response function (output) and a vehicular loading (input) in the form of a time dependent transfer (TDT) function. The characteristics of the TDT function can be used as follows:
>
> a) To reflect performance and condition of a pavement system.
>
> b) To indicate the effects of ambient conditions.
>
> c) To obtain the shape of the peak deflections curve consequent to the passage of a wide range of vehicles.
>
> d) To assess the lateral attenuation of energy following the passage of a vehicle.
>
> e) To predict the time response of a pavement system.

II) Data Reduction

At each of the test sites, and for each test, pavement deflections were recorded at different lateral distances from the edge of the intermediate tire(the datum of measured lateral distances) on a line perpendicular to the path of the vehicle (see Appendix A). The output signal for each of the LVDT gages was continuously recorded (on a photographic paper) using a six channels light beam recorder, as shown in Figure (5.1). These output signals were digitized to discrete values at an equal time interval that ranged between two-tenths of a second (0.2 sec.) to one hundredth of a second (0.01 sec.), using a LARR-V digitizer. The time

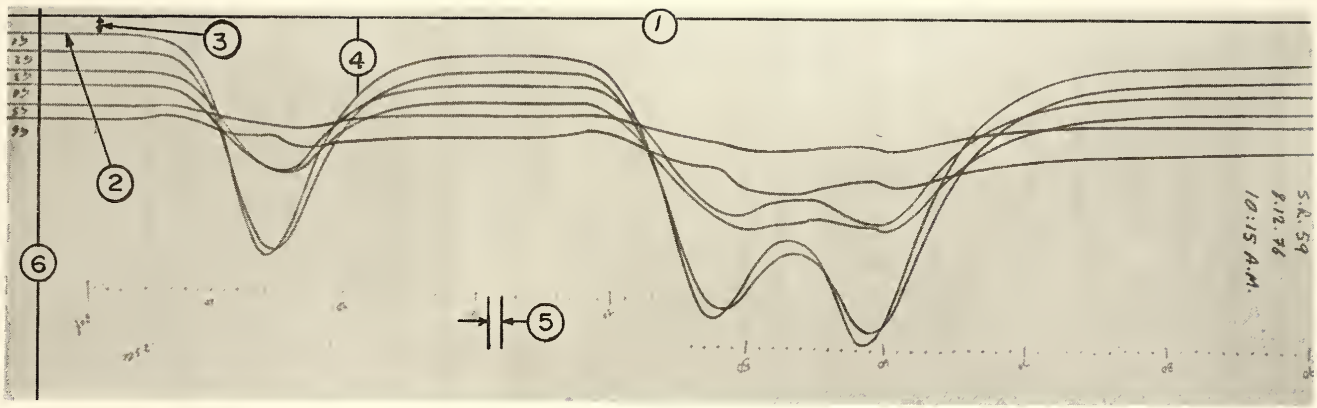

1_ Arbitrary Datum

2_ Reference Line for G_1

3_ Distance from Datum to Reference Line of G_1, $RF(G_1,0)$

4_ Distance from Datum to a Point on the Signal Curve from G_1, $SI(G_1,t)$

5_ One Delta Time

6_ Line of Zero Time

FIGURE 5.1 OUTPUT SIGNAL ON A SIX CHANNELS LIGHT BEAM RECORDER.

interval was dependent on the loading vehicle's velocity. The maximum number of data points, that were obtained from a single record, was restricted to be less than one hundred and fifty values.

Pavement deflections, at each of the LVDT gages were calculated using the following equation:

$$y(G_i,t) = [SI(G_i,t) - RF(G_i,0)].\ CAL(G_i)$$

where,

$y(G_i,t)$ = Pavement deflections (inches) at gage G_i and time t

G_i = Gage number

$SI(G_i,t)$ = Digitized electrical signal of gage G_i at time t

$RF(G_i,0)$ = Reference point of gage G_i at time zero, i.e. pavement at rest.

$CAL(G_i)$ = Calibration factor of gage G_i.

Figure (5.1) shows the output signals of six LVDT gages, a digitized electrical signal with repect to an arbitrary datum and the reference point for each LVDT gage.

III) Formulation of Solution

The Kelvin model, shown in Figure (3.1), was assumed in this study to represent the reaction of a point on a flexible pavement to an induced vehicular loading. Equation (3.3), repeated here for convenience, was the governing differential equation of motion (37):

$$m\ddot{y}(t) + c\dot{y}(t) + ky(t) = F(t) \qquad (3.3)$$

The forcing function [F(t)] in equation (3.3) also can be obtained using a numerical procedure; such as, by implicit convolution, equation (3.11b):

$$F(t_k) = m \left[\frac{y(t_k) - \Delta \sum_{n-1}^{k-1} F(t)\, G(t_{k+1-n})}{\Delta\, G(t_1)} \right] \tag{3.11b}$$

In the subsequent development, the solution of equation (3.3) will be refered to as the Newtonian solution

a) Signature

The pavement deflection response function at the edge of the tire [y(0,t)] was calculated using equation (4.1). The lateral distance (x) in equation (4.1) was measured with reference to either the intermediate or the rear tire. This was done because the front tire of a truck is offset from the path of the intermediate and rear tires, Figure (5.2b). This offset distance varies with the particular truck model. Consequently, the lateral distance between the edge of the front tire and the first LVDT gage is generally not the same as that of intermediate or rear tires. Also, if the path of the truck is not maintained perfectly perpendicular to the LVDT beam, the lateral distance will vary.

During preliminary testing, using installed LVDT gages, results showed that the parameters N and B in equation (4.1) are independent of the wheel load. Based upon this finding, the parameters N and B were calculated using peak deflection values caused by, and recorded at different lateral distances from, the intermediate and rear tires. These calculated N and B values were then used with the measured peak deflections produced by the front tire at different gages to calculate the lateral distance between the edge of the front tire and the first LVDT gage.

a. Truck on Scale (Static Wheel Loads)

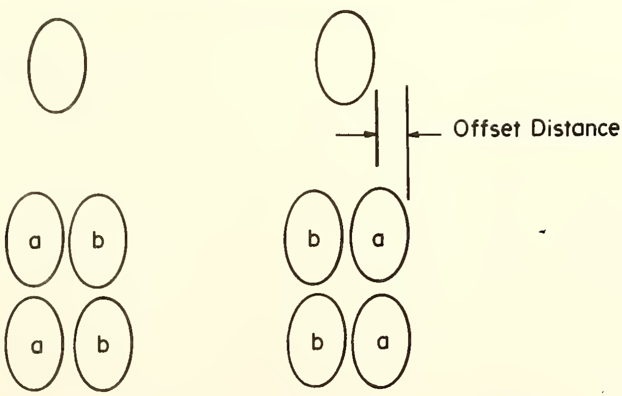

b. Tandem Gear Configuration

FIGURE 5.2 STANDARD HIGHWAY TRUCK (a) ON SCALES AND (b) GEAR CONFIGURATION.

The signature was calculated in two parts. The first part was obtained using equation (4.1) and the calculated lateral distance for the front tire. In the second part, for the intermediate and rear tires, equation (4.1), and the measured lateral distance were used.

b) Pavement's Velocity and Acceleration

After calculating the signature y(0,t), the velocity and acceleration [$\dot{y}(0,t)$, and $\ddot{y}(0,t)$] were obtained numerically. Figure (5.3) shows a typical signature and its associated velocities and accelerations. Note that as shown in Figure (5.4), only two values on the deflection curve are required to calculate the velocity at a point, numerically:three points enter with the calculation for the acceleration.

c) Forcing Function F(t)

The loading vehicle was weighed prior to testing at each site, as shown in Figure (5.2a), and the static wheel loads were recorded. The total weight on each of the intermediate and rear dual tires, tires a and b in Figure (5.2b), is assumed to be equally divided between the two tires.

The lateral distance between tires a and b, Figure (5.2b), of a dual set varies with truck model and tire size. To account for this effect, an equivalent static force was obtained for each set of dual wheels. The first approximation of this force is obtained as shown in Figure (5.5). Subsequent iterations will be explained in the next subsection.

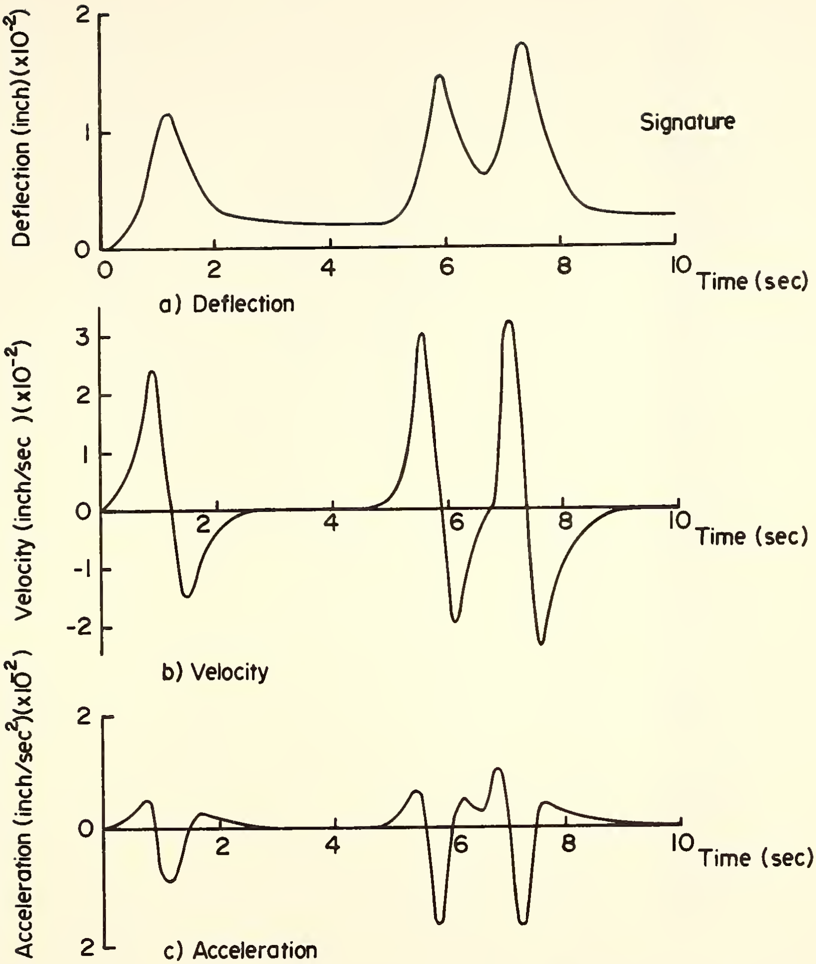

FIGURE 5.3 TYPICAL PLOTS OF SIGNATURE, VELOCITY, AND ACCELERATION Vs. TIME.

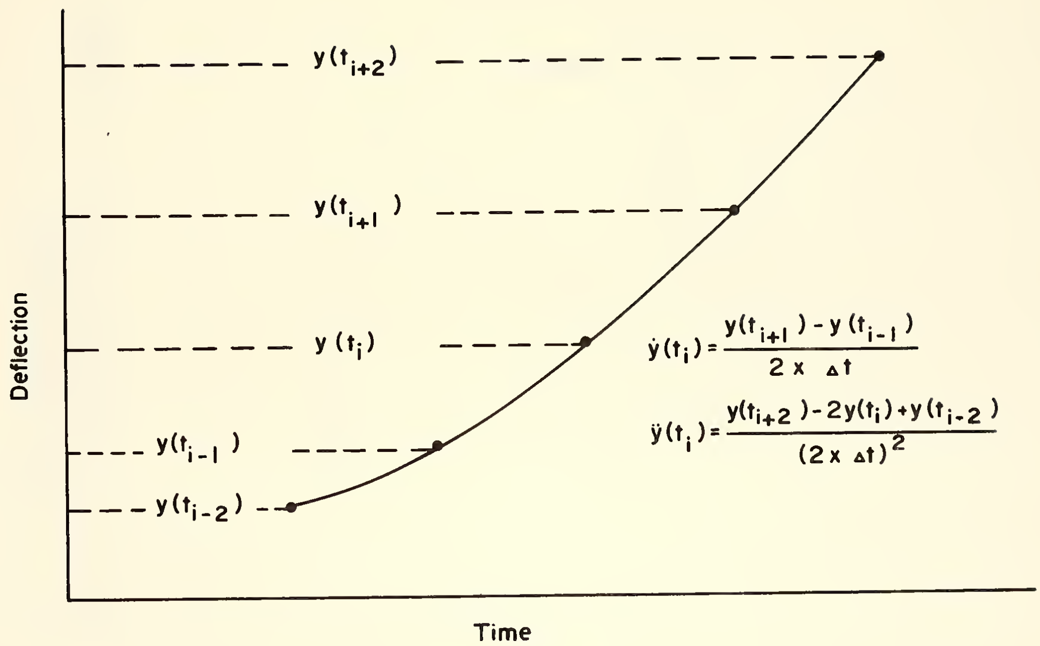

FIGURE 5.4 NUMERICAL DIFFERENTIATION PROCEDURE FOR CALCULATING THE VELOCITIES AND ACCELERATIONS OF A PAVEMENT.

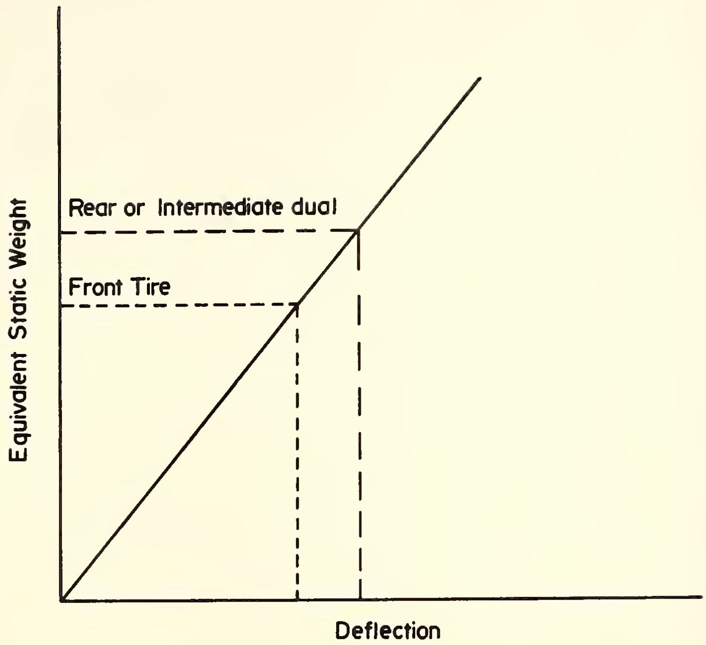

FIGURE 5.5 FIRST APPROXIMATION OF THE EQUIVALENT STATIC WEIGHTS OF THE INTERMEDIATE AND/OR REAR DUALS.

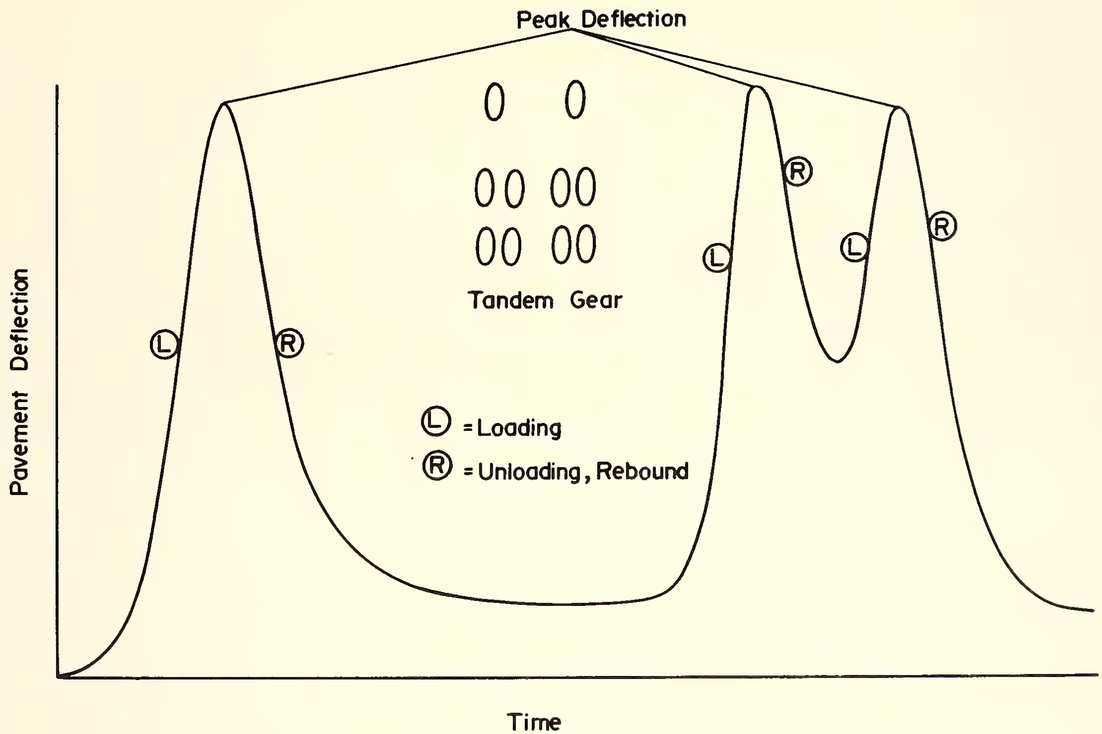

FIGURE 5.6 TYPICAL SIGNATURE PRODUCED BY A TANDEM TRUCK.

d) Newtonian Solution

Suppose that the curve in Figure (5.6) represents a typical signature that is caused by the passage of a tandem gear truck. Pavement deflections, velocities, and accelerations can be obtained for each increment of time, by procedures previously outlined. With the dynamic wheel loads* taken as the equivalent static weights, as a first approximation, equation (3.3) produces the following three equations:

$$
\begin{aligned}
m\ddot{y}(t_{PFF}) + c\dot{y}(t_{PFF}) + ky(t_{PFF}) &= F(t_{PFF}) \\
m\ddot{y}(t_{PFI}) + c\dot{y}(t_{PFI}) + ky(t_{PFI}) &= F(t_{PFI}) \qquad (5.1) \\
m\ddot{y}(t_{PFR}) + c\dot{y}(t_{PFR}) + ky(t_{PFR}) &= F(t_{PFR})
\end{aligned}
$$

where, t_{PFF}, t_{PFI}, and t_{PFR} are the times of occurence of peak forces due to the front, intermediate, and rear tires, respectively.

The three equations (5.1) are seen to contain six unknowns: m, c, k, t_{PFF}, t_{PFI}, and t_{PFR}. The following methodology was developed to overcome the indeterminancy and provide a solution.

Step 1

Because of the inertia of a pavement, the times of peak deflections and peak forces do not coincide. Suppose that each of these three time differences, for each of the wheel sets, are assigned arbitrary values. Then, the corresponding deflection curves, such as Figure (5.6), can be used to provide the times t_{PFF}, t_{PFI}, and t_{PFR} in equation (5.1). Given these times, the parameters m, c,

* As truck velocities in this study range from creep speed to five miles per hour, the dynamic force of the front tire is taken to be equivalent to the static weight.

and k can then be calculated

Having the parameters m, c, and k, and equation (3.3), the forcing function F(t) can be computed at each increment of time. These computations will also provide the three times at which the peak values of F(t) take place. If these values agree with those times chosen arbitrarily, the process is transfered to step 2 below. On the other hand, if the calculated three times do not agree with those values originally assigned, the new calculated times are used in equations (5.1) and new numerical values of the parameters m, c, and k are obtained.

The procedure is repeated until the times to peak forces at the beginning and the end of an iteration are equal. When this is satisfied, the first step in the solution procedure is had.

<u>Step 2</u>

Six regions of the signature are shown in Figure (5.6). Three regions represent the loading portions of the curve (labeled L in the figure) corresponding to the front, intermediate, and rear tires. The other three regions represent the unloading or rebound portions of the curve (labelled R in the figure).

The points of inflection on each loading part of the curve represent conditions of zero acceleration of the pavement. The respective times at these points of inflection were obtained by a numerical differentiation procedure.

Figure (5.6) also shows three points of peak deflections, which represent conditions of zero velocity. Using equation (3.3), with the conditions at the three points of inflection and at the three points of peak deflections; the following six equations were obtained:

$$c\dot{y}(t_{IF}) + ky(t_{IF}) = F(t_{IF})$$
$$c\dot{y}(t_{II}) + ky(t_{II}) = F(t_{II}) \qquad (5.2)$$
$$c\dot{y}(t_{IR}) + ky(t_{IR}) = F(t_{IR})$$

$$m\ddot{y}(t_{PF}) + ky(t_{PF}) = F(t_{PF})$$
$$m\ddot{y}(t_{PI}) + ky(t_{PI}) = F(t_{PI}) \qquad (5.3)$$
$$m\ddot{y}(t_{PR}) + ky(t_{PR}) = F(t_{PR})$$

where, (t_{IF}), (t_{II}), (t_{IR}) are the times at the points of inflection that were produced by the front, intermediate and rear tires, respectively: (t_{PF}), (t_{PI}), (t_{PR}) are the corresponding times at the peak deflections.

The three equations (5.2) are seen to contain five unknowns: c, k, $F(t_{IF})$, $F(t_{II})$, and $F(t_{IR})$. Assigning arbitrary values for two of the F's, the parameters c, and k can be computed.

The three equations (5.3) display four unknowns: m, $F(t_{PF})$, $F(t_{PI})$, and $F(t_{PR})$. With the k parameter known from above [equations (5.2)], after assigning an arbitrary value to any one of the F's the remaining unknowns can also be found.

With the first iteration of step 2 providing measures of k, c, and m, the forcing function F(t), equation (3.3), can be calculated at every increment of time. The calculated values of F(t) are then examined with respect to the following questions:

1. are the calculated values of F(t) at the points of inflection and the points of peak deflections equal to those originally assigned?
2. are the calculated parameters m, c, and k compatible with those calculated in step 1?
3. are the time differences corresponding to the peak forces and peak deflections equal to those calculated in step 1?
4. are the calculated peak forces in steps 1 and 2 of equal magnitude?

If the answer to any of these questions is negative, the process reverts to step 1. On the other hand, if all answers are affirmative, the Newtonian phase of the solution is had.

The values of the parameters m, c, k obtained in the Newtonian solution must also satisfy the results of implicit convolution.

e) Implicit Convolution Solution

Having the m, c, k parameters from the Newtonian solution, the time dependent transfer (TDT) function can be calculated using either equation (3.6) or (3.7). The equivalent forcing function can be computed using equation (3.11b) at the edge of the tire, as well as at each LVDT gage. The equivalent forcing functions are then compared, at each increment of time, with the corresponding Newtonian forcing functions. If the two show agreement at each increment of time, the m, c, and k parameters can then be considered to represent those of the pavement system.

If the agreement between the two procedures is not good, the values of the m, c, k parameters are altered, and the process returns to step 1 of the Newtonian solution, expect that the time delay can now be calculated and need not be assumed.

Figure (5.7) presents several typical representations of the forces obtained from the Newtonian and implicit convolution procedures. Had the check been perfect, the dotted and solid lines would have coincided. Not granted such results, the methodology then increments the value of the parameters (m, c, and k) to effect the coincidence of the lines, this will be called the <u>rotation of the axis of convolution</u> (Appendix B). The successful accomplishment of the rotation yields the desired m, c, k parameters.

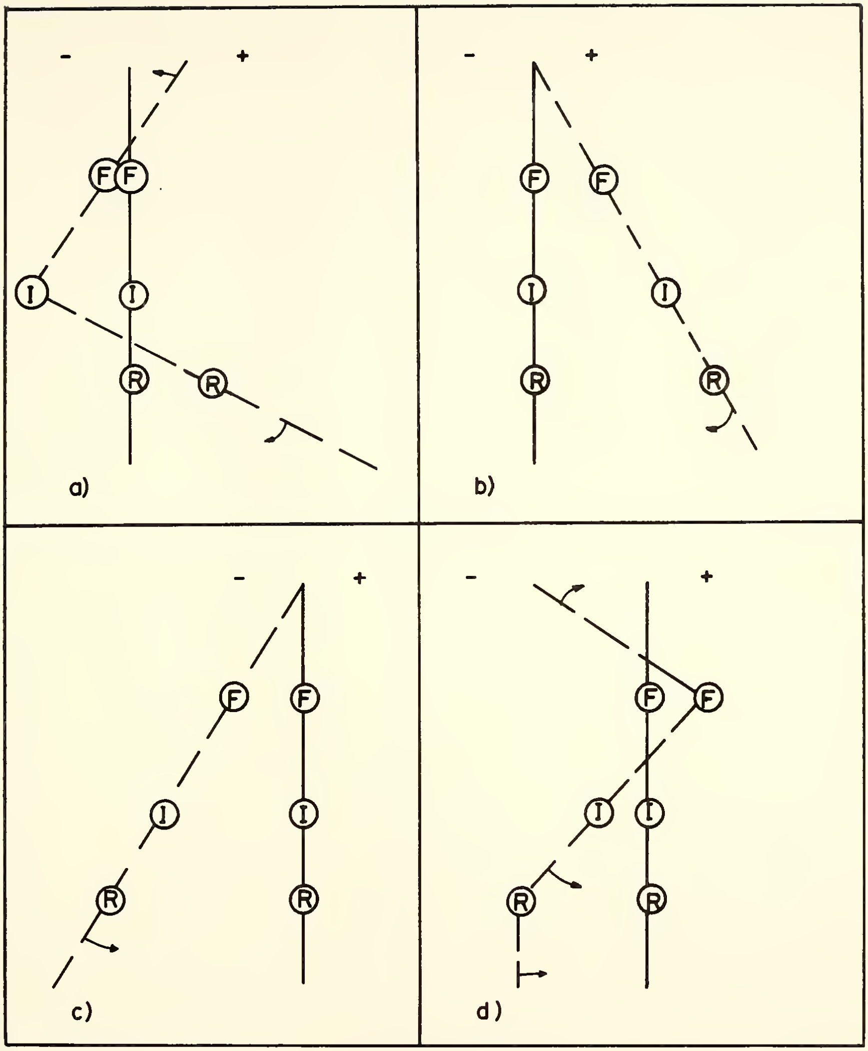

Forces Obtained Using Equation 3.3 (Newtonian)
Forces Obtained Using Equation(3.11b) (Implicit Convolution)

FIGURE 5.7 REPRESENTATION OF THE FORCE OBTAINED BY NEWTONIAN AND IMPLICIT CONVOLUTION SOLUTIONS.

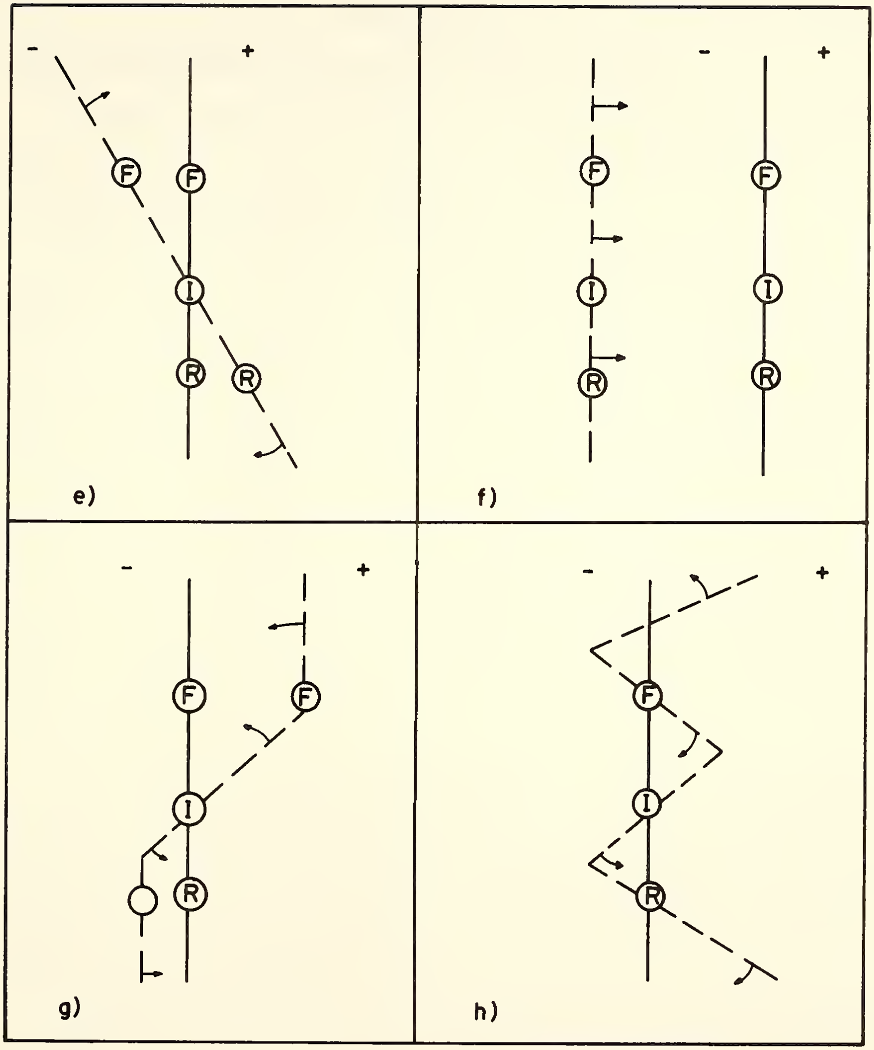

FIGURE 5.7 CONTINUED

CHAPTER 6

TEST RESULTS

I) Data for the Measured Deflection Response Functions

Appendix D provides lists of the relevant* digitized data of the deflection response functions that were obtained at the test sites.

II) Time Dependent Deflection Response Functions

Figures (6.1) through (6.7) display typical measured pavement deflection responses at seven sites [see Tables (4.1) and (4.2)], and the calculated signature (G_0) at the edge of the tire, using the standard highway truck. The sequence of letters, G_i, on the figures desigantes the particular gage number at which deflections were recorded. For example, G_2 denotes the second gage from the edge of the tire. Shown also are the measured lateral distances (x) between the gages and the tire. Figures (6.8) and (6.9) show measured deflections at site 1 (Table 4.1) due to the passage of a single axle, and a double tandem truck, respectively.

Five test series were performed using the standard highway truck at sites 1-4 under varying ambient conditions. Some results are presented in Tables (6.1) and (6.2). Note that no measurable deflections were recorded at any of the test sites for an ambient temperature of twelve degrees below zero Fahrenheit (-12^oF).

Pavement deflections at the edge of the tire (the datum of lateral measurment) were calculated using equation (4.1). Some corresponding values of N and B parameters are given in Tables (6.1) and (6.2). Also

* Relevancy will be discussed in section I of Chapter 7.

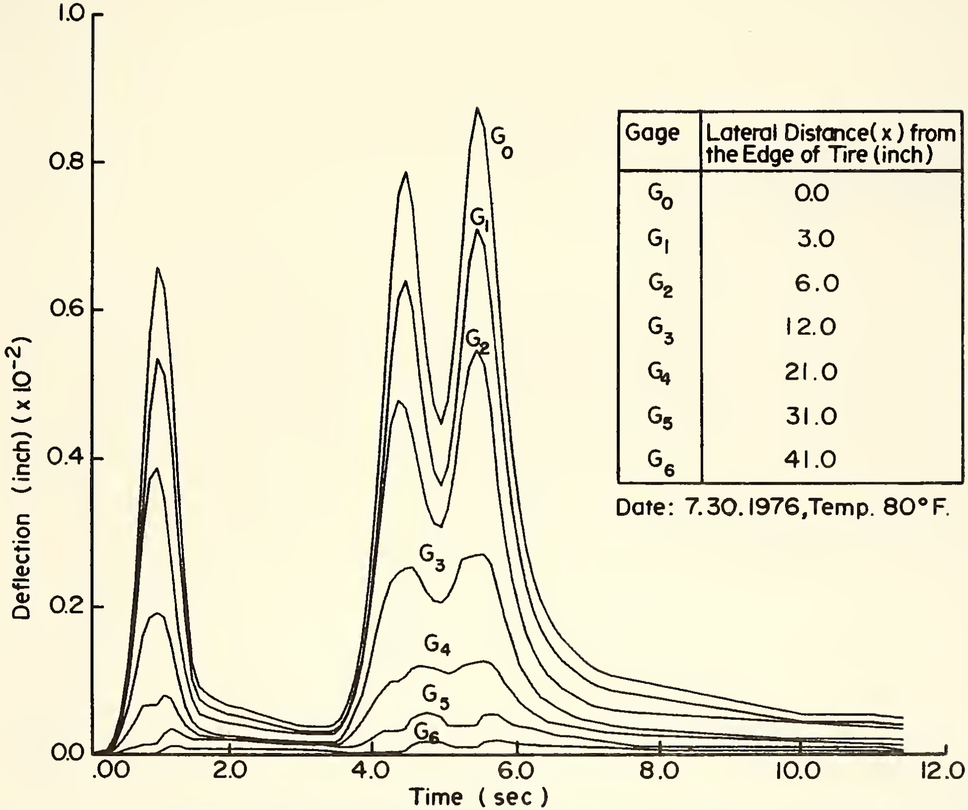

Gage	Lateral Distance(x) from the Edge of Tire (inch)
G_0	0.0
G_1	3.0
G_2	6.0
G_3	12.0
G_4	21.0
G_5	31.0
G_6	41.0

FIGURE 6.1 TYPICAL MEASURED DEFLECTIONS AND CALCULATED SIGNATURE (G_0) Vs. TIME. SITE 1, STANDARD HIGHWAY TRUCK.

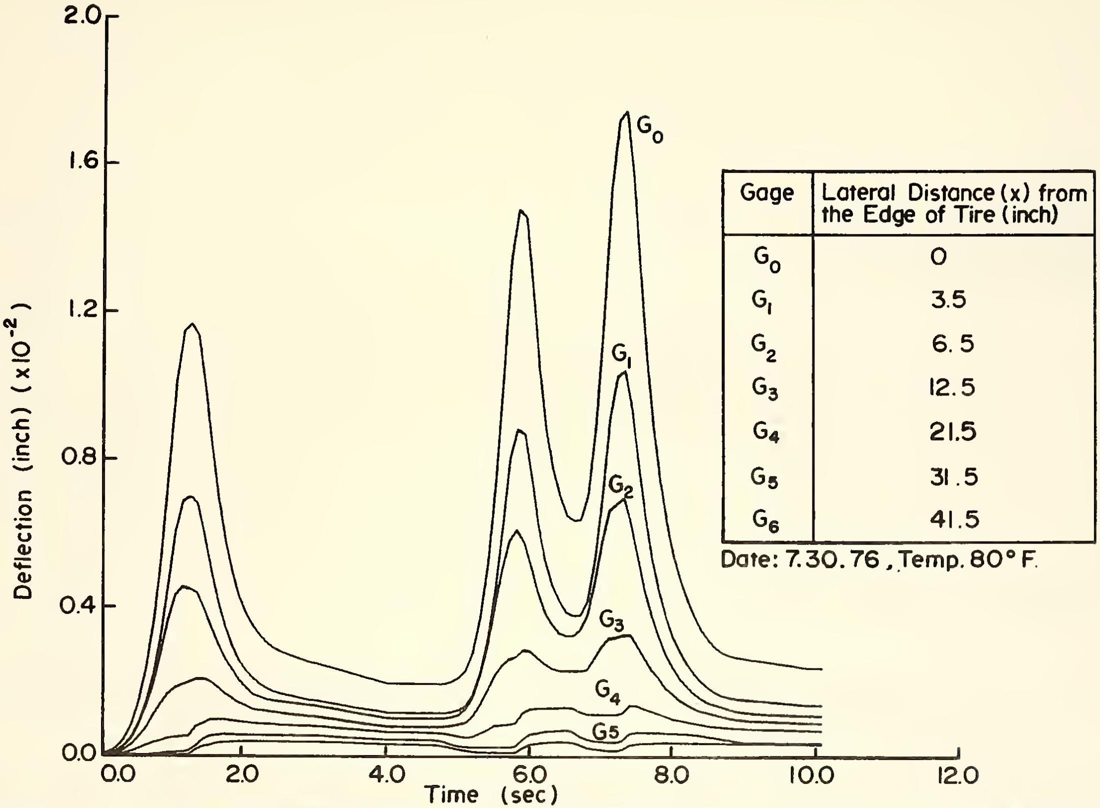

Gage	Lateral Distance (x) from the Edge of Tire (inch)
G_0	0
G_1	3.5
G_2	6. 5
G_3	12.5
G_4	21.5
G_5	31 .5
G_6	41.5

Date: 7.30.76 , Temp. 80° F.

FIGURE 6.2 TYPICAL MEASURED DEFLECTIONS AND CALCULATED SIGNATURE (G_0) Vs. TIME. SITE 2, STANDARD HIGHWAY TRUCK .

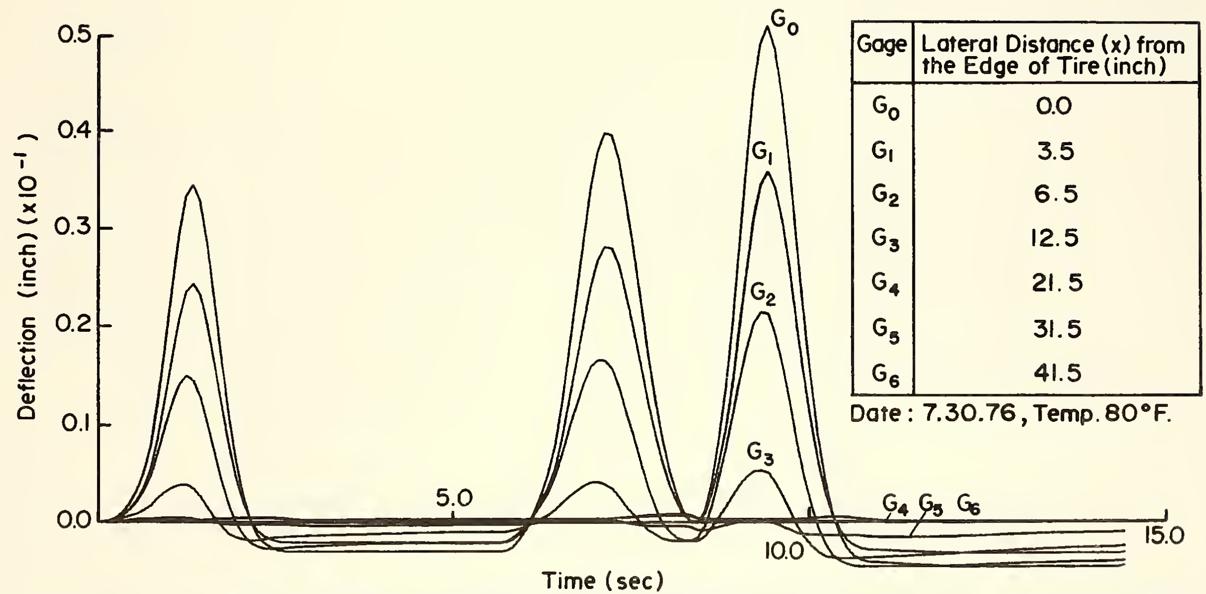

Gage	Lateral Distance (x) from the Edge of Tire (inch)
G_0	0.0
G_1	3.5
G_2	6.5
G_3	12.5
G_4	21.5
G_5	31.5
G_6	41.5

Date : 7.30.76, Temp. 80°F.

FIGURE 6.3 TYPICAL MEASURED DEFLECTIONS AND CALCULATED SIGNATURE (G_0) Vs. TIME. SITE 3, STANDARD HIGHWAY TRUCK.

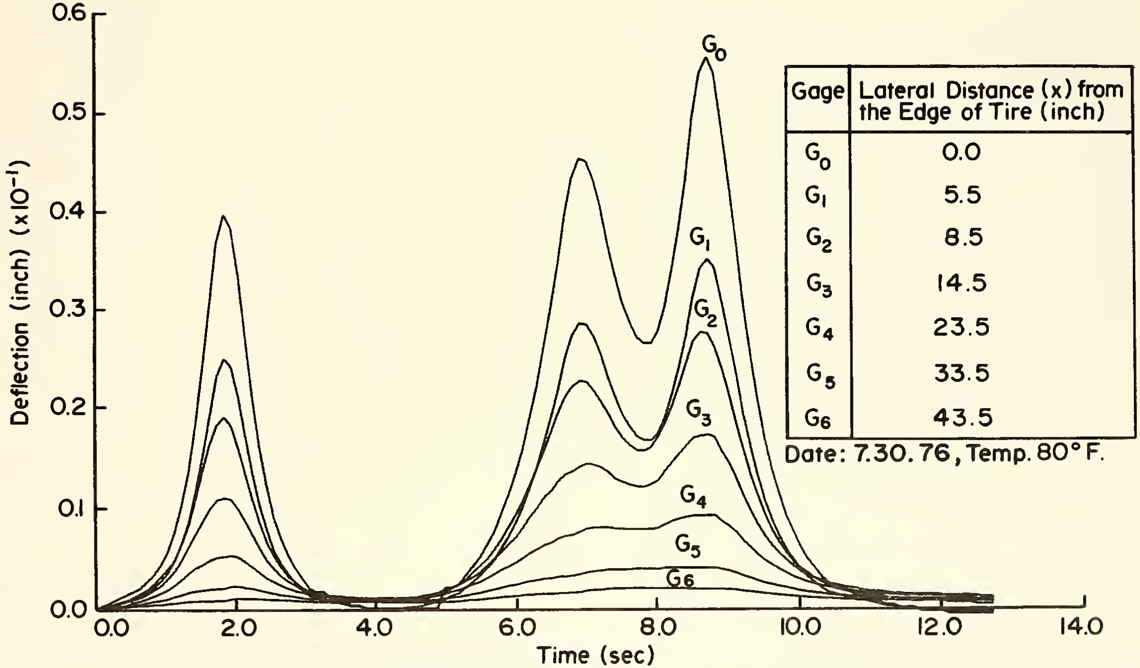

FIGURE 6.4 TYPICAL MEASURED DEFLECTIONS AND CALCULATED SIGNATURE (G_0) Vs. TIME. SITE 4, STANDARD HIGHWAY TRUCK.

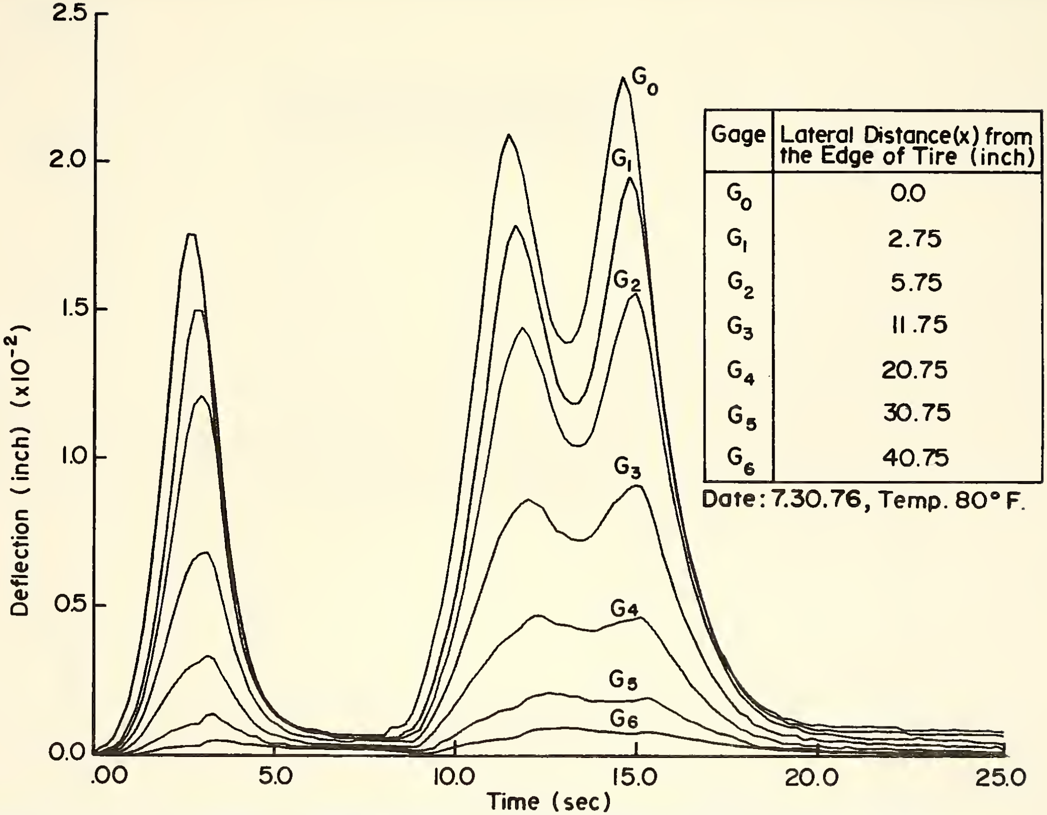

Gage	Lateral Distance(x) from the Edge of Tire (inch)
G_0	0.0
G_1	2.75
G_2	5.75
G_3	11.75
G_4	20.75
G_5	30.75
G_6	40.75

FIGURE 6.5 TYPICAL MEASURED DEFLECTIONS AND CALCULATED SIGNATURE (G_0) Vs. TIME. SITE 5, STANDARD HIGHWAY TRUCK.

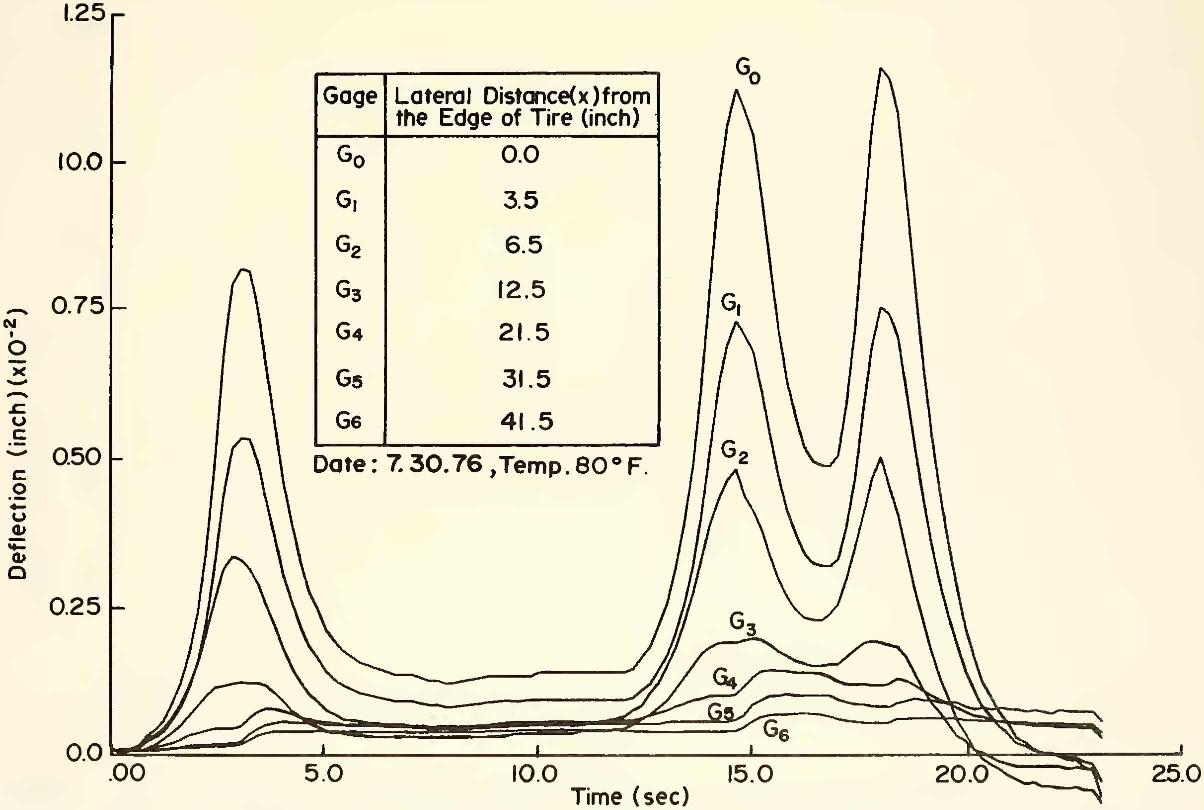

FIGURE 6.6 TYPICAL MEASURED DEFLECTIONS AND CALCULATED SIGNATURE (G_o) Vs. TIME. SITE 6, STANDARD HIGHWAY TRUCK.

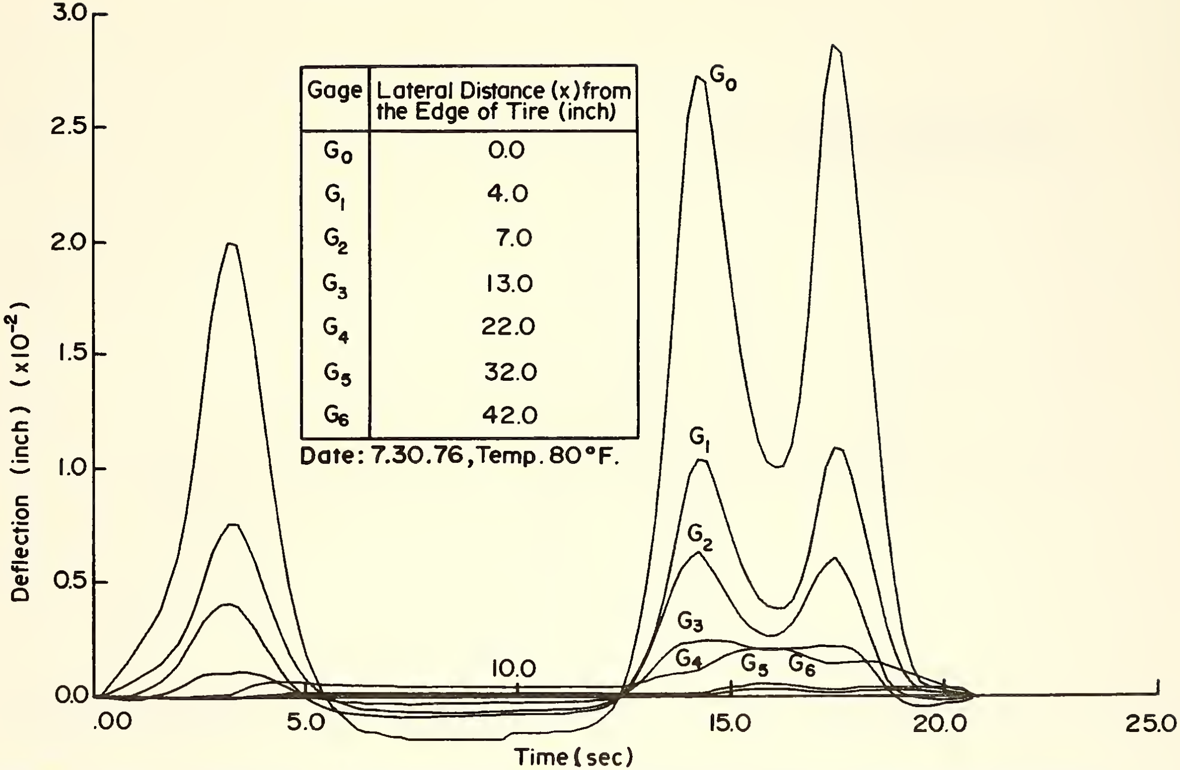

FIGURE 6.7 TYPICAL MEASURED DEFLECTIONS AND CALCULATED SIGNATURE (G_0) Vs. TIME. SITE 7, STANDARD HIGHWAY TRUCK.

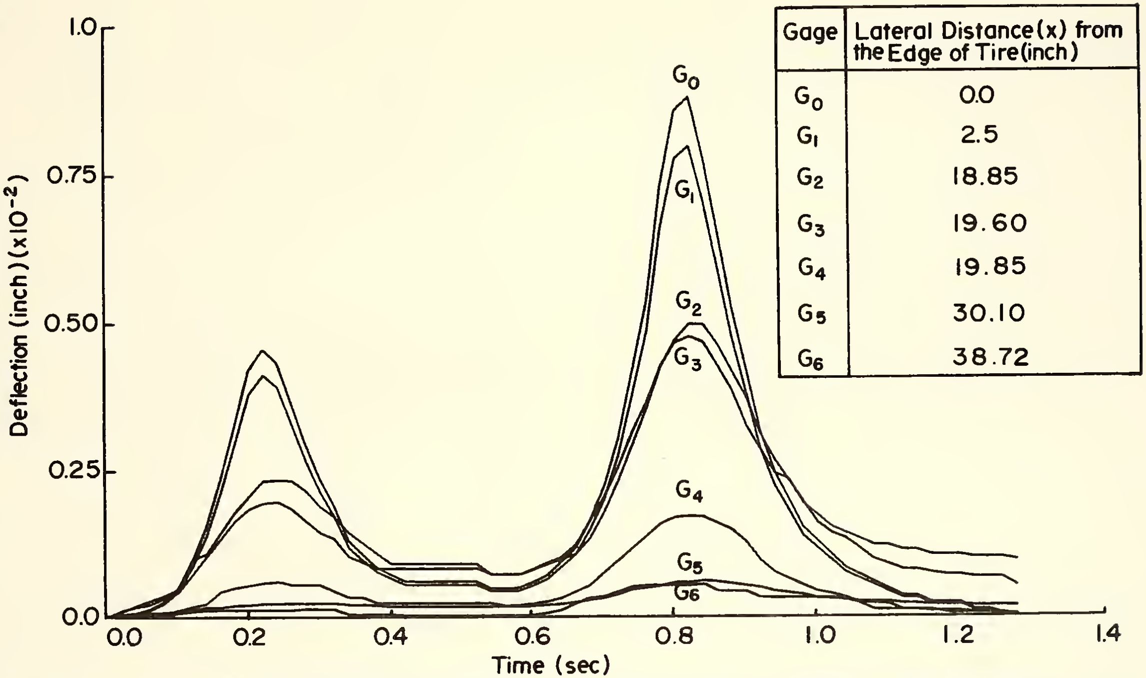

FIGURE 6.8 MEASURED DEFLECTIONS AND CALCULATED SIGNATURE (G_0) Vs. TIME, SITE 1, SINGLE AXLE TRUCK.

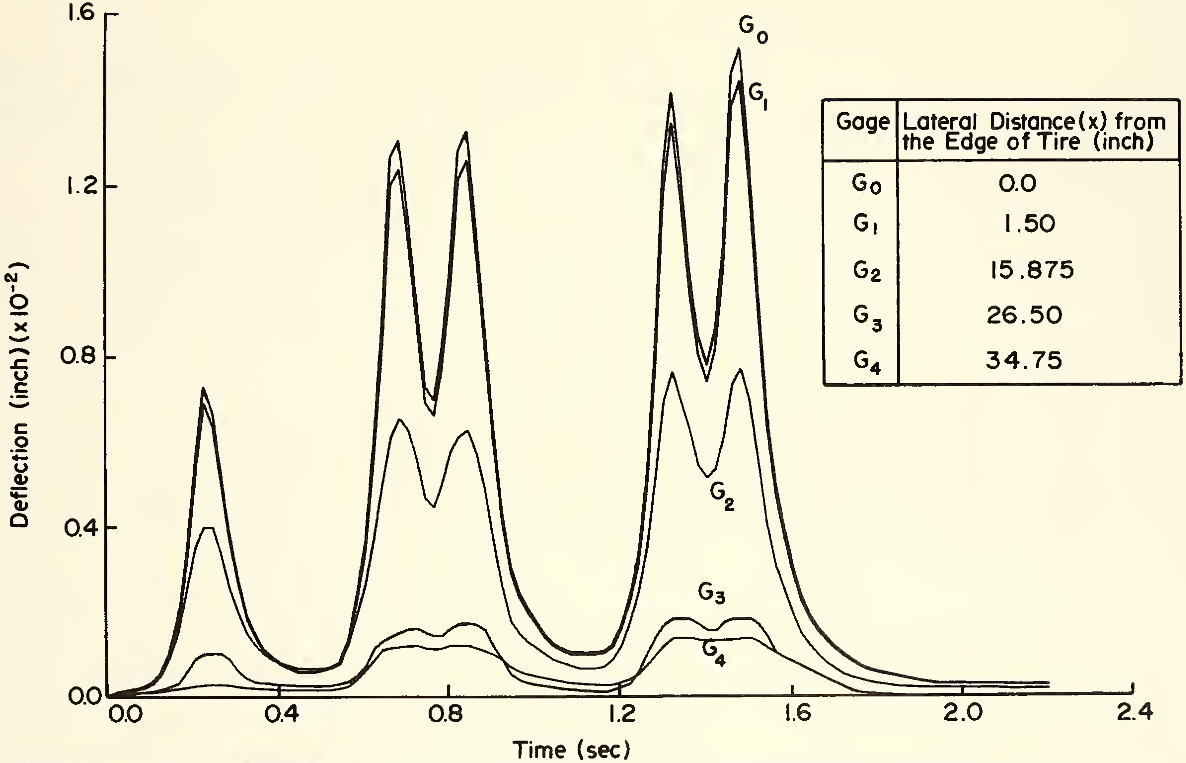

FIGURE 6.9 MEASURED DEFLECTIONS AND CALCULATED SIGNATURE (G_0) Vs. TIME. SITE I, DOUBLE TANDEM TRUCK.

TABLE 6.1 SOME RESULTS AT SITES 1 and 2 (STANDARD HIGHWAY TRUCK)

SITE	DATE	AIR TEMP. °F	WHEEL LOAD (lbs)			PEAK DEFLECTIONS (inch)			VEHICLE VELOCITY (ft/sec)	DEFLECTION BASIN PARAMETERS	
			FRONT	INTER-MEDIATE	REAR	FRONT	INTER-MEDIATE	REAR		N	B
1	8-26-75	75	6616	6827	6836	.0066	.0068	.0067	2.67	1.26	31.64
		75	6611	6668	6842	.0066	.0068	.0068	2.81	1.26	31.82
	1- 5-76	-12	6500	6700	6750	.0000	.0000	.0000	2.70	-	-
		-12	6500	6720	6775	.0000	.0000	.0000	2.90	-	-
	3-17-76	22	6276	8715	9554	.0050	.0069	.0074	3.55	1.38	53.30
		22	6295	8638	9433	.0053	.0069	.0073	3.25	1.38	52.28
	5-13-76	64	6478	8307	8759	.0057	.0073	.0076	2.54	1.22	26.28
		64	6481	8281	8699	.0058	.0075	.0077	2.35	1.22	23.62
	7-30-76	78	6681	8454	8728	.0065	.0082	.0083	3.56	1.14	17.25
		78	6748	8093	9210	.0065	.0078	.0087	4.16	1.15	17.04
	9-13-76	80	4500	2800	3500	.0055	.0033	.0043*	2.21	1.128	15.62
		80	1000		900	.0011		.0009†	2.36	1.13	15.60
2	8-25-75	82	6388	7177	7038	.0104	.0113	.0111	3.12	1.01	8.46
		82	6423	7500	6793	.0135	.0154	.0136	3.60	1.07	10.70
	1- 5-76	-12	6100	6900	6800	.0000	.0000	.0000	2.61	-	-
		-12	6120	7200	6600	.0000	.0000	.0000	2.91	-	-
	3-17-76	22	6975	7881	8205	.0117	.0134	.0139	2.97	1.37	31.95
		22	6991	8227	8346	.0115	.0132	.0136	2.63	1.34	32.24
	5-13-76	68	7069	8054	7773	.0156	.0180	.0170	2.52	.99	6.54
		68	7069	8000	7800	.0157	.0181	.0171	2.67	.99	6.54
	7-30-76	80	6130	8044	8131	.0099	.0191	.0195	3.00	.87	5.81
		80	6113	7822	8270	.0100	.0182	.0199	2.51	.88	6.75

* Standard highway truck(empty).
† Automobile(Ford).

TABLE 6.2 SOME RESULTS AT SITES 3, 4, 5, 6 AND 7 (STANDARD HIGHWAY TRUCK)

SITE	DATE	AIR TEMP. °F	WHEEL LOAD (lbs)			PEAK DEFLECTIONS (inch)			VEHICLE VELOCITY (ft/sec)	DEFLECTION BASIN PARAMETERS	
			FRONT	INTER-MEDIATE	REAR	FRONT	INTER-MEDIATE	REAR		N	B
3	8-26-75	75	6003	7477	7668	.0326	.0409	.0415	3.33	1.60	37.29
		75	5979	7714	8274	.0268	.0361	.0364	1.10	1.57	34.67
	1- 5-76	-12	6500	7900	8000	.0000	.0000	.0000	2.61	-	-
		-12	6450	7960	8120	.0000	.0000	.0000	1.89	-	-
	3-17-76	24	6615	8762	9847	.0104	.0135	.0152	2.08	1.86	241.39
		24	6615	8742	9817	.0104	.0134	.0151	2.08	1.88	252.09
	5-13-76	68	6592	8749	8719	.0232	.0308	.0306	2.57	1.52	32.01
		68	6589	9022	8563	.0245	.0332	.0316	2.43	1.53	32.39
	7-30-76	80	6900	7882	9682	.0377	.0444	.0539	3.38	1.45	16.77
		80	6908	7832	9947	.0339	.0391	.0500	2.20	1.48	18.28
4	8-25-75	82	5602	8022	7295	.0323	.0385	.0341	2.92	1.05	16.15
		82	5602	8000	7310	.0323	.0381	.0342	3.12	1.05	16.15
	1- 5-76	-12	6500	8000	8100	.0000	.0000	.0000	.92	-	-
		-12	6448	7800	8300	.0000	.0000	.0000	4.12	-	-
	5-13-76	68	6522	8927	9162	.0378	.0512	.0512	2.74	.99	10.11
		68	6500	8825	8775	.0386	.0521	.0523	2.72	.99	10.64
	7-30-76	80	7000	8200	9872	.0399	.0453	.0556	2.81	.93	10.81
		80	6984	8187	9975	.0399	.0455	.0557	2.62	.93	10.80
5	8-12-76	80	7001	8521	9342	.0175	.0210	.0229	1.48	1.15	20.17
6	8-12-76	80	6401	8826	9222	.0081	.0112	.0116	1.24	.87	6.87
7	8-12-76	80	6401	8802	9285	.0229	.0313	.0329	1.31	.50	2.08

tabulated are some typical calculated peak deflections at the edge of the tire for the front, intermediate, and rear tires of the loading vehicle.

III) Peak Deflections

Figures (6.10 - 6.16) show the peak deflections corresponding to the passage of the standard highway truck at sites 1-7. The solid curves in the figures represent measured peak deflections versus lateral distances from the edge of the tire. Calculated peak deflections [A(0,t), equation (4.1)] are shown as dashed lines.

IV) Equivalent Forcing Functions

Figures (6.17 - 6.23) show the equivalent forcing functions at the indicated lateral distances from the edge of the tire. These functions were obtained by the implicit convolution procedure [equation (3.11b)]. The sequence of letters, G_i, as before, designates the gage number at which the equivalent forces were calculated. The equivalent forces denoted as G_0, represent the loading vehicle's forcing function.

V) Energy Attenuation in the Pavement

Figures (6.24 - 6.30) provide plots of the calculated equivalent peak forces versus lateral distances from the edge of the tire.

VI) Time Dependent Transfer Function

Figures (6.31 - 6.37) show typical plots of the time dependent transfer functions (TDT) for each of the test sites.

Table (6.3) provides a listing of the following characteristics of the TDT functions at sites 1-4:

a) peak value of the TDT function.

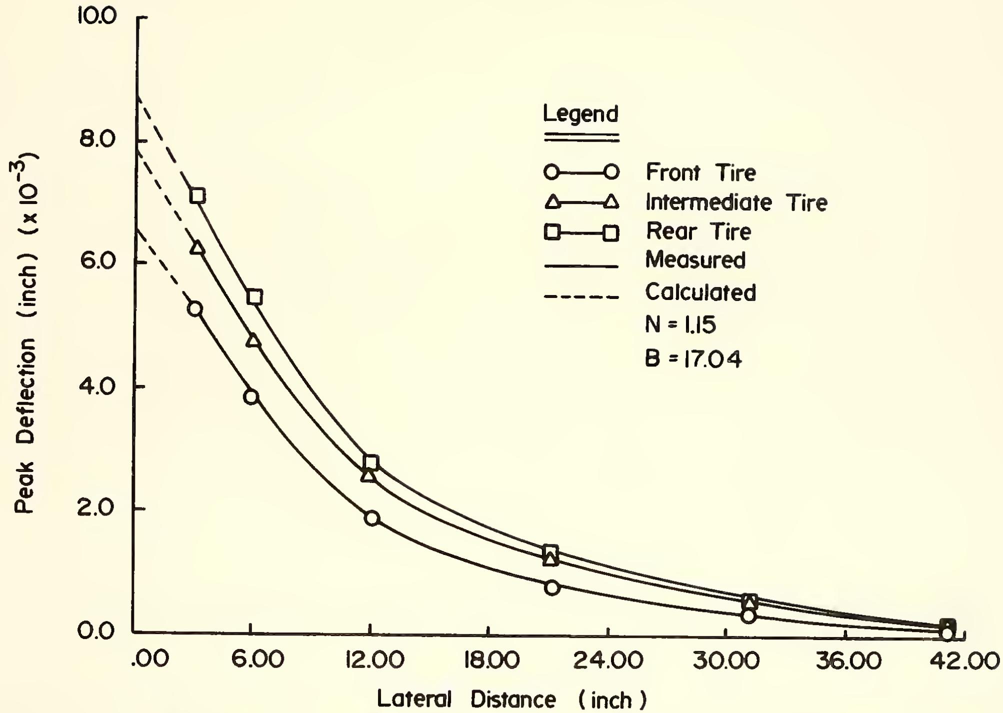

FIGURE 6.10 MEASURED AND CALCULATED PEAK DEFLECTIONS Vs. LATERAL DISTANCES. SITE 1, STANDARD HIGHWAY TRUCK.

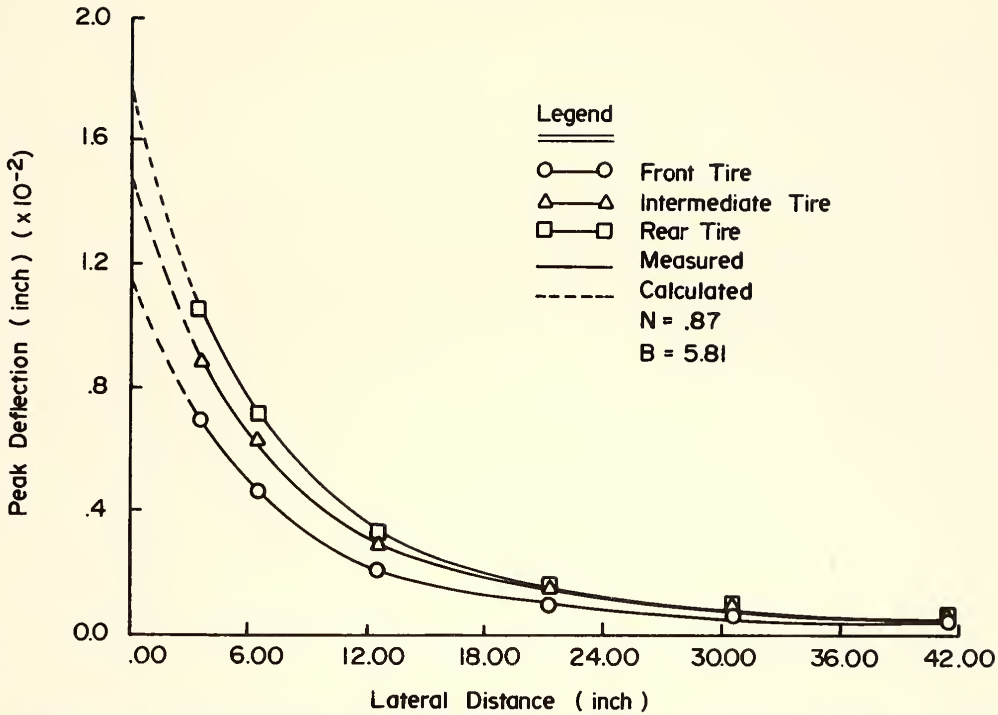

FIGURE 6.11 MEASURED AND CALCULATED PEAK DEFLECTIONS Vs. LATERAL DISTANCES. SITE 2, STANDARD HIGHWAY TRUCK.

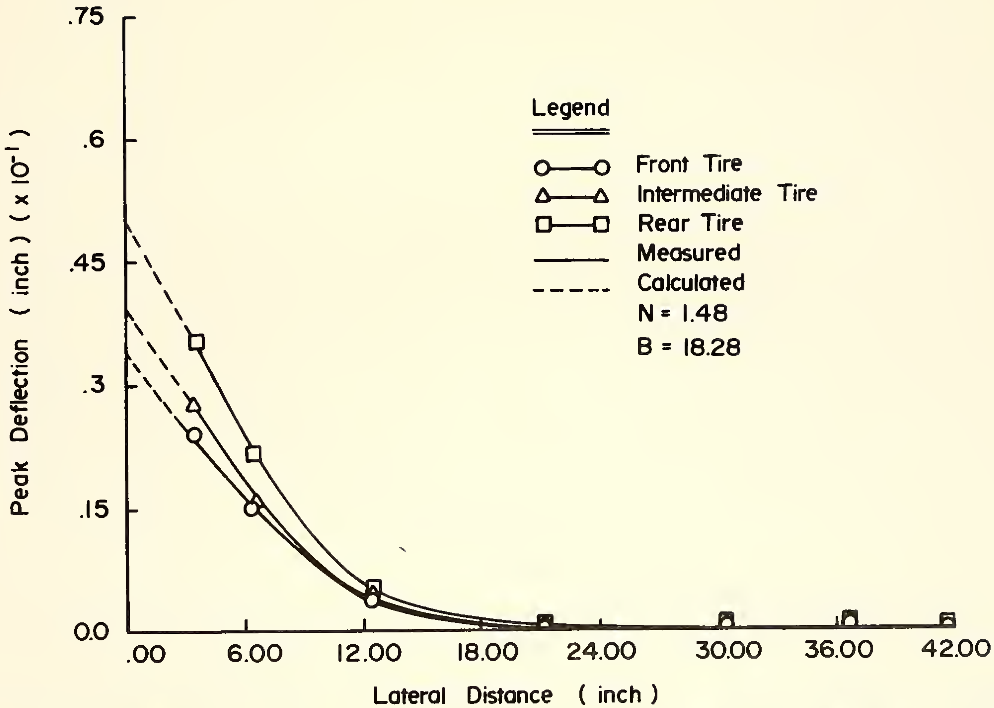

FIGURE 6.12 MEASURED AND CALCULATED PEAK DEFLECTIONS Vs. LATERAL DISTANCES. SITE 3, STANDARD HIGHWAY TRUCK.

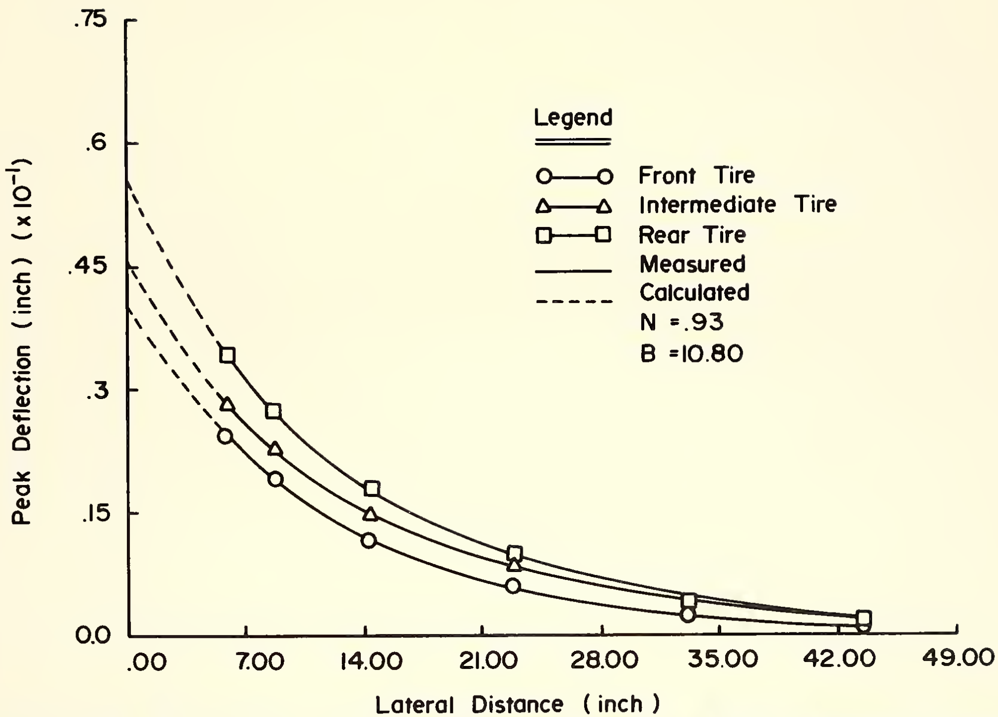

FIGURE 6.13 MEASURED AND CALCULATED PEAK DEFLECTIONS Vs. LATERAL DISTANCES. SITE 4, STANDARD HIGHWAY TRUCK.

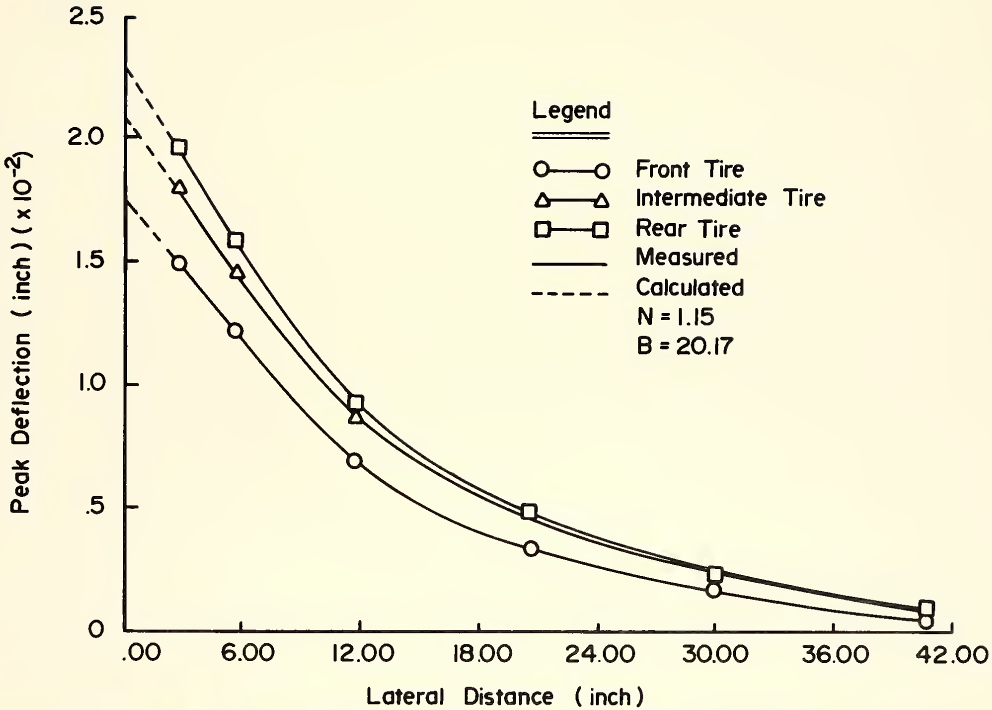

FIGURE 6.14 MEASURED AND CALCULATED PEAK DEFLECTIONS Vs. LATERAL DISTANCES. SITE 5, STANDARD HIGHWAY TRUCK.

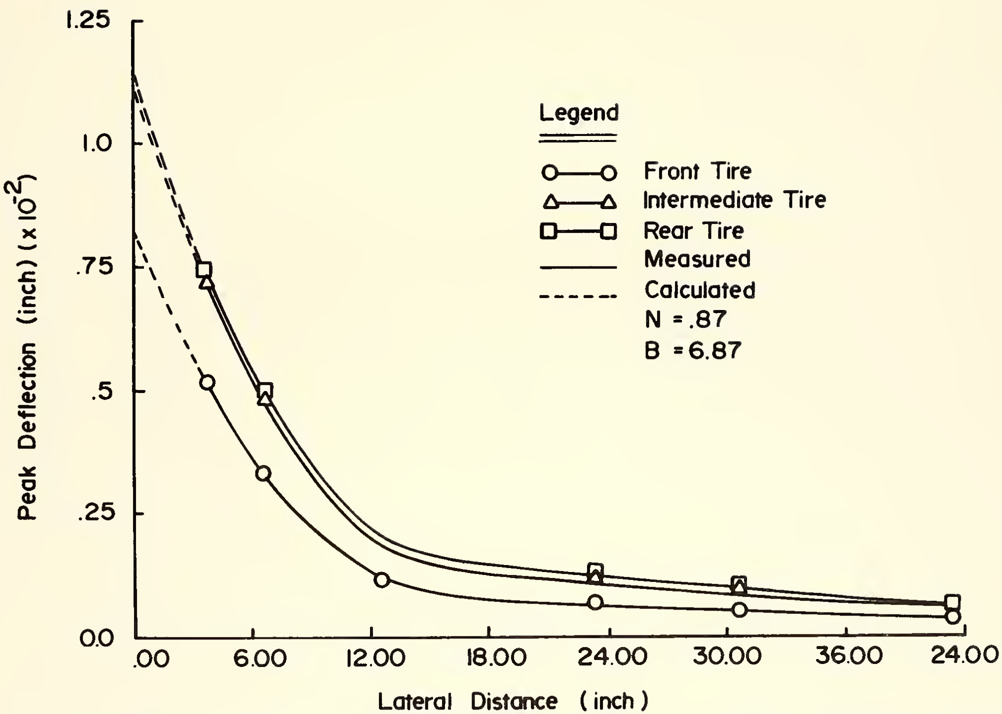

FIGURE 6.15 MEASURED AND CALCULATED PEAK DEFLECTIONS Vs. LATERAL DISTANCES. SITE 6, STANDARD HIGHWAY TRUCK.

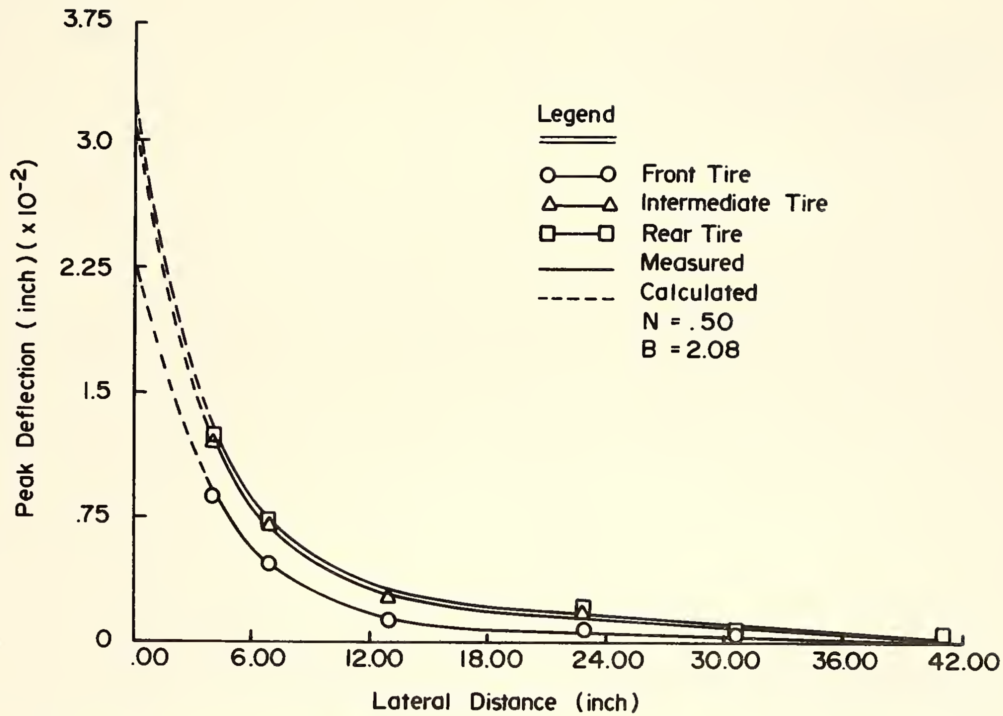

FIGURE 6.16 MEASURED AND CALCULATED PEAK DEFLECTIONS Vs. LATERAL DISTANCES. SITE 7, STANDARD HIGHWAY TRUCK.

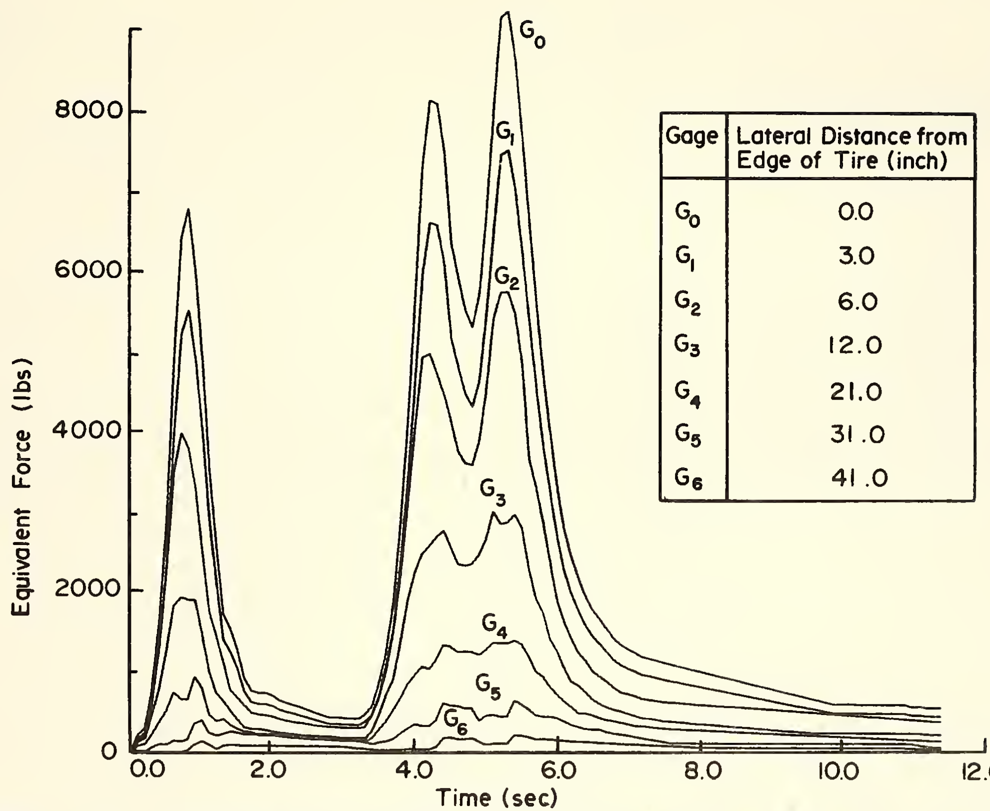

FIGURE 6.17 CALCULATED EQUIVALENT FORCING FUNCTIONS Vs. TIME. SITE I, STANDARD HIGHWAY TRUCK.

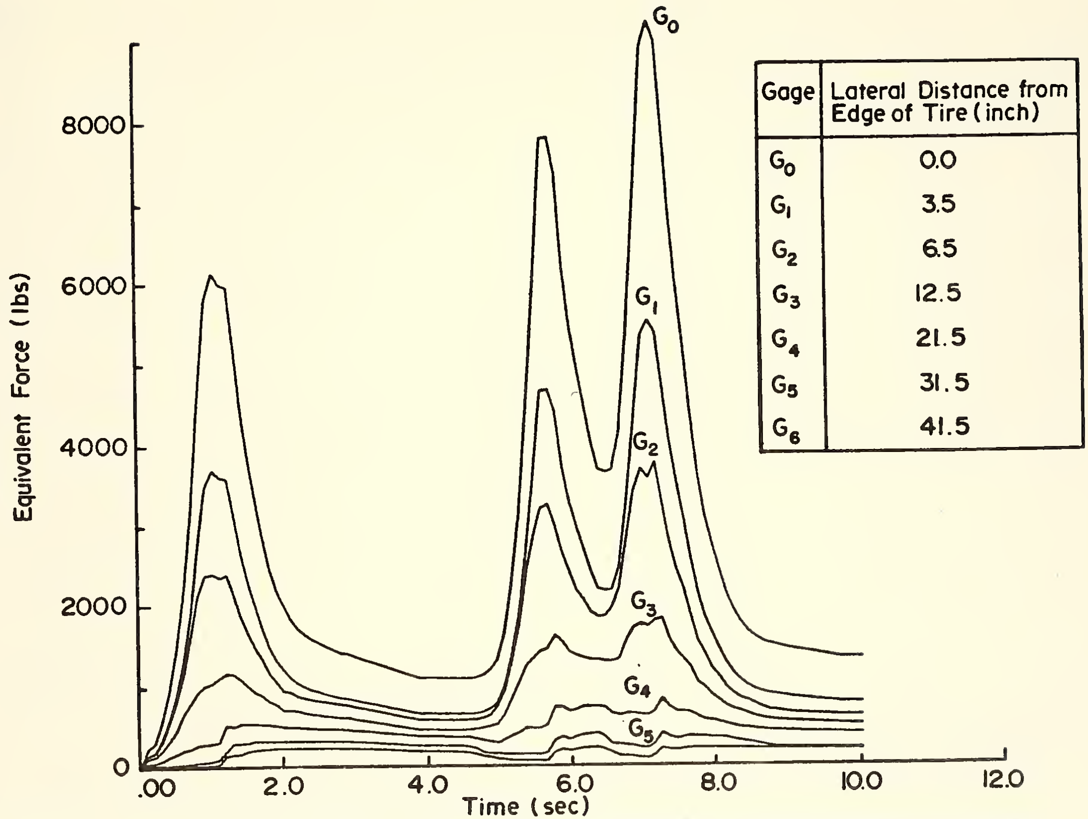

FIGURE 6.18 CALCULATED EQUIVALENT FORCING FUNCTIONS Vs. TIME. SITE 2, STANDARD HIGHWAY TRUCK.

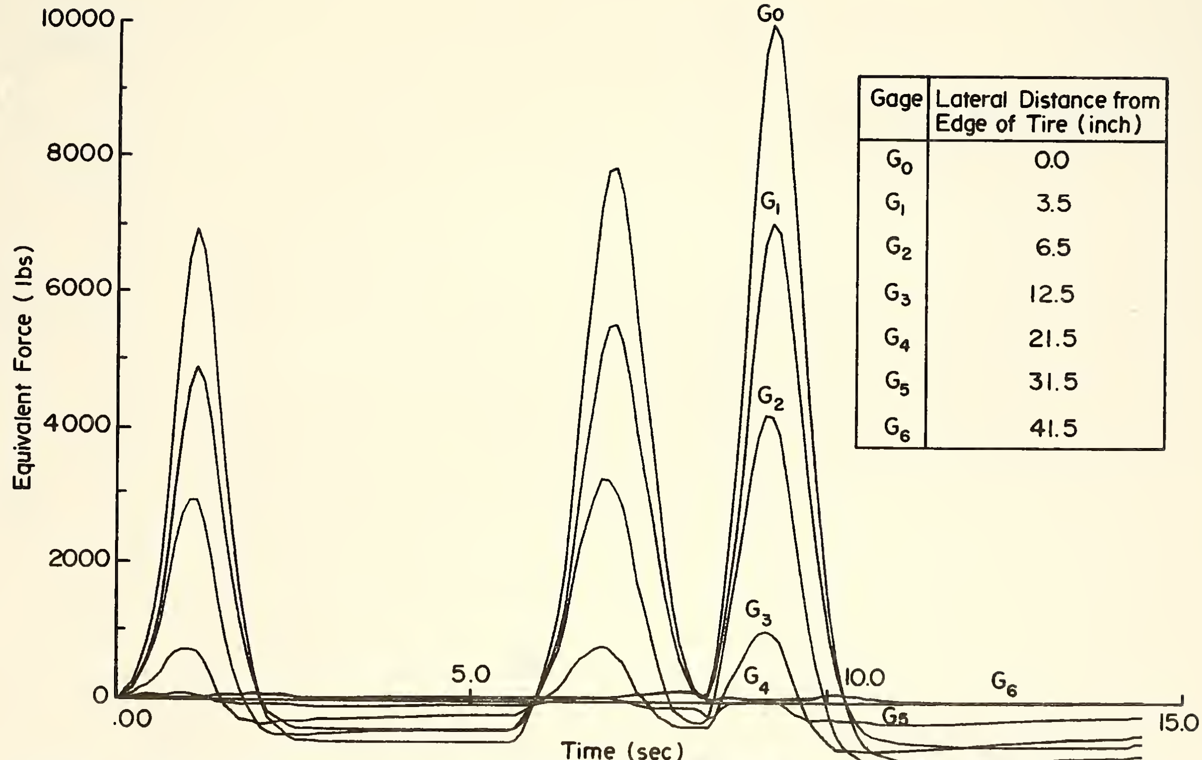

FIGURE 6.19 CALCULATED EQUIVALENT FORCING FUNCTIONS Vs. TIME . SITE 3, STANDARD HIGHWAY TRUCK .

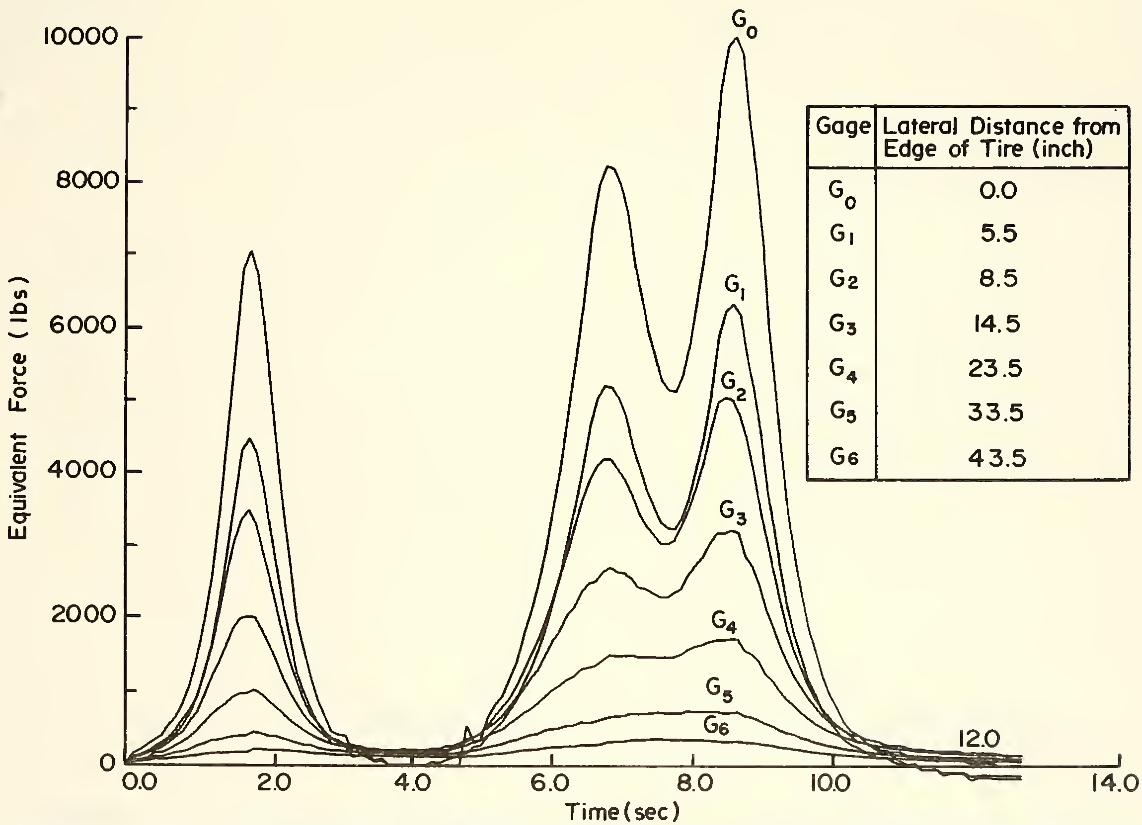

FIGURE 6.20 CALCULATED EQUIVALENT FORCING FUNCTIONS Vs. TIME. SITE 4, STANDARD HIGHWAY TRUCK.

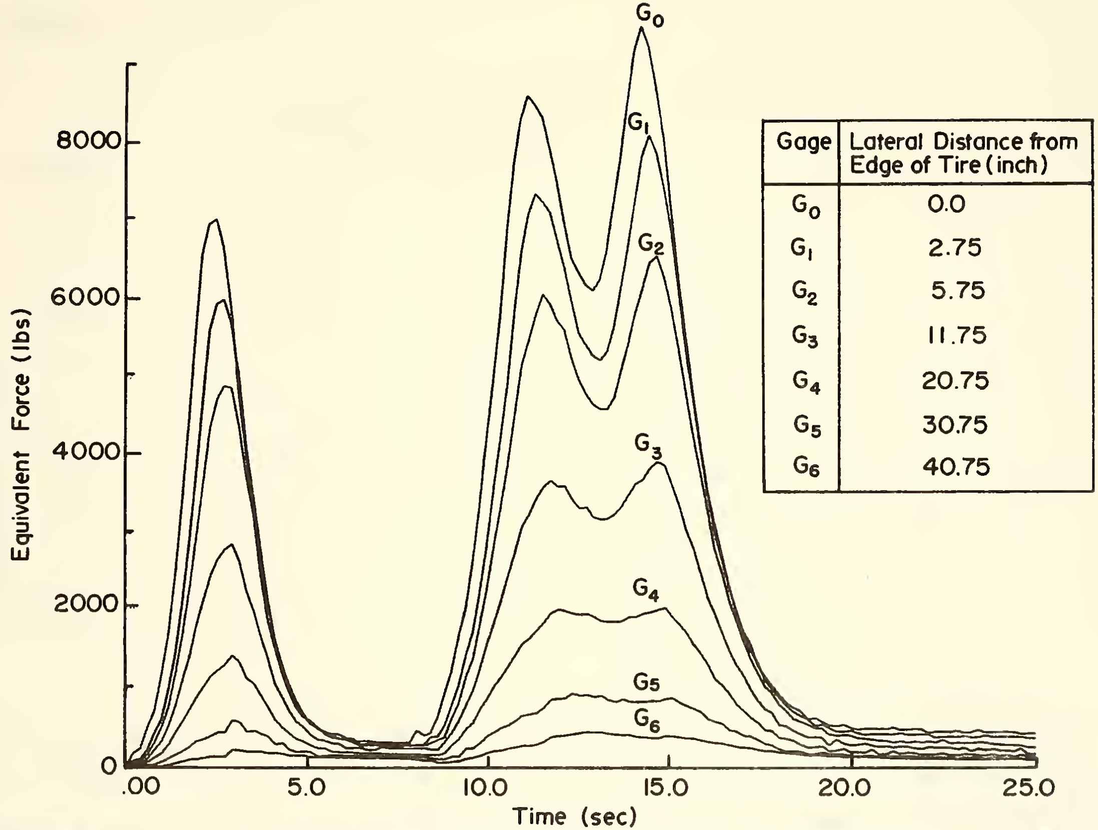

FIGURE 6.21 CALCULATED EQUIVALENT FORCING FUNCTIONS Vs. TIME. SITE 5, STANDARD HIGHWAY TRUCK.

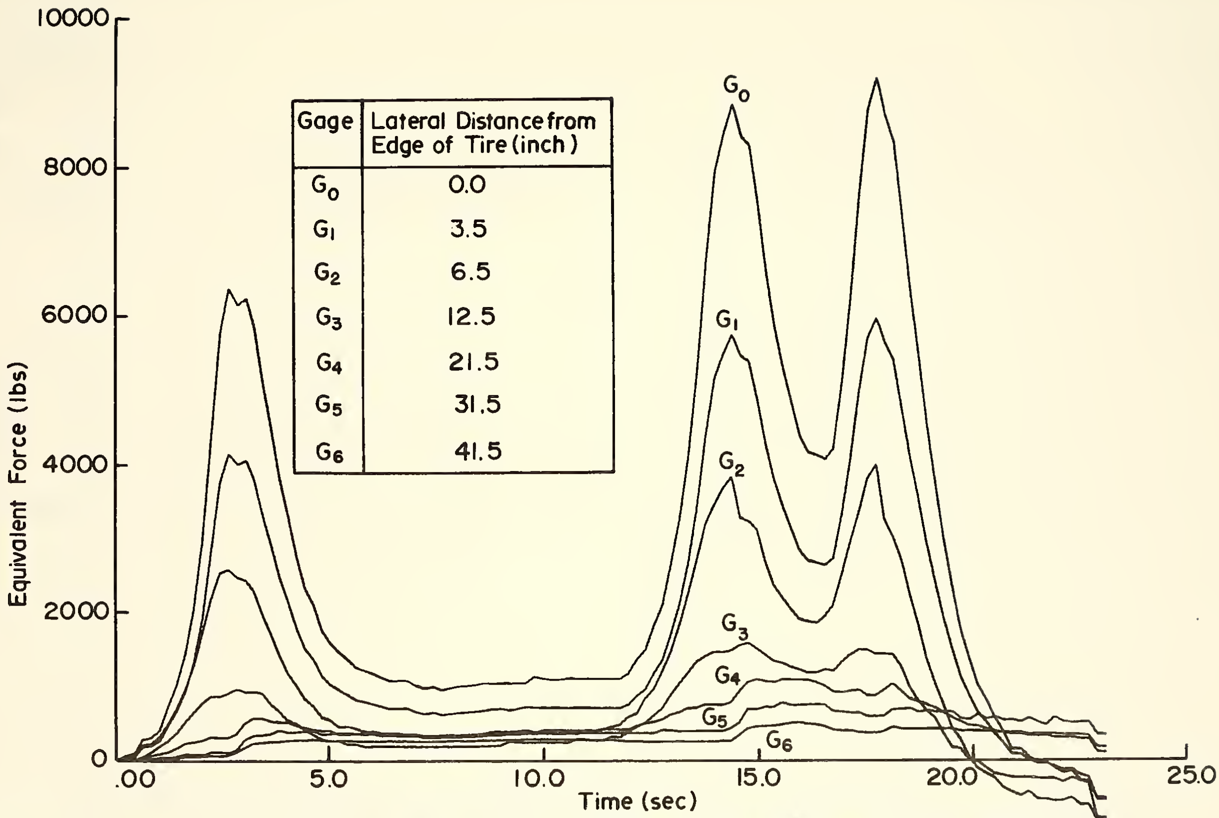

FIGURE 6.22 CALCULATED EQUIVALENT FORCING FUNCTIONS Vs. TIME. SITE 6, STANDARD HIGHWAY TRUCK.

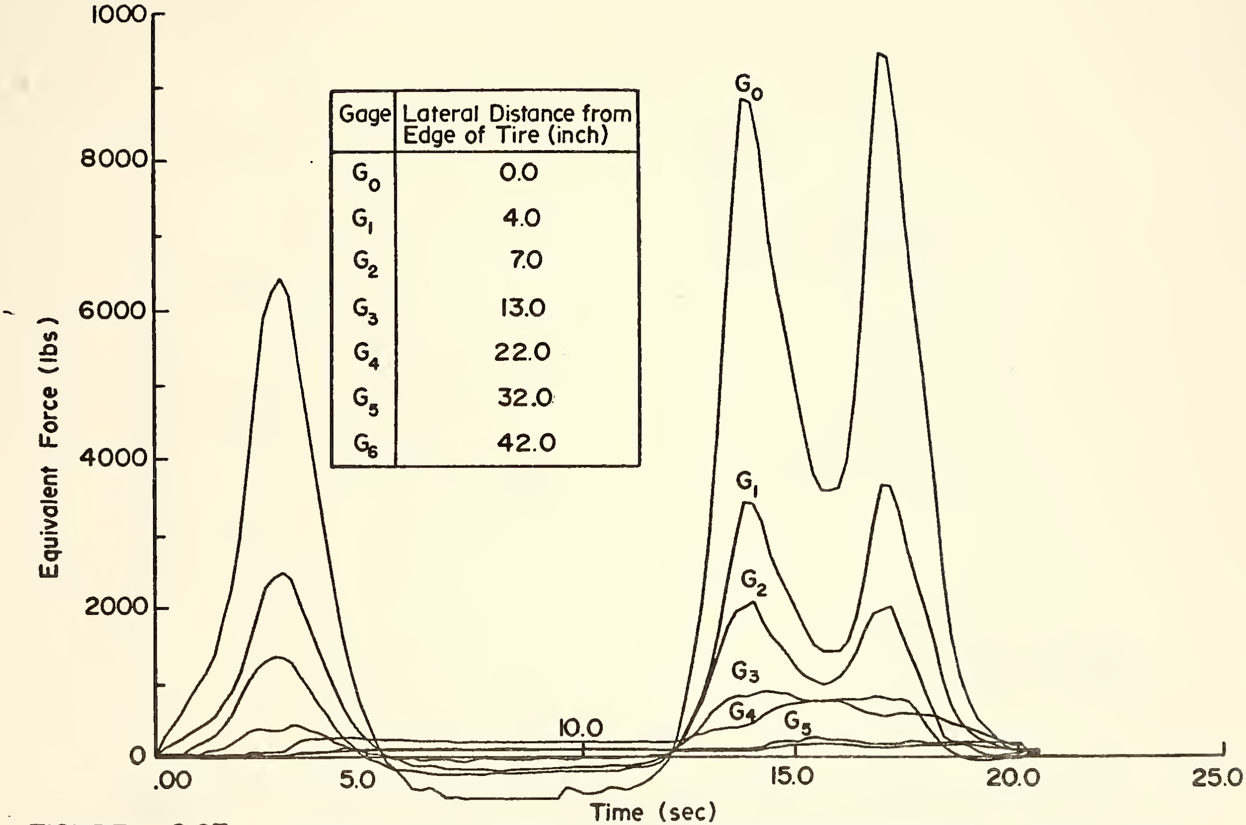

FIGURE 6.23 CALCULATED EQUIVALENT FORCING FUNCTIONS Vs. TIME. SITE 7, STANDARD HIGHWAY TRUCK.

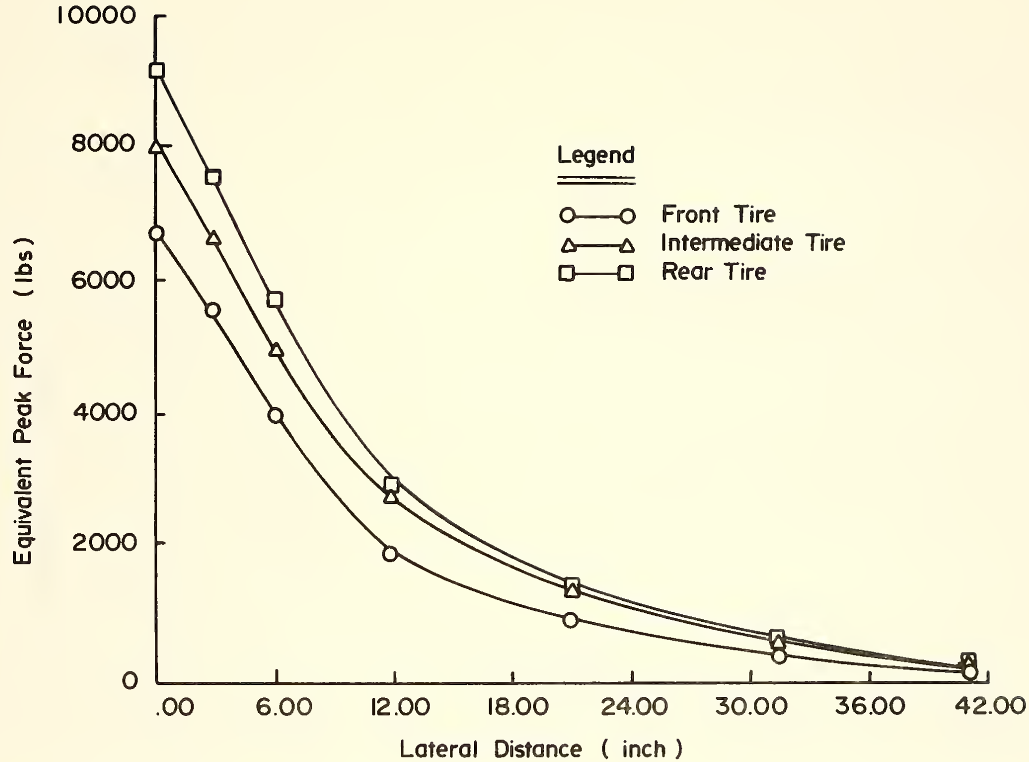

FIGURE 6.24 EQUIVALENT (CALCULATED) PEAK FORCES Vs. LATERAL DISTANCES. SITE I, STANDARD HIGHWAY TRUCK.

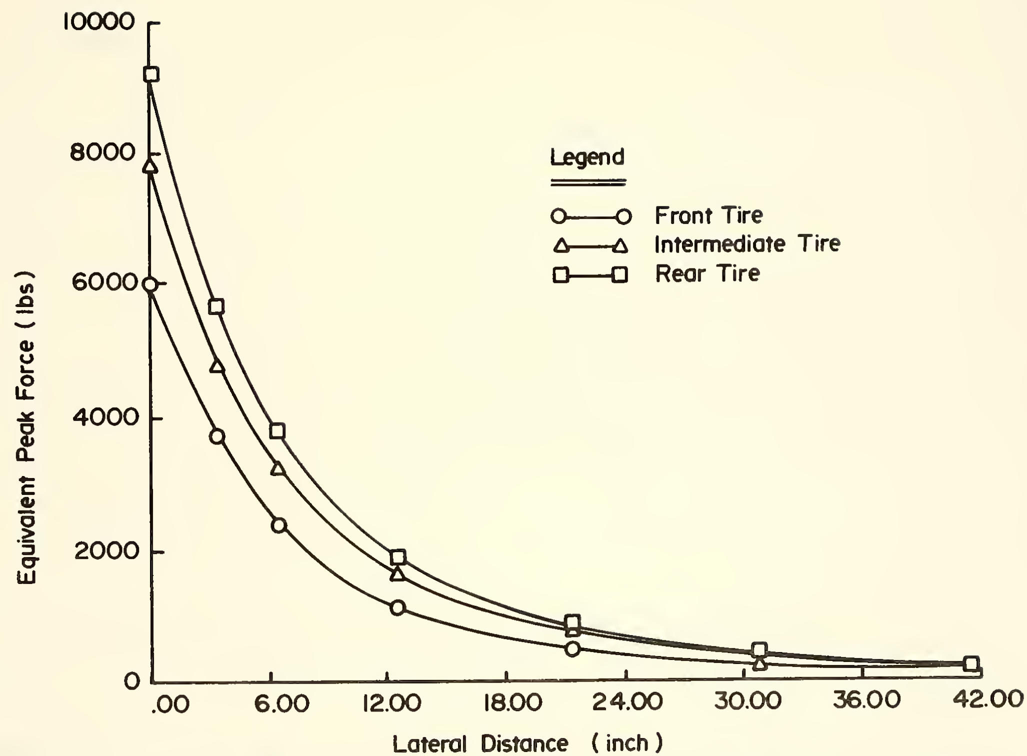

FIGURE 6.25 EQUIVALENT (CALCULATED) PEAK FORCES Vs. LATERAL DISTANCES. SITE 2 , STANDARD HIGHWAY TRUCK.

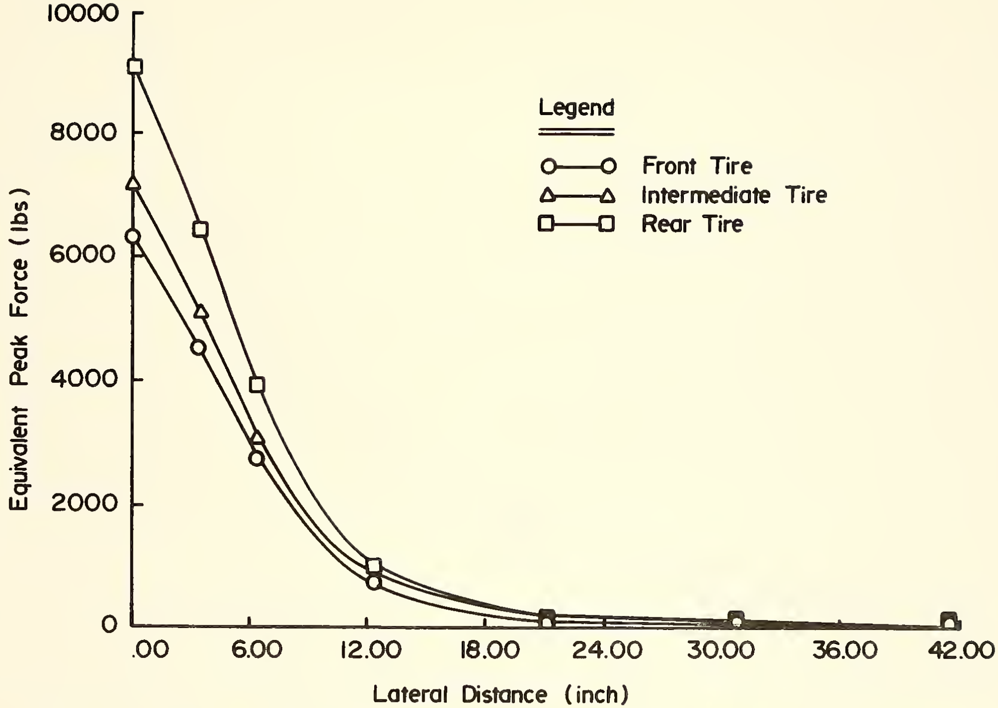

FIGURE 6.26 EQUIVALENT (CALCULATED) PEAK FORCES Vs. LATERAL DISTANCES. SITE 3, STANDARD HIGHWAY TRUCK.

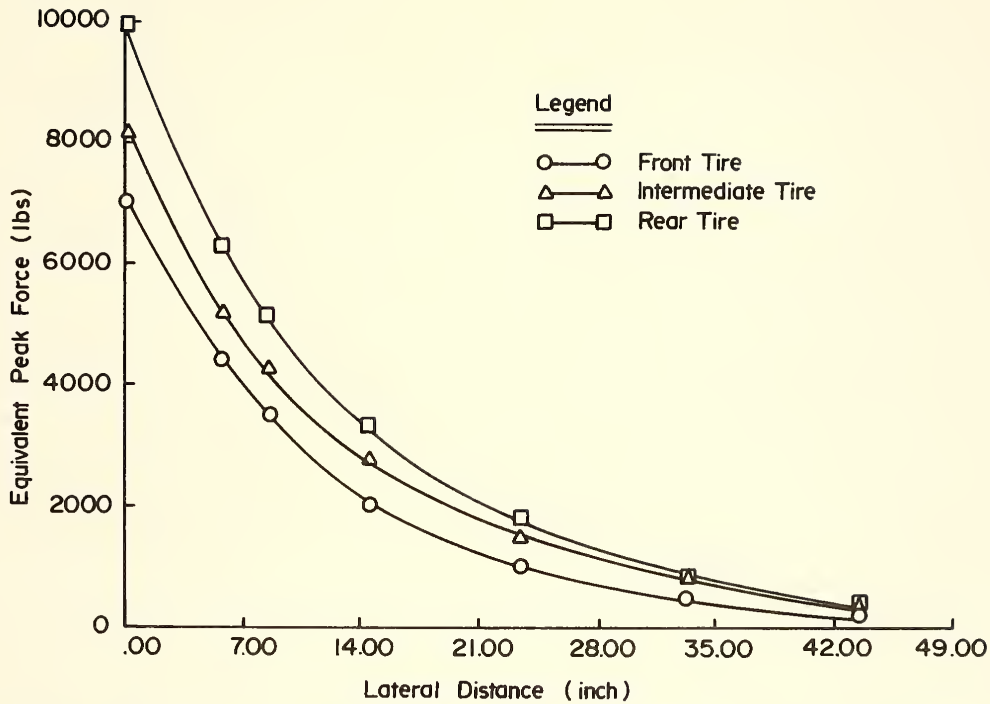

FIGURE 6.27 EQUIVALENT (CALCULATED) PEAK FORCES Vs. LATERAL DISTANCES. SITE 4, STANDARD HIGHWAY TRUCK.

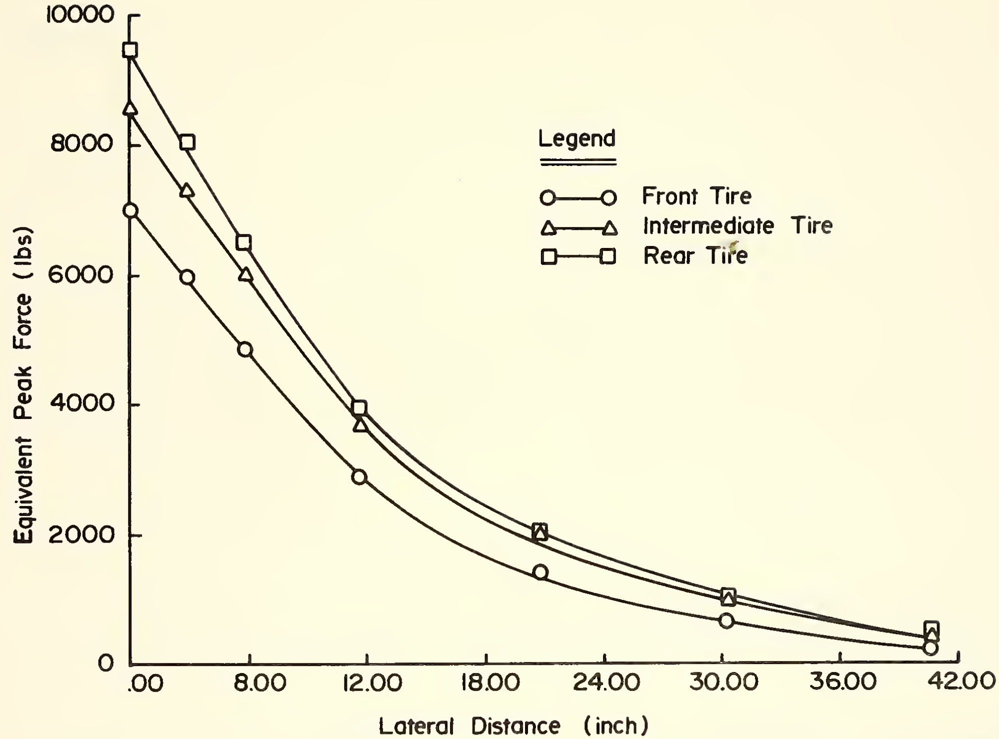

FIGURE 6.28 EQUIVALENT (CALCULATED) PEAK FORCES Vs. LATERAL DISTANCES. SITE 5, STANDARD HIGHWAY TRUCK.

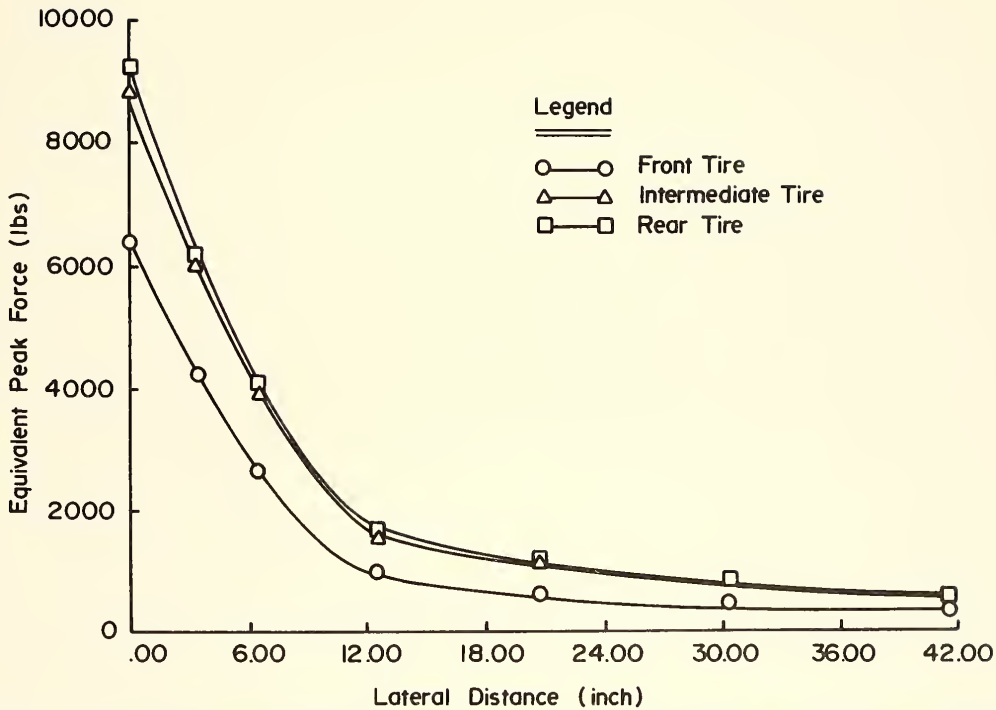

FIGURE 6.29 EQUIVALENT (CALCULATED) PEAK FORCES Vs. LATERAL DISTANCES. SITE 6, STANDARD HIGHWAY TRUCK.

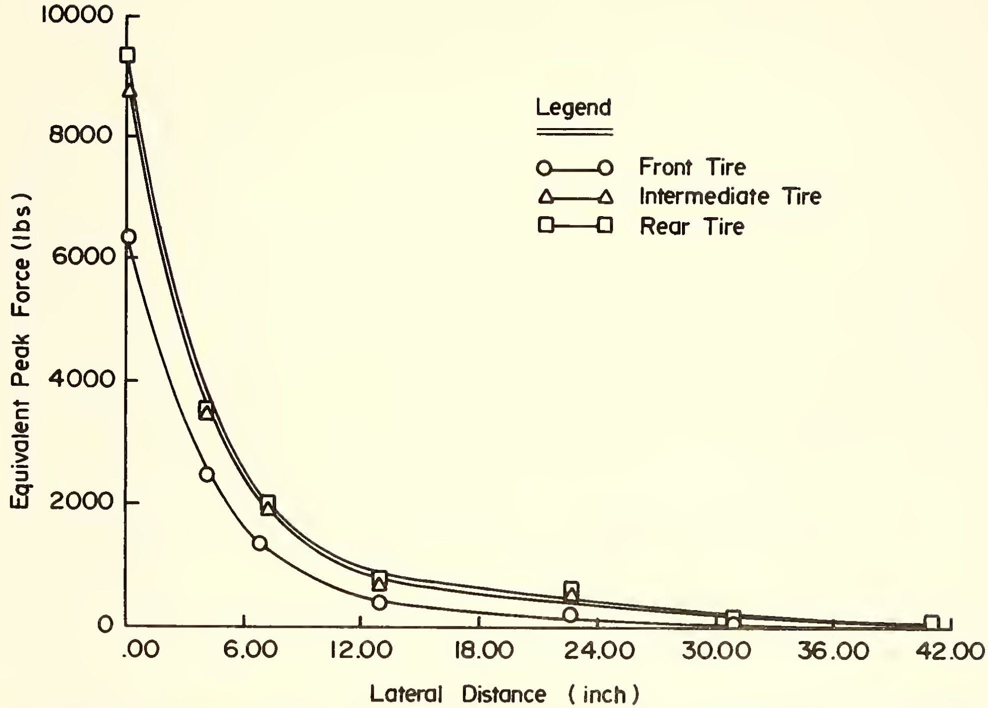

FIGURE 6.30 EQUIVALENT (CALCULATED) PEAK FORCES Vs. LATERAL DISTANCES. SITE 7, STANDARD HIGHWAY TRUCK.

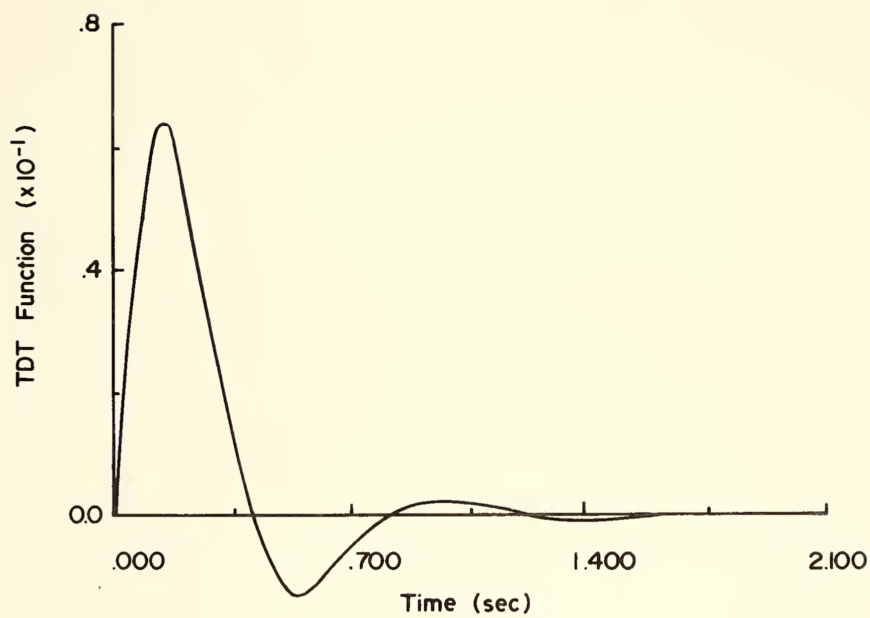

FIGURE 6.31 TYPICAL TIME DEPENDENT TRANSFER FUNCTION Vs. TIME. SITE I, STANDARD HIGHWAY TRUCK.

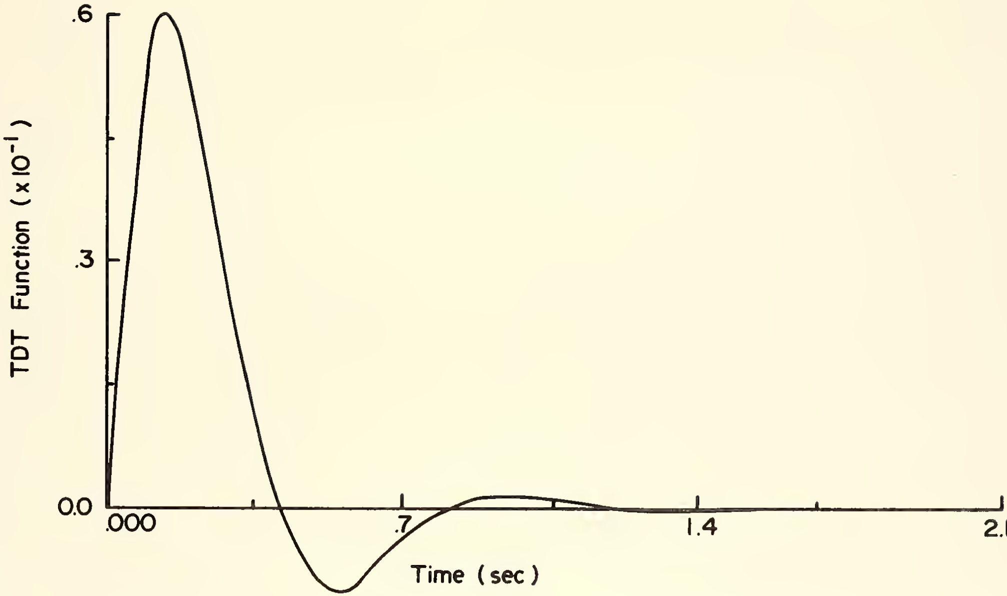

FIGURE 6.32 TYPICAL TIME DEPENDENT TRANSFER FUNCTION Vs. TIME. SITE 2, STANDARD HIGHWAY TRUCK.

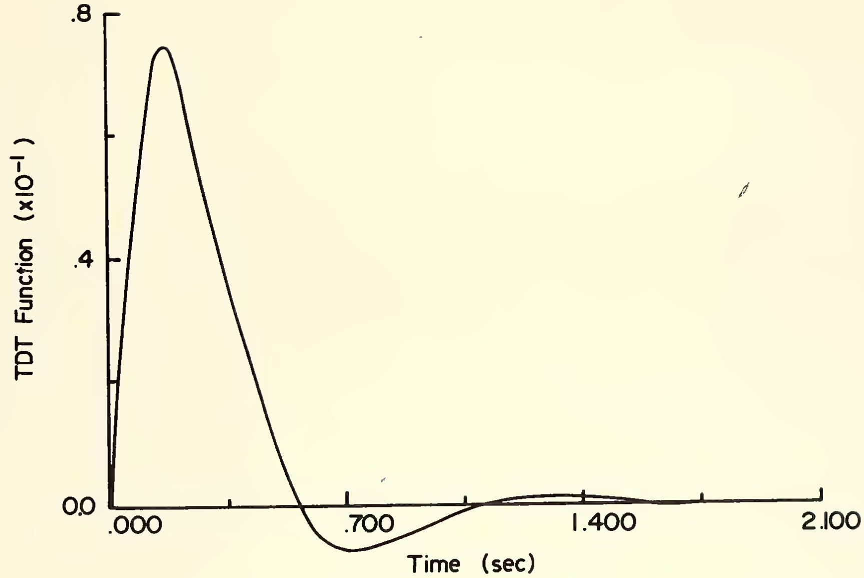

FIGURE 6.33 TYPICAL TIME DEPENDENT TRANSFER FUNCTION Vs. TIME. SITE 3, STANDARD HIGHWAY TRUCK.

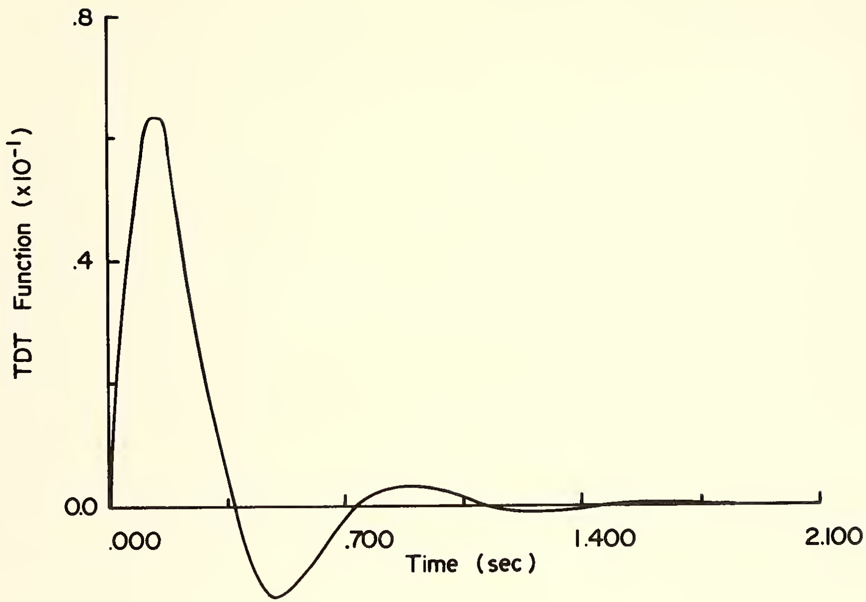

FIGURE 6.34 TYPICAL TIME DEPENDENT TRANSFER FUNCTION Vs. TIME.
SITE 4, STANDARD HIGHWAY TRUCK.

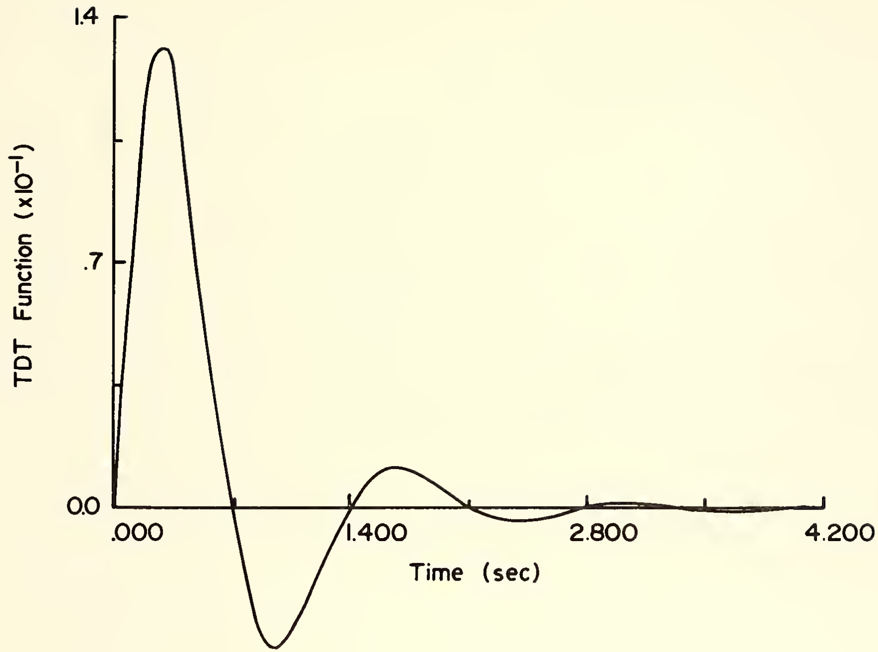

FIGURE 6.35 TYPICAL TIME DEPENDENT TRANSFER FUNCTION Vs. TIME. SITE 5, STANDARD HIGHWAY TRUCK.

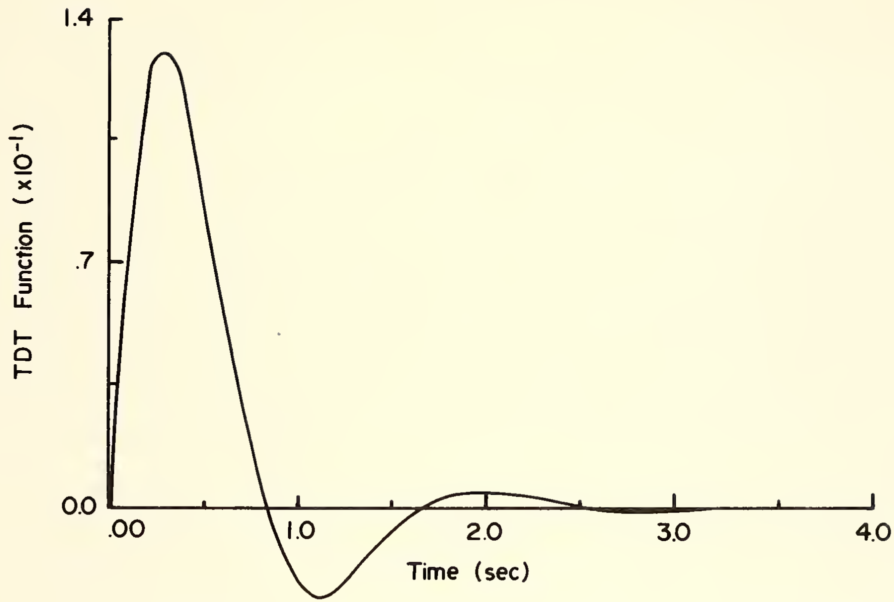

FIGURE 6.36 TYPICAL TIME DEPENDENT TRANSFER FUNCTION Vs. TIME. SITE 6, STANDARD HIGHWAY TRUCK.

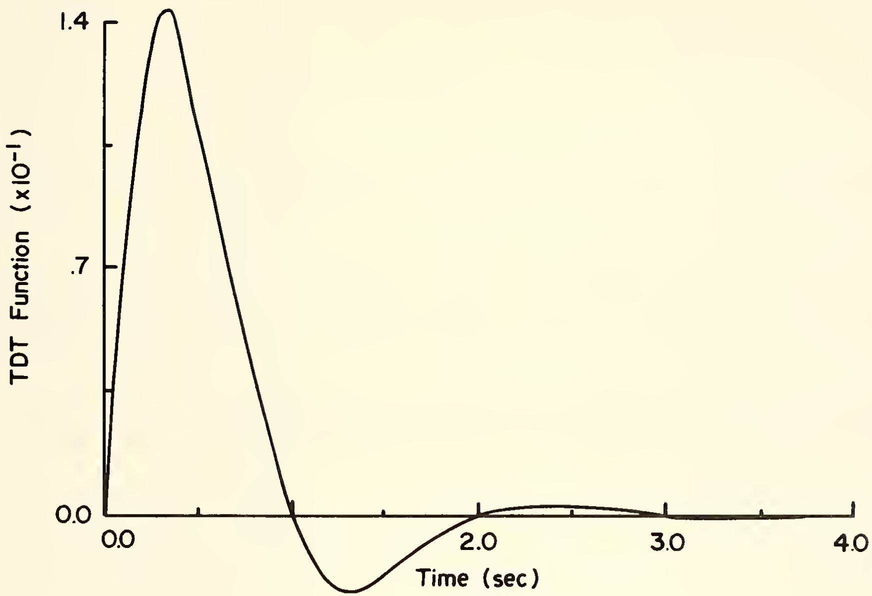

FIGURE 6.37 TYPICAL TIME DEPENDENT TRANSFER FUNCTION Vs. TIME.
SITE 7, STANDARD HIGHWAY TRUCK.

TABLE 6.3 PEAK VALUES OF TDT FUNCTIONS, TIME TO PEAK AND TIME TO FIRST ZERO FOR SITES 1-7.

SITE	AIR TEMPERATURE (°F)	DATE	MAGNITUDE OF FIRST PEAK	TIME TO FIRST PEAK (sec)	TIME TO FIRST ZERO (sec)
1	75	8-26-75	.064	.142	.430
	75		.064	.141	.422
	22	3-17-76	.065	.143	.436
	22		.064	.145	.452
	64	5-13-76	.064	.141	.425
	64		.063	.141	.428
	78	7-30-76	.064	.139	.402
	78		.064	.141	.417
	80	9-13-76	.064	.141	.420
	80		.064*	.141	.420
2	82	8-25-75	.061	.138	.433
	82		.061	.138	.432
	22	3-17-76	.065	.162	.721
	22		.065	.161	.728
	68	5-13-76	.061	.138	.431
	68		.061	.138	.431
	80	7-30-76	.061	.136	.418
	80		.061	.136	.416
3	75	8-26-75	.062	.132	.374
	75		.063	.137	.398
	24	3-17-76	.152	.357	1.245
	24		.152	.357	1.245
	68	5-13-76	.066	.146	.435
	68		.067	.147	.437
	80	7-30-76	.063	.135	.378
	80		.064	.135	.378
4	82	8-26-75	.066	.138	.370
	82		.066	.138	.370
	68	5-13-76	.064	.133	.361
	68		.066	.137	.369
	80	7-30-76	.063	.133	.365
	80		.063	.133	.364
5	80	8-12-76	.144	.314	.906
6	80	8-12-76	.130	.284	.993
7	80	8-12-76	.143	.321	.830

* The loading vehicle was an automobile (Ford).

b) time from zero to the peak value .

c) time from zero th the first zero value of the TDT function .

The values of the m, c, k parameters used in the calculation of the TDT functions are listed in Table (6.4).

TABLE 6.4 EQUIVALENT MASS (m), EQUIVALENT DASHPOT CONSTANT (c) AND EQUIVALENT SPRING CONSTANT (k), FOR SITES 1-7

SITE	AIR TEMPERATURE (^{o}F)	DATE	m $\frac{lb\text{-}sec^2}{in}$	c $\frac{lb\text{-}sec}{in}$	k $\frac{lb}{in}$
1	75	8-26-75	14737	126768	1057555
	75		14011	120523	1036256
	22	3-17-76	16811	146677	1191238
	22		17837	156771	1205615
	64	5-13-76	14211	122100	1040020
	64		14411	125212	1049215
	78	7-30-76	14008	116203	1096398
	78		14587	121616	1081680
	80	9-13-76	14287•	120921	1056121
	80		14287*	120921*	1056121*
2	82	8-25-75	5779	53400	427321
	82		6726	61860	498594
	22	3-17-76	12744	130815	577461
	22		13149	136041	596908
	68	5-13-76	6392	58944	475394
	68		6344	58577	471831
	80	7-30-76	6629	60994	514653
	80		6412	58321	497851
3	75	8-26-75	2108	17553	184913
	75		2835	23665	226159
	24	3-17-76	62579	249574	647449
	24		62508	249294	646721
	68	5-13-76	4258	34922	293205
	68		3960	32121	270032
	80	7-30-76	2295	18263	194587
	80		2287	18163	194001
4	82	8-26-75	2075	15024	176436
	82		2075	15011	176438
	68	5-13-76	2043	15413	184164
	68		2669	19245	228302
	80	7-30-76	2068	16163	184582
	80		2060	16153	185482
5	80	8-12-76	29681	107914	455321
6	80	8-12-76	44764	182826	828039
7	80	8-12-76	24027	94407	333023

* The loading vehicle was an automobile (Ford).
• Standard highway truck(empty).

CHAPTER 7

DISCUSSION

It was hypothesized herein that there exists a relationship between a pavement's deflection response function (output) and a vehicular loading (input) in the form of a time dependent transfer (TDT) function. The characteristics of the TDT function can be used as follows:

a) as indicators of the performance and condition of a pavement system.

b) to indicate the effects of ambient conditions.

c) to obtain the shape of the peak deflection curves consequent to the passage of a wide range of vehicles.

d) to assess the lateral attenuation of energy following the passage of a vehicle.

e) to predict the time response of a pavement system.

The procedures for obtaining TDT function were previously outlined in Chapter 5. Analyses of the data included:

1. Modeling the peak deflections as a function of lateral distance to calculate the signature (pavement's deflection, with time, under the edge of a tire).
2. Calculating the vertical velocity and acceleration at various points on the surface of a loaded pavement.
3. Calculating the TDT function.
4. Calculating equivalent forces at various lateral distances from the edge of a tire.
5. Predicting a pavement's deflection response for a range of loading vehicles.

Items 1 and 2 are required to calculate the TDT function. Items 3, 4 and

5 are necessary to investigate the validity of the working hypothesis.

I) Signature

Deflection data collected at the test sites were considered good and sufficient only when the paths of loading vehicles were such that the intermediate and rear tires passed within eight inches, laterally, from the front of the LVDT beam. All passes at greater lateral distances were disregarded (and were not digitized).

The overhang of the LVDT beam and the bulge of the side of the tire prevented the loading wheel from coming closer than three inches from the front of the beam. The signature was obtained using equation (4.1) and the measured deflections from the LVDT beam.

The LVDT beam was placed at the side of the embedded LVDT gages at site 1 (gravel pit road). The loading vehicle was then driven, so that the intermediate and rear tires passed over one of the embedded gages. Pavement deflections were recorded under the tire and at the various gage positions on the LVDT beam. The signature was calculated using equation (4.1).

The region between the straight lines in Figure (7.1) designates the locus of the pairs of calculated and measured signatures for various lateral positions of loading vehicles. The solid line represents the correspondence between the measured and calculated signatures within the accuracy of the measurements (0.0001 inch). This last condition was found to hold for all tests when the intermediate and rear tires of the loading vehicle passed within eight inches (8") from the front of the LVDT beam.

Discrepancies between calculated and measured values were noted for vehicular paths at greater lateral distances than eight inches (8"). For

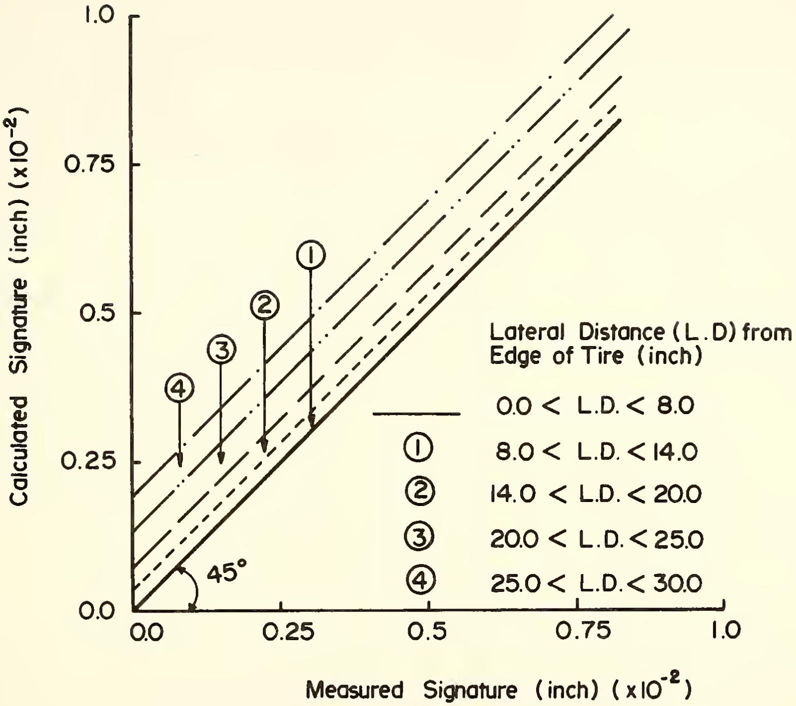

FIGURE 7.1 CALCULATED Vs. MEASURED SIGNATURES. SITE 1.

this reason, deflection data collected at the test sites were not used when the intermediate and/or rear tires of loading vehicles passed at a lateral distance greater than eight inches from the front of the LVDT beam. Care was taken throughout the testing period to direct the loading vehicle as close to the front of the LVDT beam as the bulge of the side of tires permitted.

II) N and B Parameters of Equation (4.1)

In general, throughout this research study, four passes of the test vehicle were made, during each testing period at each of the test sites. On the average, one of these paths was more than eight inches laterally from the front of the LVDT beam which did not satisfy the criterion of calculating the signature (see section I above). Hence, from the other three paths, the two closest to the beam were chosen for analysis.

The field testing phase of this study lasted about one and a half years. Therefore, analysis and/or discussion of test results reported herein are for the range of data collected during this period.

Values of N and B parameters, the considered test sites, and the air temperature recorded during the test, are listed in Tables (6.1) and (6.2).

Figure (7.2) shows plots of the values of N parameter (to an arithmetic scale) against the corresponding values of B (to logarithmic scale), for sites 1, 2, 3 and 4. Examination of the figure suggests that N and B may be related functionally as

$$N = C_1 + C_2 \log B \qquad (7.1)$$

where C_1, C_2 are constants depending on the characteristics of the pavement section at each site. Analyses of the data have indicated the constants to be independent of temperature, number of load repetitions

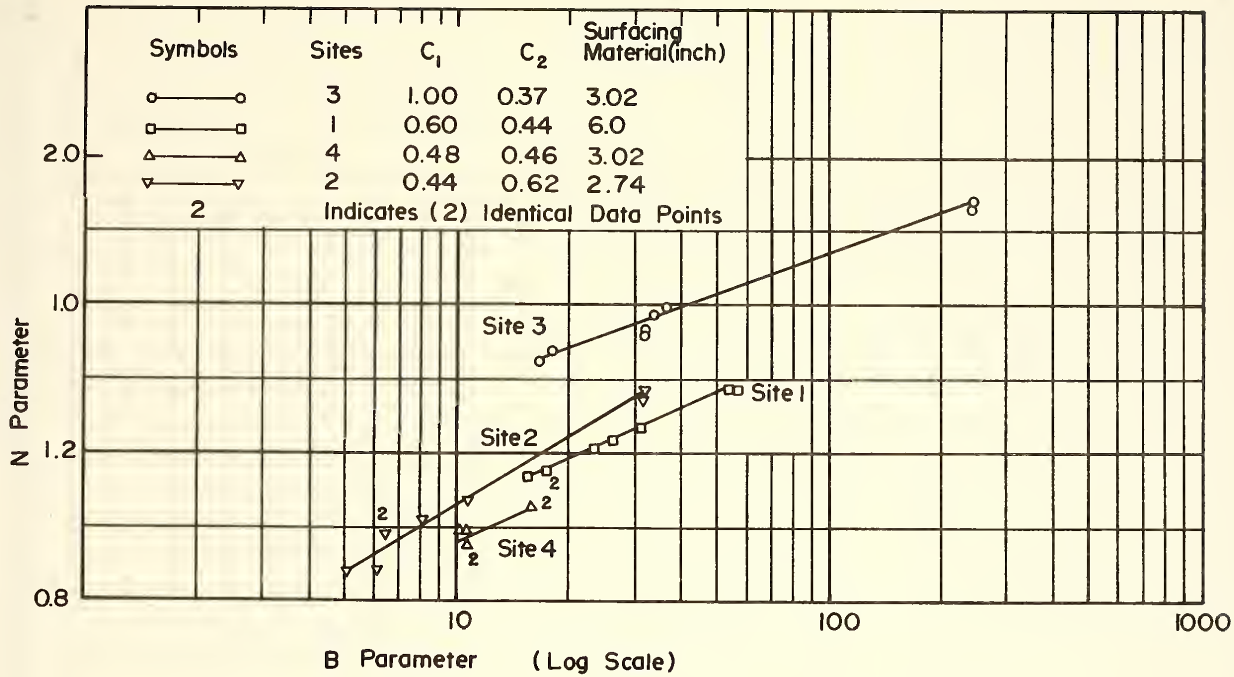

FIGURE 7.2 N Vs. LOG B .

and loading vehicle. Corresponding values of the constants were calculated for each of the four sites and are listed in the figure.

The N and B parameters of equation (4.1) may be thought of as descriptors of the distribution of deflections from the edge of a loading tire. For example, if N is equal to two, equation (4.1) resembles the normal (gaussian) distribution with B being proportional to the variance. Thus, as might be expected, changes in values of N and B for a pavement section reflect the distribution of deflections and structural characteristics of that section.

Figure (7.3) represents four typical normalized* peak deflection curves as a function of lateral distance for sites 1, 2, 3 and 4. The corresponding values of N and B parameters and the values of ($\sqrt[N]{B}$) are indicated in the figure. It can be seen that the higher the value of ($\sqrt[N]{B}$), the farther the lateral spread of the deflection. Again, the analogy to the normal distribution should be noted for N equal to two. For this state, ($\sqrt{B}$) is seen to be proportional to the standard deviation, the well-known measure of the scatter of data about its mean. Most tests were conducted with the same loading vehicle at creep speed, and hence the input energy was fairly constant, the amount of the lateral spread may be thought of as a measure of the lateral attenuation of energy in the pavement. These observations gave rise to the use of the N and B parameters as indicators of a pavement's performance.

Figure (7.4) shows plots of the B parameter as a function of the number of load repetitions (see Table 4.5) for sites 1, 2, 3 and 4. The solid symbols in the figure designate conditions at a temperature of twenty two degrees Fahrenheit (22°F). Open symbols indicate the

* Normalized with respect to the deflection value under the edge of loading tire, the maximum deflection.

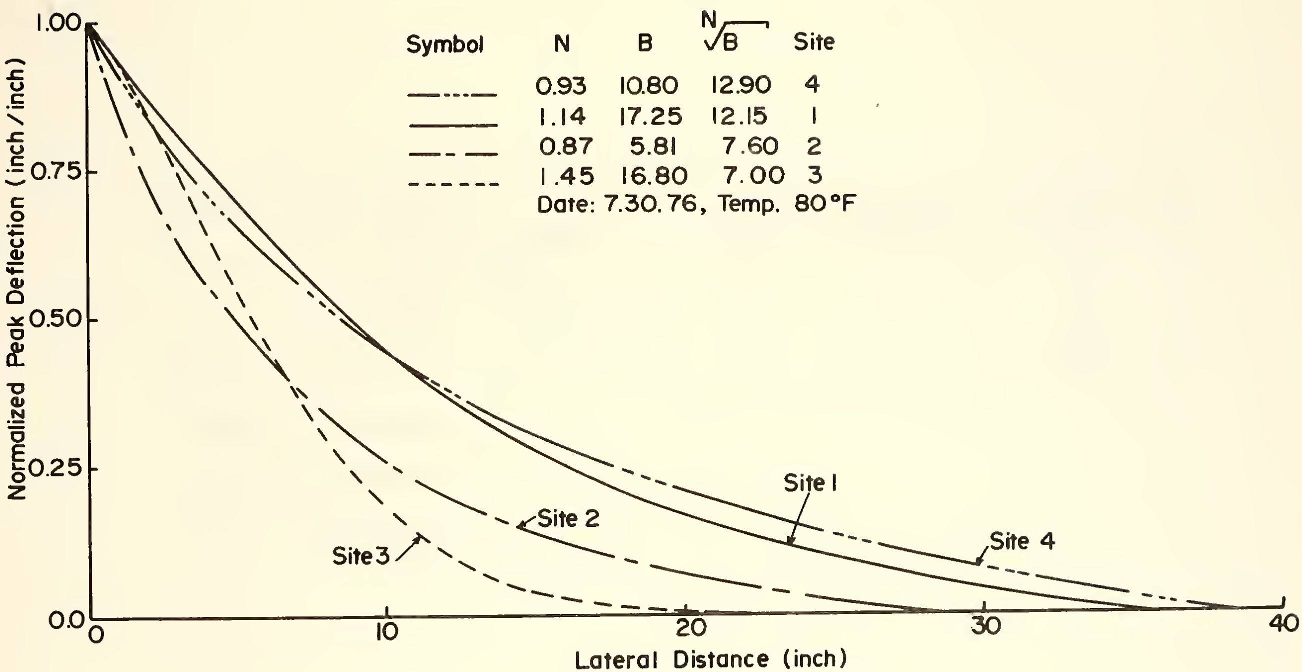

FIGURE 7.3 NORMALIZED PEAK DEFLECTIONS Vs. LATERAL DISTANCE.

Symbol	Site	Slope $\times 10^{-5}$	Y Intercept	R^2(%)	Percentage of Total Traffic (%)		
					Truck	Pick up	Automobile
○	1	-7.4	32.51	94.6	90	0	10
△	3	-5.4	37.45	80.4	10	20	70
□	4	-3.2	15.93	95.8	5	15	80
▽	2	-1.5	9.51	89.6	5	0	95

● ▲ ▼ Temperature 22° F

○ △ ▽ Temperature 64 - 80° F

(15.4) = Equivalent Load Repetitions (Year)

2 = (2) Identical Data Points

(Part of Figure 7.4)

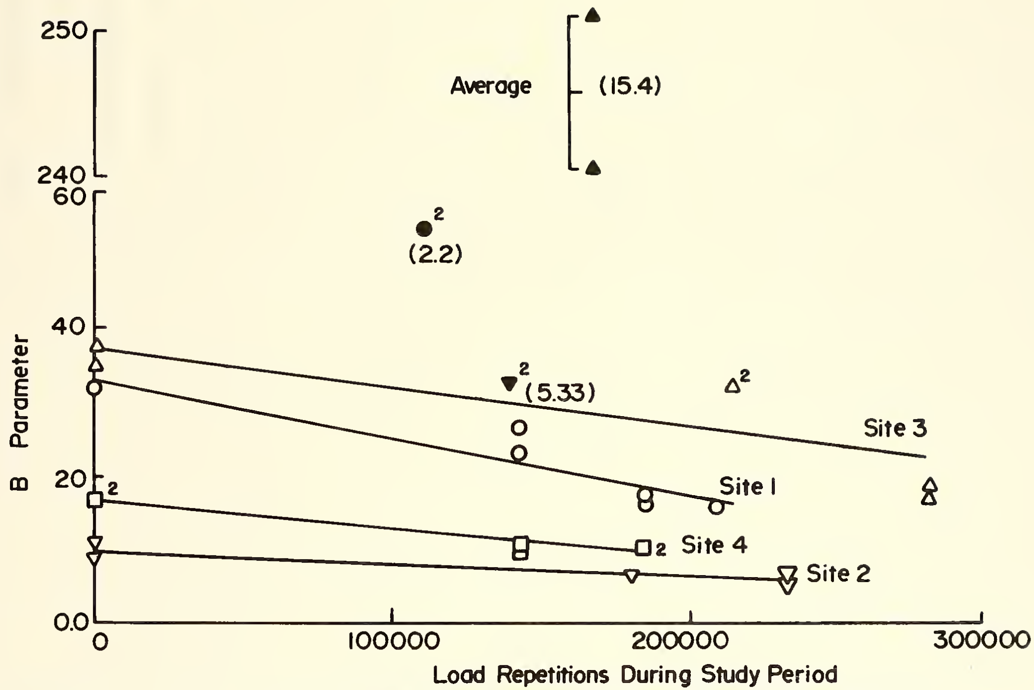

FIGURE 7.4 THE B PARAMETER Vs. LOAD REPETITIONS.

temperature range of sixty four to eighty degrees Fahrenheit. The straight lines between the data points were obtained from a least squares analysis. The coefficients of correlation, (R^2), the y-intercepts and the slope of the lines are indicated in the figure (page 100). The number of trucks, pickup(s) and automobiles traveling over each of the road sites is also listed in the figure as a percentage of the total traffic at the site. Examination of Figure (7.4) indicates that in all cases, the B parameter decreases with increasing load repetitions during the period of study. In addition, the steeper the slope of the line, the higher the percentage of trucks traveling the site. For example, in the case of site 1, the gravel pit road, which displays the steepest slope for the B parameter, ninety percent of the vehicles were trucks. Whereas at site 2, which gave the flattest slope, there were only five percent trucks. The percentages for the two intermediate sites were as listed in the figure. Recalling that the B parameter reflects the lateral spreading of the peak deflection basin, it follows that the steeper the slope the more rapidly will the peak deflection be channelized. Consequently, more work will be done to the pavement in the near vicinity of the wheel.

Plots of the N parameter with load repetitions are shown in Figure (7.5). It can be noticed that the N parameter also decreases with increasing load repetitions. However, the slope of the lines, obtained from a least squares analysis, show much less variations than did those for the B parameter.

Figure (7.6) shows a schematic representation of the typical deflection basin with corresponding relative values of the N and B parameters

Symbol	Site	Slope $\times 10^{-7}$	y Intercept	R^2(%)
○	1	-5.8	1.27	90.6
▽	2	-6.0	1.05	83.5
△	3	-3.9	1.59	92.5
□	4	-5.9	1.05	95.4

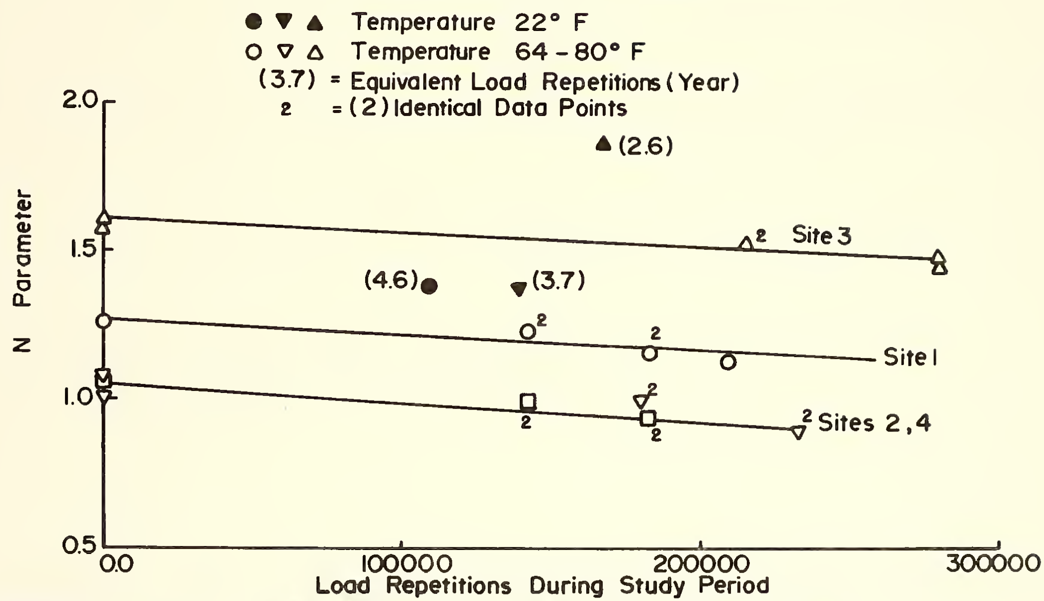

FIGURE 7.5 THE N PARAMETER Vs. LOAD REPETITIONS.

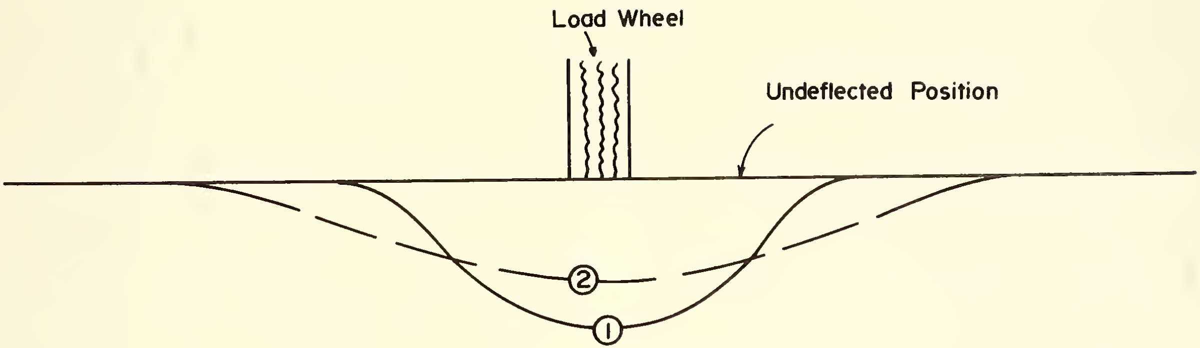

1 Smaller N and B , High Load Repetitions

2 Larger N and B , Low Load Repetitions

FIGURE 7.6 SCHEMATIC REPRESENTATION OF THE TYPICAL DEFLECTION BASIN.

at one site. It can be seen that the smaller the value of the parameters the more rapid the lateral attenuation of enery and consequently the deeper it penetrates under the wheel. As noted above, implicit in this is that as N and B decrease, more work is done to the pavement section in the vicinity of the wheel load. Consequently, greater distress might be expected to occur with fewer passes. Visual observations tend to confirm this. Site 2, which showed the smallest values of N and B was the site which exibited the greater distress, even though this section had the least number of trucks as a percentage of vehicles.Unfortunately, it was not possible to determine when the various sites were constructed. However, it is interesting to speculate that the construction might be related inversely with the sequence of the B and N values. For example, site 2 might have preceded site 4 which in turn would precede sites 1 and 3.

The N and B parameters were also determined for two sites on interstate highway 64 in Indiana (see Table 4.2). Site 6 was trafficked six months prior to the testing period. Site 7 had been completed but was not opened to traffic prior to the date of testing. Both sites had the same pavement cross-section. Figure (7.7) shows plots of normalized peak deflections as functions of lateral distance for both sites. The N and B parameters, as well as the peak deflections under the edge of the front, intermediate and rear tires are also listed in the figure. It can be seen that: a) the N and B parameters for the trafficked section (site 6) are higher than those of the closed section (site 7), b) the deflection basin for site 6 is wider than that of site 7, and c) deflections under the edge of tires on site 7 are much higher than those of site 6. Recall that

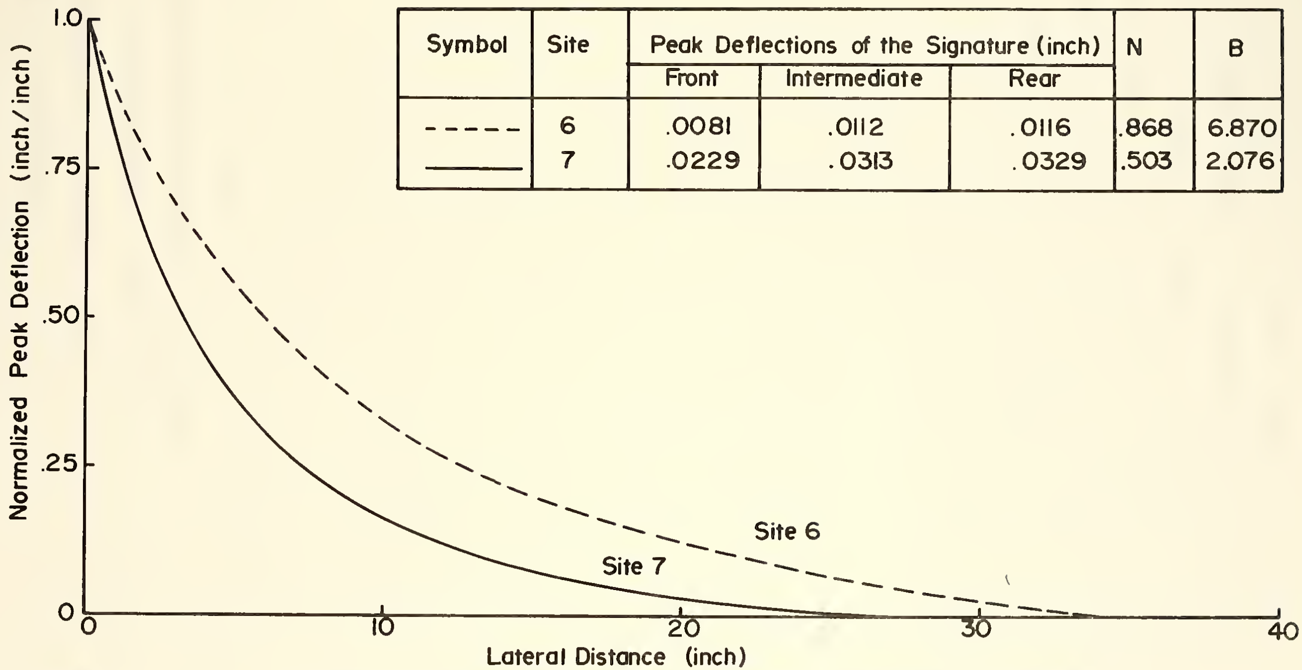

Symbol	Site	Peak Deflections of the Signature (inch)			N	B
		Front	Intermediate	Rear		
- - - - -	6	.0081	.0112	.0116	.868	6.870
———	7	.0229	.0313	.0329	.503	2.076

FIGURE 7.7 NORMALIZED PEAK DEFLECTIONS Vs. LATERAL DISTANCE, INTERSTATE I 64, INDIANA.

the higher the values of the N and B parameters, the lower the peak deflection and the wider the deflection basin. The rather narrow deflection basin of the closed section is a consequence of the pavement not having been subjected previously to a wide lateral distribution of vehicles. Given normal lateral traffic distribution which had occured on the trafficked section, the deflection basin would then be expected to widen as shown in Figure (7.7). This observation indicates the need of monitoring newly constructed pavements more closely (see suggestions for future research).

Further examination of Tables (6.1) and (6.2) indicates that at an air temperature of twenty two degrees Fahrenheit,the values of N and B parameters are larger than those listed at higher temperatures. This is a consequence of the more uniform deflection for the colder pavement. Conditions for a temperature of twenty two degrees Fahrenheit are designated in Figures (7.4) and (7.5) by the solid symbols. The number shown in brackets next to each of these symbols indicates the equivalent number of years of traffic needed to travel over the road site so that the data point will fall back on the straight line representing the site. These numbers were calculated using the noted slopes of the lines and relating observed load repetitions with time.

Some additional aspects and uses of N and B parameters will be presented in the subsequent section entitled "Pavement Evaluation".

III) Time Dependent Transfer (TDT) Function

The characteristics of the time dependent transfer (TDT) function may be thought of as scaling a pavement system's interactive mechanism, which acts to transfer an induced loading (input) to a deflection response (output).

Figures (6.31) through (6.37) presented typical plots of the TDT functions for sites (1-7). Various characteristics of these functions were summarized in Table (6.3); viz. the first peak (maximum), time to first peak, and time to first zero. These may be thought of as the basic descriptors of the TDT functions. The values are seen to be independent of the wheel load (Table 6.1), of the type of loading vehicle, and of the gear configuration.

The response of a pavement section to a loading vehicle is sensitive to changes in temperature (28). This is mirrored in the characteristics of the TDT function. In Table (6.3), the characteristic values of the TDT function were seen to be higher at an air temperature of twenty two degrees Fahrenheit relative to those at higher temperatures.These range from small differences at site 1 (the thickest surface course) to a factor of three for the time to first zero for site 3.

The characteristics values of the TDT functions for sites 5, 6 and 7 (Table 6.3) are higher than those for the other four sites (site 5 was overlaid in 1975, sites 6 and 7 were constructed in 1976, sites 1, 2, 3 and 4 have been in service over five years without major rehabilitation). These three sites are in better conditions than the others. Hence, the possibility exists of using the characteristic values as indicators of performance. The data studied in this work indicates this area to be a fruitful pursuit for further research. Of special importance at the present writing is the noted relationship between these measures and the action of pavement systems.

The TDT functions were also used to examine the lateral attenuation of energy. Figures (6.24) through (6.30) showed typical plots of the distribution of equivalent peak forces as a function of lateral distance. Examination of the figures indicates that energy (as scaled by the equivalent force) follows an exponentially decaying function. The more rapid the attenuation, the more energy is available to do detrimental work in the vicinity of the tire. Some additional discussion of energy attenuation will be presented in the section entitled "Pavement Evaluation".

The characteristics of the TDT function (as stated above) of a pavement section were found to be independent of wheel load, of type of loading vehicle, and of the gear configuration. This implies that if the TDT function of a pavement section is known, then its time response deflection function can be predicted for another loading vehicle. The TDT functions for sites 1, 2, 3 and 4 were obtained and cataloged using a loaded Indiana State Highway truck, which had a gross-weight of about fifty thousand pounds. The forcing functions were also obtained for an automobile and for the same truck when empty at site 1. The gross-weights of the automobile and of the empty standard highway truck were approximately forty-four hundred and twenty-four thousand pounds, respectively. The forcing function for each of these vehicles was then explicitly convoluted with each of the TDT functions for sites 2, 3 and 4; the predicted pavement deflection response functions were obtained. The automobile and the empty standard highway truck were then driven to sites 2, 3 and 4 and deflection measurements were made consequent to the passage of the two vehicles next to the LVDT beam. Figures (7.8) through (7.10) show plots of the predicted and the measured deflections as

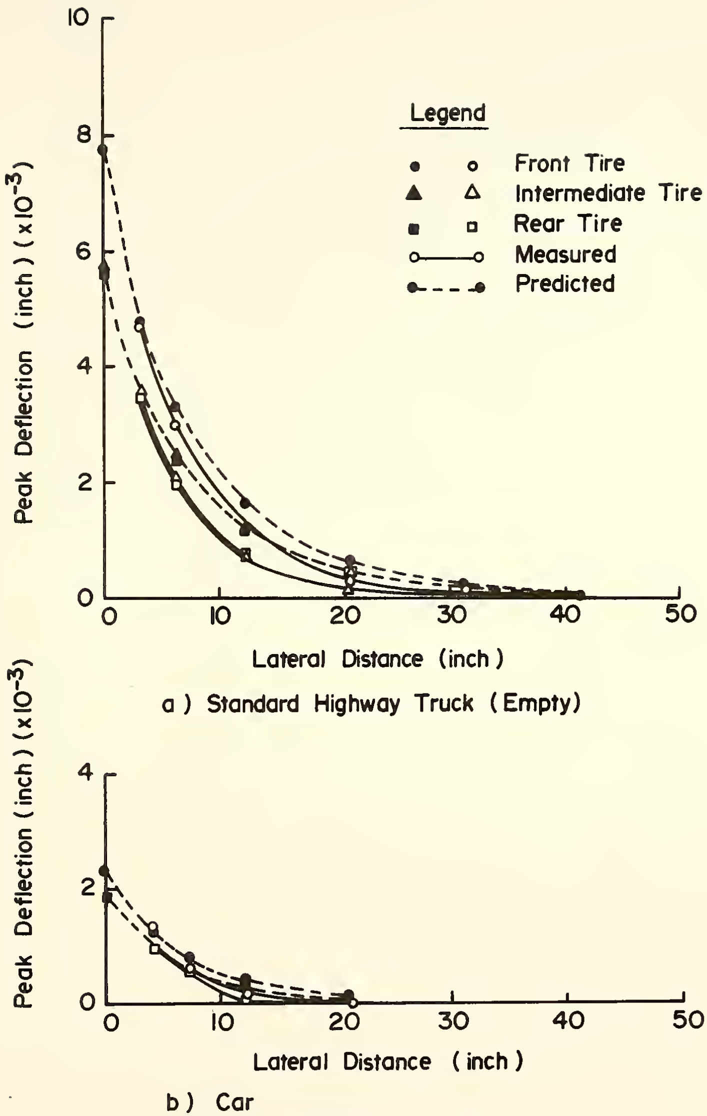

FIGURE 7.8 MEASURED AND PREDICTED PEAK DEFLECTION BASIN. SITE 2

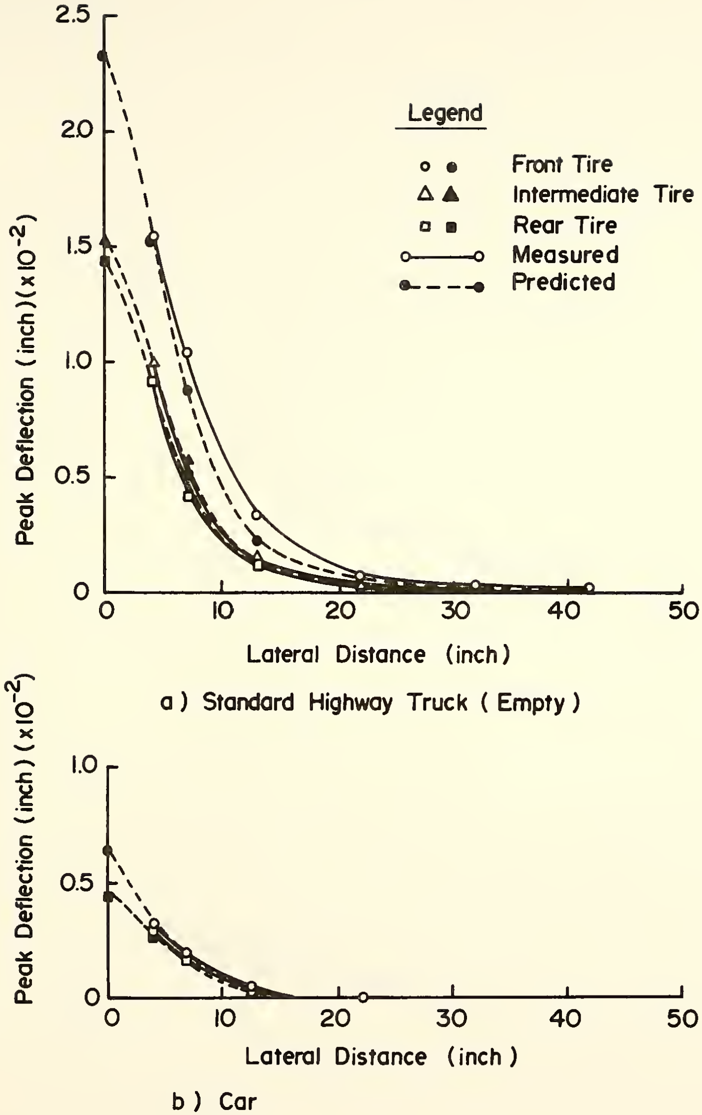

FIGURE 7.9 MEASURED AND PREDICTED PEAK DEFLECTION BASIN. SITE 3

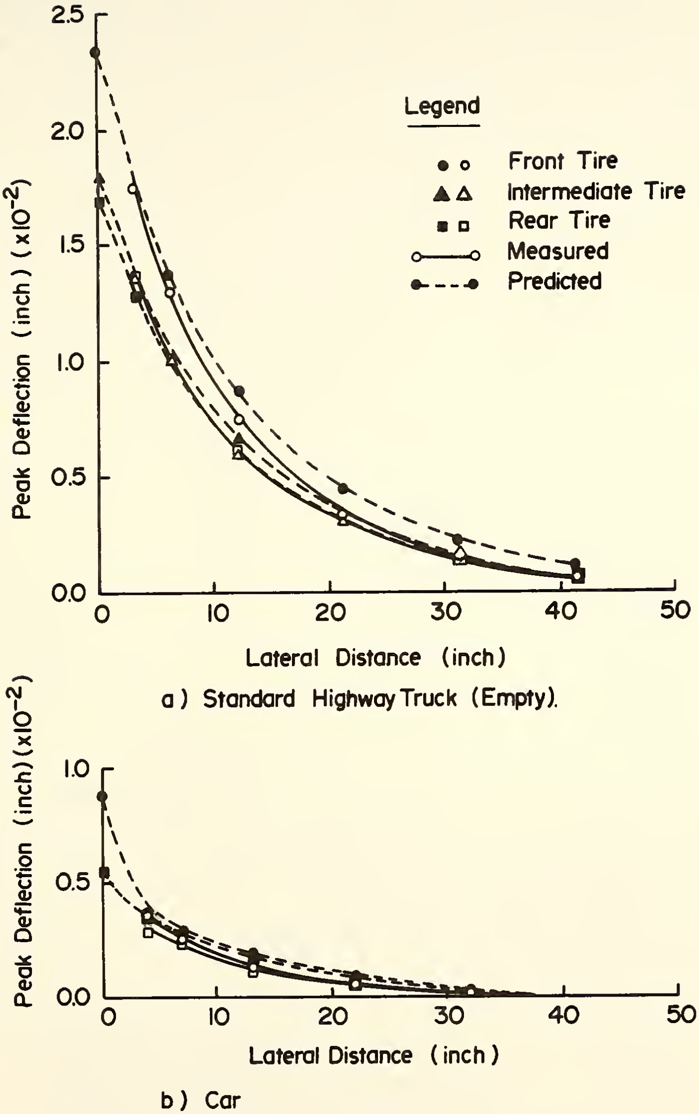

FIGURE 7.10 MEASURED AND PREDICTED PEAK DEFLECTION BASIN. SITE 4

functions of lateral distance. The success of the method is evident. The same order of results had been reported previously by Boyer and Harr (55) and Highter and Harr (56). However, in the present series the correspondence could even be demonstrated for an automobile.

Figure (7.11) shows the time response of measured and predicted deflections for site 2. The time scale on these figures was adjusted so as to provide for the coincidence of the peak values. This was necessary because it was not possible to control the speed of the vehicles so as to be the same at all sites.

The successful prediction of pavement deflection response functions for a wide range of axle loads, gross loads and gear configurations should not be interpreted as <u>unlimited liscense to use transfer function theory</u>. Even though the transfer was made between an automobile and a truck, the induced loadings produced small strains and the material acted in its "elastic" range. This condition is the basic to the use of superposition and of convolution.

IV) <u>Pavement Evaluation</u>

Pavement evaluation consisted herein of two phases: a) subgrade evaluation using the TDT function and its parameters and b) structural evaluation using deflections and the N and B parameters of equation (4.1).

IV.I <u>Subgrade Evaluation</u>

a) <u>Modulus of Subgrade Reaction (k_s)</u>

Table (6.4) provided a list of the equivalent mass (m), equivalent spring (k) and equivalent dashpot (c) of the

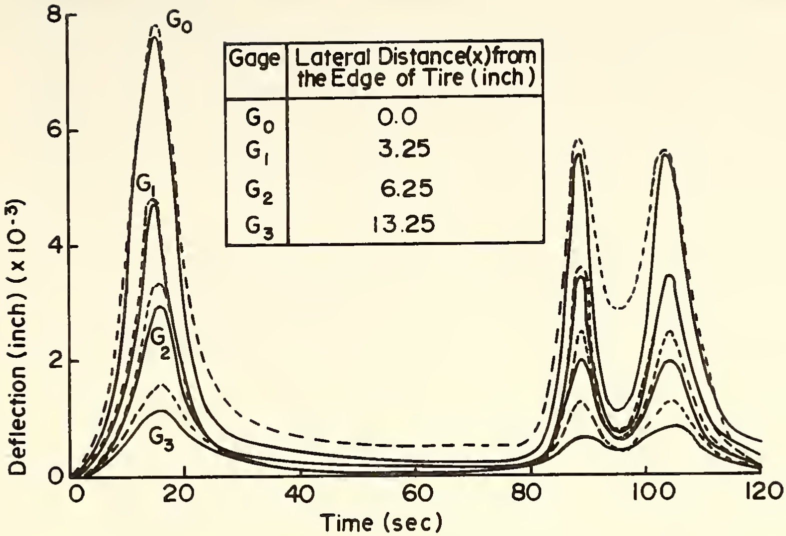

a) Standard Highway Truck (Empty)

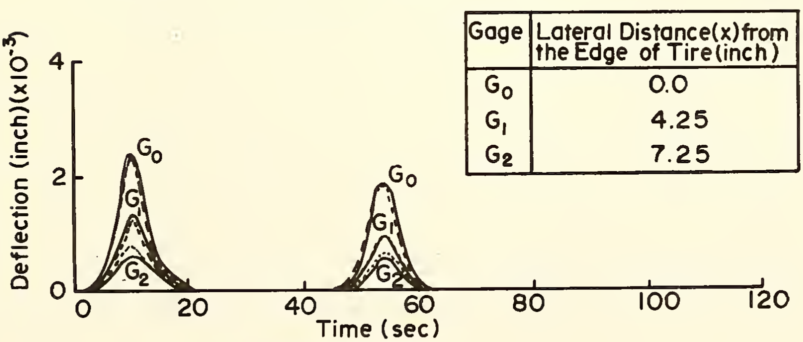

b) Automobile (Ford)

——— Measured

- - - - - - Predicted

FIGURE 7.11 MEASURED AND PREDICTED DEFLECTION Vs. TIME. SITE 2.

Kelvin-mass-spring-dashpot model used in this study. A methodology was developed whereby the modulus of subgrade reaction (k_s) can be estimated from the spring constant (k), the tire pressure (p) and the wheel load (Q). The procedure is as follows:

1) The contact area (a) and its radius (r) are calculated as shown in equations (1) and (2) in Figure (7.12).

2) The equivalent contact area (a_e) at the surface of the subgrade, at depth (T) is obtained using equation (3). It is assumed that the applied load is distributed 1 : β as shown in Figure (7.12). For thin pavements (surface course thickness less than three inches) experience indicates (58) that β can be taken as unity. For thicker surfaces β = 1.5 recommended.

3) The modulus of subgrade reaction (k_s) is defined as the ratio of the reactive pressure under a slab relative to its deflection, under standardized test conditions (see Reference 58). Symbolically, using notation in Figure (7.12) and assuming* $y_p = y_s$, this becomes

$$k_s = \frac{Q}{a_e \, y_p} \tag{7.2}$$

Examination of the results in Tables (6.1), (6.2) and (6.4) show that Q/y_p can be approximated by the Kelvin model's (k) to within about ten percent. For example,

* This assumption is conservative in the sense that $y_p \geq y_s$

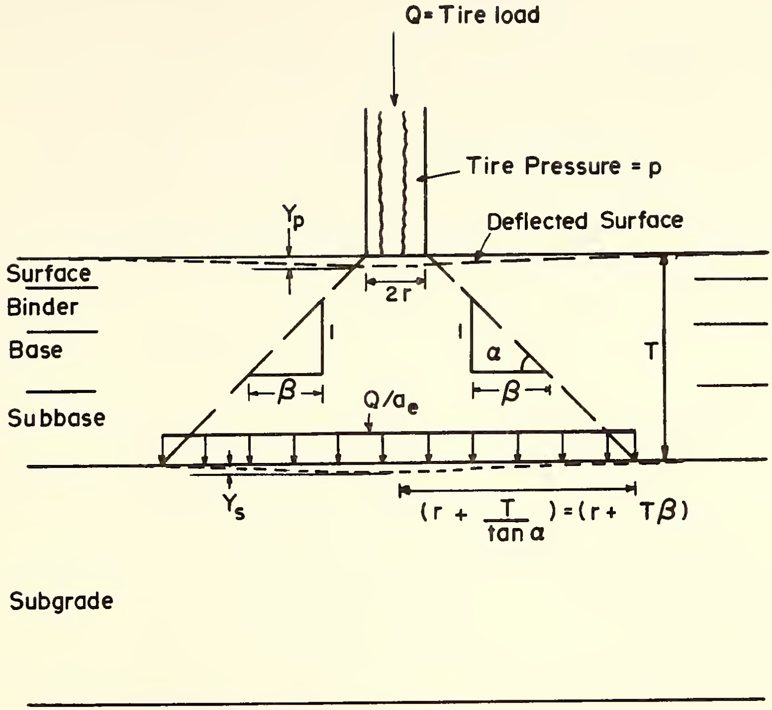

Contact Area = $a = \frac{Q}{p}$ (1)

Radius of Contact Area = $r = \sqrt{\frac{a}{\pi}}$ (2)

Equivalent Contact Area = $a_e = \pi(r + T\beta)^2$ (3)

Modulus of Subgrade Reaction = $k_s = \frac{k}{a_e}$ (4)

"k" in Equation (4) is the Spring Constant of the Kelvin-Model.

FIGURE 7.12 ILLUSTRATION OF THE CALCULATION OF MODULUS OF SUBGRADE REACTION USING THE SPRING CONSTANT (k) OF THE KELVIN-MODEL.

in Table (6.1) for site 1 on 3-17-76,

$$Q = (\frac{1}{3})\ (6276 + 8715 + 9554) = 8182,$$

$$y_p = (\frac{1}{3})\ (0.0050 + 0.0069 + 0.0074) = 0.0064,$$

hence, Q/y_p = 1,272,000 lb/in. From Table (6.4), the spring constant (k) for this case is 1,191,238 lb/in. (A ratio of 1.07). Hence, equation (7.2) may be taken as

$$k_s = \frac{k}{a_e}$$

which is given as equation (4) in Figure (7.12)

b) California Bearing Ratio (CBR_k)

Using the relationship developed by AASHO (54), Figure (7.13), the value of CBR_k can be obtained once the modulus of subgrade reaction is had.

c) Soil Support Value (SSV)

Figure (7.14) shows a plot of SSV as a function of CBR_k as given by AASHO (57). Hence, having the values of the CBR_k from (b) above, SSV is had.

d) Elastic Modulus (E)

Huekelom and Foster (61) have correlated the modulus of elasticity and CBR's using results of a wave propagation test in the linear elastic range. This correlation, Figure (7.15), takes the form,

$$E = 1500\ CBR \qquad (7.3)$$

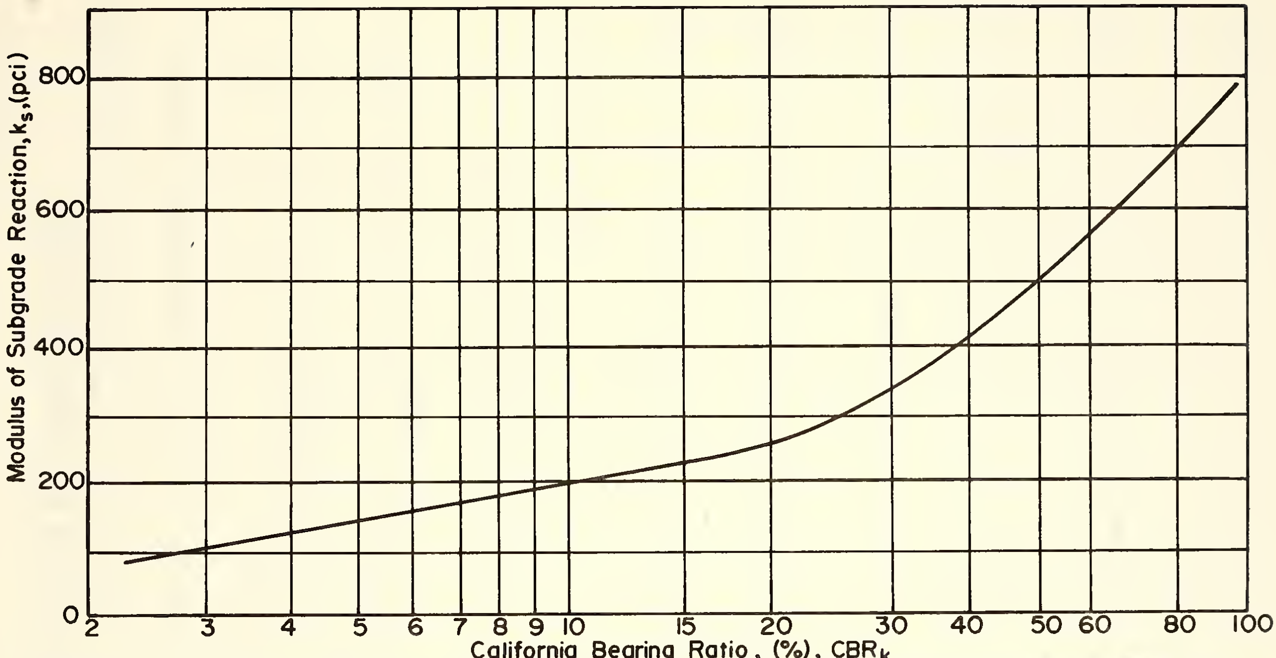

FIGURE 7.13 RELATIONSHIP BETWEEN CALIFORNIA BEARING RATIO AND MODULUS OF SUBGRADE REACTION (54).

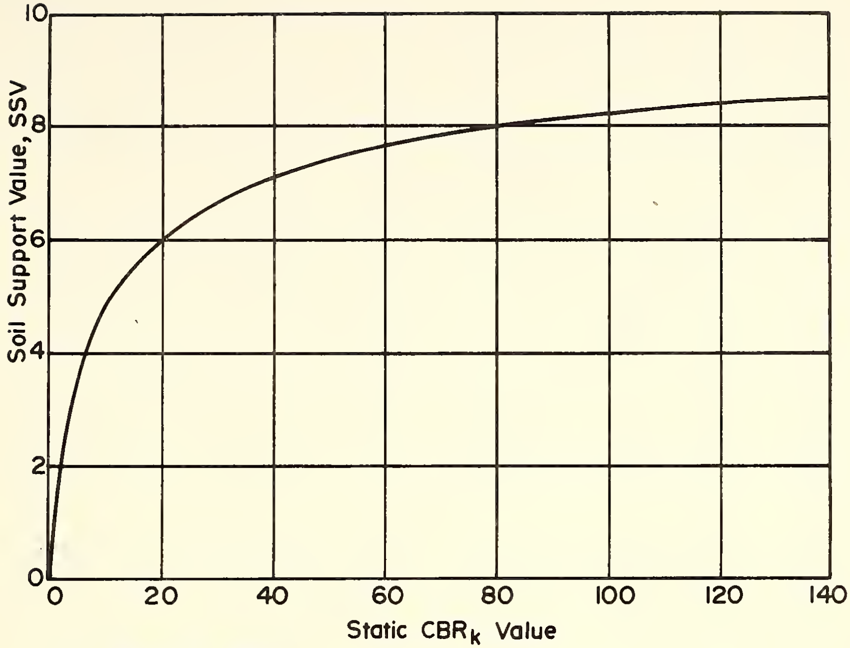

a) SSV Vs. CBR_k

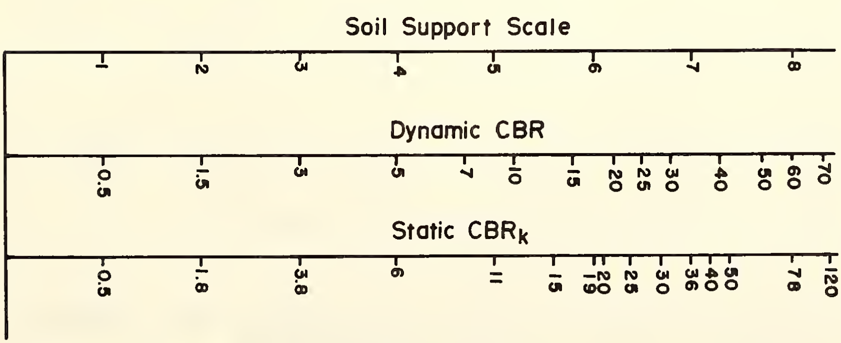

b) Correlation between SSV, Dynamic CBR and Static CBR.

FIGURE 7.14 CORRELATION BETWEEN SOIL SUPPORT VALUE, DYNAMIC AND STATIC CBR_k(57).

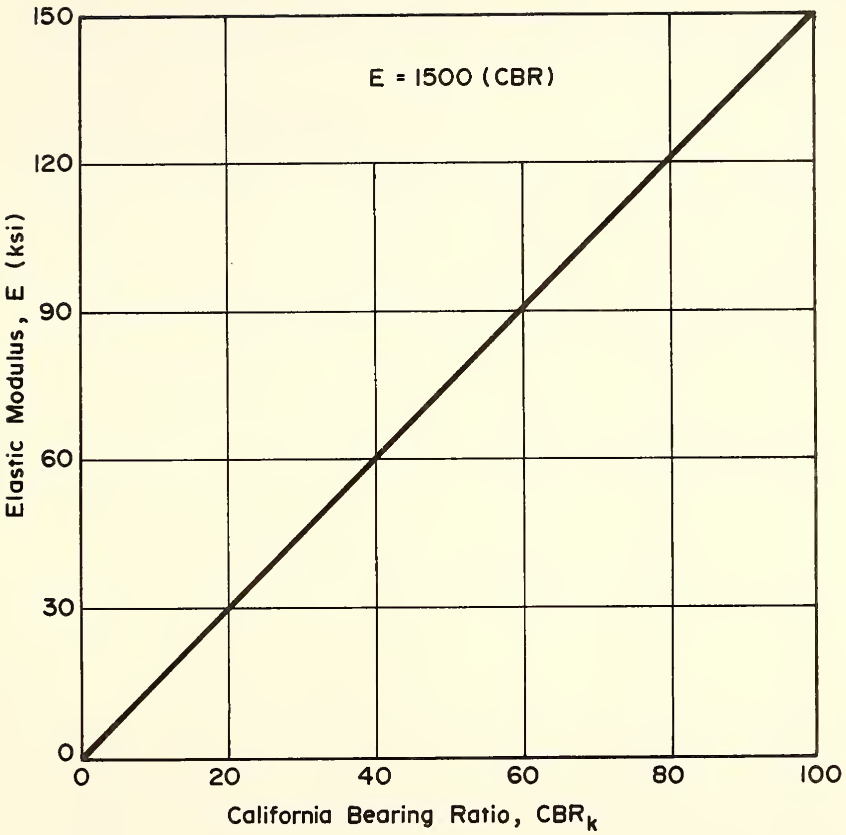

FIGURE 7.15 CORRELATION BETWEEN CALIFORNIA BEARING RATIO AND ELASTIC MODULUS, AFTER (61).

In Table (7.1) is given calculated values of (k_s), (CBR_k), (SSV) and (E) for the data obtained in this study. In the last column are shown CBR values provided this writer by the Indiana State Highway Department after the values for CBR_k had been calculated.

e) Dynamic Stiffness Modulus (DSM)

Figure (7.16) shows a typical plot of normalized equivalent forcing function as a function of normalized signature. Normalized here means that all numerical values of the equivalent force and the signature were divided by the peak values of the equivalent force and the peak deflection, respectively. The break point on the curve has been found to correspond to the point of inflection (point of zero acceleration) on the signature-time plots, Figures (6.1) through (6.8).

A dynamic stiffness modulus (DSM) was calculated as

$$DSM = \frac{1}{2} \left(\frac{F_1}{\Delta_1} + \frac{F_2}{\Delta_2} \right) \qquad (7.3)$$

where F_1, Δ_1 and F_2, Δ_2 are the values at the point before and the point after the point of inflection on the signature-time plot. A listing of calculated values of DSM (are given in Table (7.2). It should be noted that the DSM values increase with decreasing temperature. This had been reported earlier by Green and Hall (28) in their discussion of Waterway Experiment Station (WES) evaluation methodology using vibratory equipment.

TABLE 7.1 TIRE PRESSURE (p), MODULUS OF SUBGRADE REACTION (k_s), CALIFORNIA BEARING RATIO (CBR_k), SOIL SUPPORT VALUE (SSV) AND MODULUS OF ELASTICITY (E), FOR THE TEST SITES.

SITE	DATE	TIRE PRESSURE (psi)			MODULUS OF SUBGRADE REACTION k_s (pci)			AVERAGE k_s (pci)	CBR_k (%) USING FIGURE (7.13)	SSV	E	CBR (HIGHWAY DEPARTMENT)
		FRONT	INTER-MEDIATE	REAR	FRONT	INTER-MEDIATE	REAR					
1	8-26-75	83	83	85	200	199	200	200	10	5.3	16500	not available
		88	93	87	197	198	196	197	10	5.3	16500	
	3-17-76	75	80	72	224	216	210	217	11	5.5	18000	
		75	80	72	226	216	213	218	11	5.5	18000	
	5-13-76	87	95	98	198	194	194	195	10	5.3	16500	
		87	95	98	200	196	196	197	10	5.3	16500	
	7-30-76	40	82	90	186	200	202	196	10	5.3	16500	
		40	82	90	183	199	198	193	10	5.3	16500	
2	8-25-75	91	91	89	165	162	162	163	6	4.4	10500	3-6
		91	91	89	192	187	190	190	9	5.2	15000	
	3-17-76	75	80	72	212	210	204	209	10	5.3	16500	
		75	80	72	219	215	210	215	11	5.3	18000	
	5-13-76	87	95	98	179	178	180	179	7	4.9	12000	
		87	95	98	178	176	178	177	7	4.9	12000	
	7-30-76	40	82	90	171	187	190	183	7	4.9	12000	
		40	82	90	165	182	183	177	7	4.9	12000	

TABLE 7.1 CONTINUED

SITE	DATE	TIRE PRESSURE (psi)			MODULUS OF SUBGRADE REACTION (k_s) (pci)			AVERAGE k_s (pci)	CBR_k(%) USING FIGURE (7.13)	SSV	E	CBR (HIGHWAY DEPARTMENT)
		FRONT	INTER-MEDIATE	REAR	FRONT	INTER-MEDIATE	REAR					
3	8-26-75	83	83	85	71	68	68	69	2	3.0	4500	4
		83	83	85	87	83	82	84	2	3.0	4500	
	3-17-76	75	80	72	240	230	220	230	15	6.0	9000	
		75	80	72	240	229	219	229	15	6.0	9000	
	5-13-76	87	95	98	112	108	109	110	4	4.0	6000	
		87	95	98	103	99	100	101	3	3.5	5250	
	7-30-76	40	82	90	63	71	70	68	2	3.0	4500	
		40	82	90	63	71	69	68	2	3.0	4500	
4	8-26-75	91	91	89	70	65	66	67	2	3.0	4500	3-6
		91	91	89	70	64	66	67	2	3.0	4500	
	5-13-76	87	95	98	70	68	68	69	2	3.0	4500	
		87	95	98	87	84	84	85	2	3.0	4500	
	7-30-76	40	82	90	59	67	66	64	2	3.0	4500	
		40	82	90	60	67	65	63	2	3.0	4500	
5	8-12-76	86	90	90	171	166	164	167	6	4.7	7050	4
6	8-12-76	76	90	90	159	152	151	154	6	4.7	7050	2.2, 6.5
7	8-12-76	76	90	90	63	61	61	62	2	3	4500	2.0, 6.3

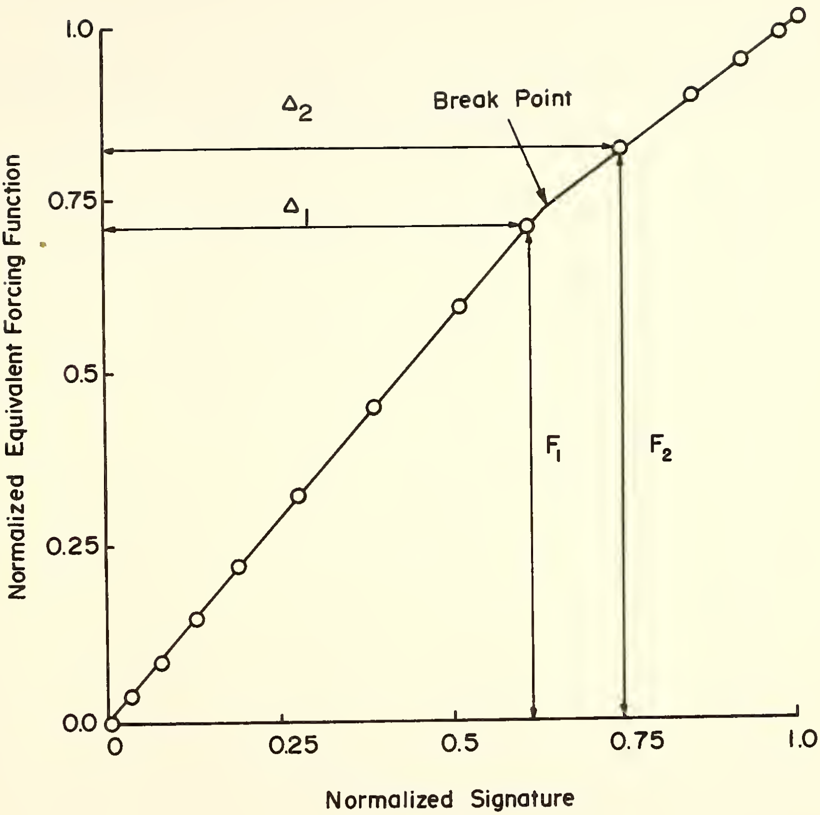

FIGURE 7.16 TYPICAL NORMALIZED EQUIVALENT FORCING FUNCTION Vs. NORMALIZED SIGNATURE.

TABLE 7.2 CALCULATED DYNAMIC STIFFNESS MODULUS (DSM), SITES 1, 2, 3, 4, 5, 6 AND 7

SITE	DATE	AIR TEMP. °F	DYNAMIC STIFFNESS MODULUS DSM kips/inch			AVERAGE DSM (kips/inch)
			FRONT	INTER-MEDIATE	REAR	
1	8-26-75	75	1342	1491	1267	1326
			1328	1304	1185	1272
	3-17-76	22	1726	1565	1386	1559
			1596	1559	1360	1505
	5-13-76	64	1544	1425	1319	1429
			1400	1381	1290	1357
	7-30-76	78	1391	1367	1373	1377
			1404	1312	1269	1328
	9-13-76	80	1357	1309	1312	1326
2	8-25-75	82	785	888	721	798
			746	744	660	717
	3-17-76	22	746	774	698	739
			856	935	762	851
	5-13-76	68	590	574	574	579
			584	568	569	574
	7-30-76	80	818	788	678	761
			827	848	842	839

TABLE 7.2 CONTINUED

SITE	DATE	AIR TEMP. °F	DYNAMIC STIFFNESS MODULUS DSM kips/inch			AVERAGE DSM (kips/inch)
			FRONT	INTER-MEDIATE	REAR	
3	8-26-75	75	267	246	237	250
			291	325	278	298
	3-17-76	24	875	854	747	825
			875	852	748	825
	5-13-76	68	360	362	338	353
			297	373	353	341
	7-30-76	80	237	279	299	272
			299	268	281	283
4	8-25-75	82	216	198	188	201
			216	197	188	200
	5-13-76	68	232	224	210	222
			233	211	211	218
	7-30-76	80	225	205	206	212
			225	205	206	212
5	8-12-76	80	579	551	506	545
6	8-12-76	80	1068	1103	960	1044
7	8-12-76	80	451	442	460	451

IV.II Structural Evaluation

a) Introduction

The performance of pavements as measured by the present serviceability index (PSI) is related to the logarithm of the number of load applications (58). The amount of energy input in a pavement system consequent to the passage of a vehicle can vary from a compact automobile to a heavy eighteen wheeled truck. Thus, any procedure to predict the performance of pavement sections with reasonable reliability must also be able to account for the induced energy of a moving traffic stream of variable composition.

Highter and Harr (56) studied deflection data gathered at the AASHO road test and collected at Kirtland and Pease Air Force Bases. Using this information, they derived a regression equation relating present serviceability index (PSI) to cumulative total peak deflection (Figures 2.1 and 7.17). Their studies indicated that "there is a threshold cumulative total peak pavement deflection at which distress develops in asphaltic concrete pavement". Based on the AASHO data, they concluded that twelve hundred feet (1200 ft) of cumulative total peak deflection will cause distress in highway pavements; twenty two hundred feet (2200 ft) for runway pavements. In this study, it was assumed that each pass produced one coverage.

In the present research, a study was conducted of the induced energy into a pavement using the concept of work.

S-B-SB
6-9-16 Surface Course 6 inches Thick
Base Course 9 inches Thick
Subbase 16 inches Thick

Predictive Equation:

$$PSI = .031 + .383S + .077B + .071SB - .0022D + 5.56 \times 10^{-7} D^2$$

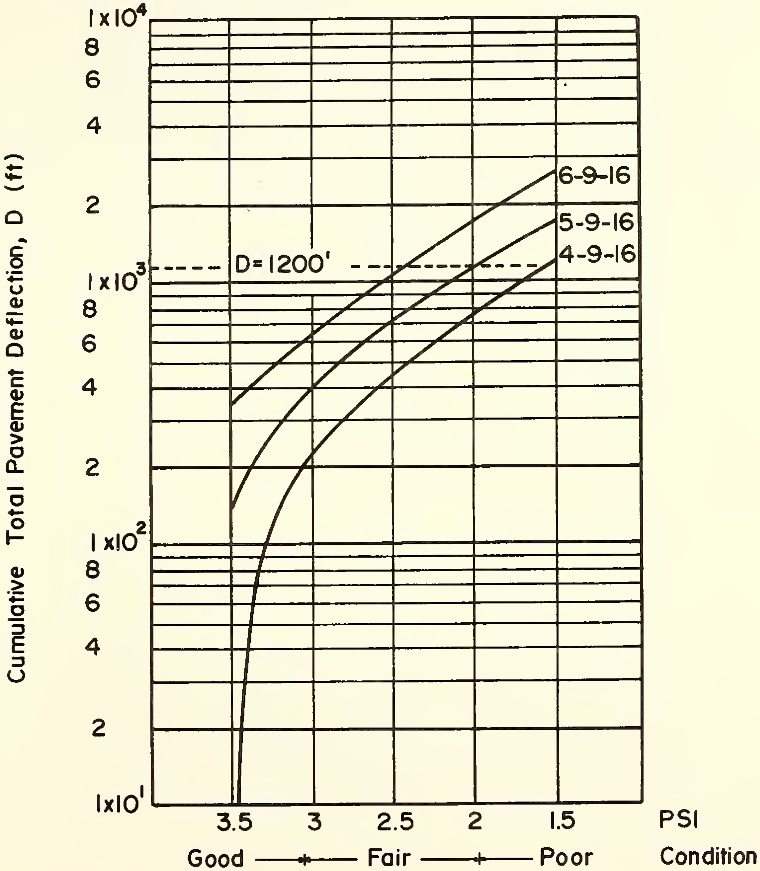

FIGURE 7.17 THE PREDICTED EFFECT OF SURFACE COURSE THICKNESS ON THE CONDITION OF A PAVEMENT AS A FUNCTION OF ITS CUMULATIVE TOTAL DEFLECTION. (56).

Figures (7.18) and (7.19) show typical plots relating the equivalent forcing function and the signature for one pass of the standard highway truck. The areas bounded by the three hysteresis loops are measures of the work done to the pavement by the moving vehicle.

Figure (7.20) shows a plot of the work done (the area encompassed by the loops) as a function of total peak deflection (the sum of the deflection of the front, intermediate and rear tires) per pass. It should be noted that the data plotted in the figure represent eight tests at different air temperatures using the same vehicle, see Table (6.3) site 3. Examination of the figure indicates that the work done to the pavement is related to the total peak deflection. Figure (7.21) shows a plot of the work done as a function of air temperature. Note that at twelve degrees Fahrenheit below zero ($-12^{\circ}F$) the pavement system is effectively rigid. Recognizing that the work done on a pavement system by a moving load is related to total peak deflection and ambient temperatures, a pavement evaluation procedure was developed as part of the present study. In concept, it is an extension of the findings of Highter and Harr (56).

b) Lateral Placement

The lateral placement is defined as the distance between the nearest edge of the pavement structure and the wheel path, Figure (7.22a). Studies indicate the position of a vehicle on

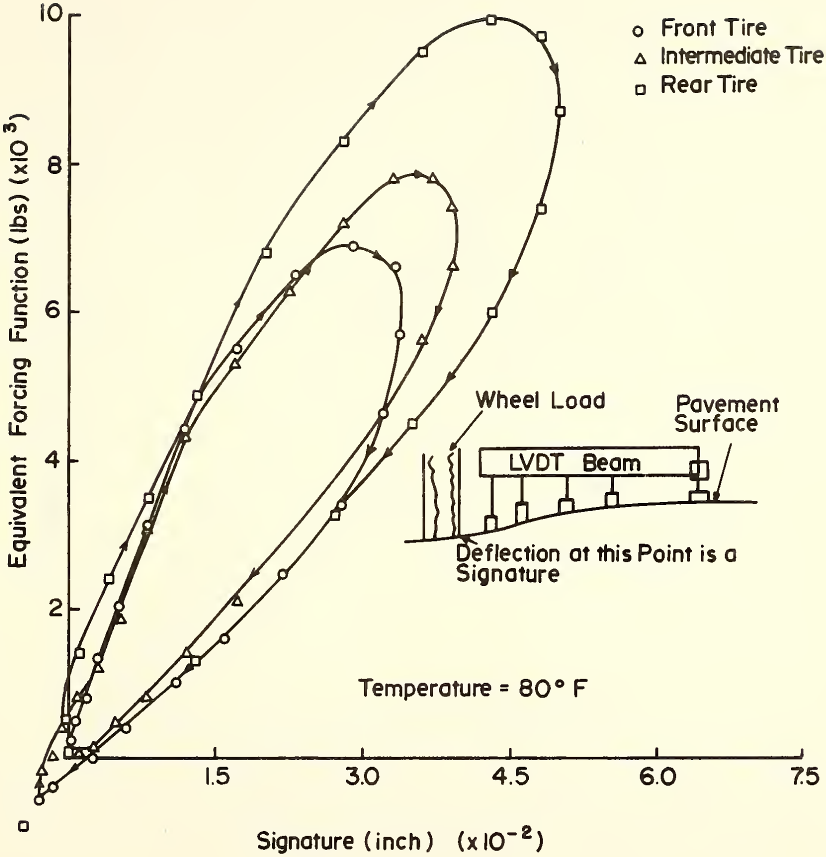

FIGURE 7.18 EQUIVALENT FORCING FUNCTION Vs. SIGNATURE, SITE 3.

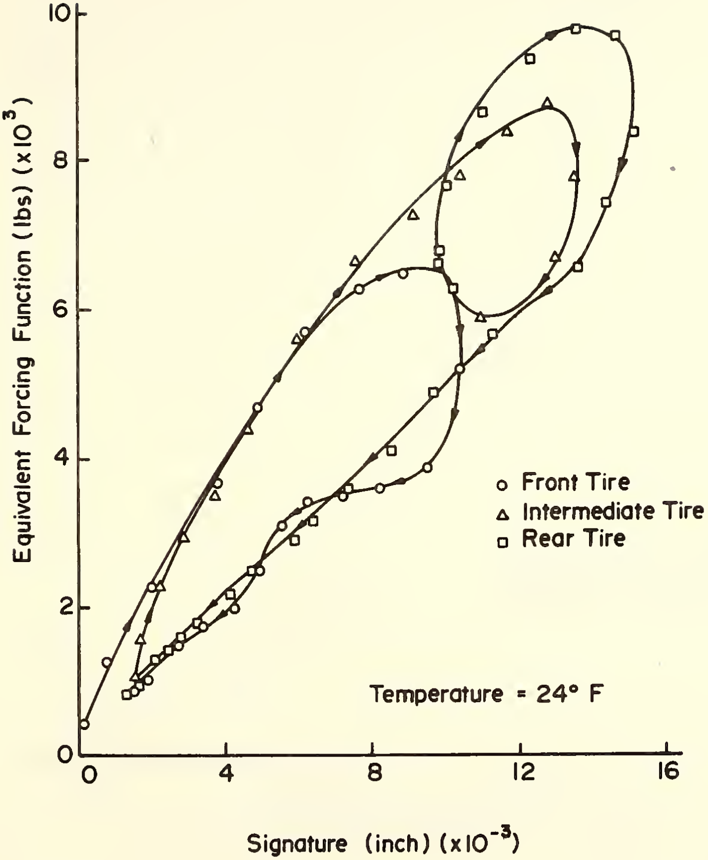

FIGURE 7.19 EQUIVALENT FORCING FUNCTION Vs. SIGNATURE, SITE 3.

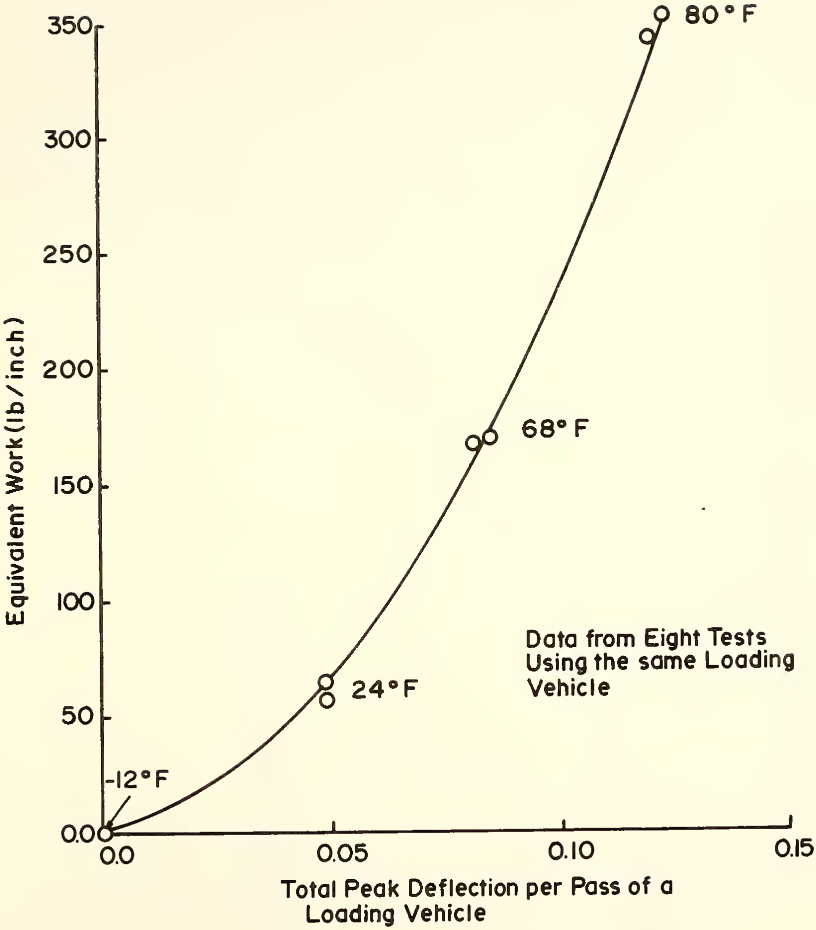

FIGURE 7.20 EQUIVALENT WORK Vs. TOTAL PEAK DEFLECTION PER PASS OF A LOADING VEHICLE, SITE 3.

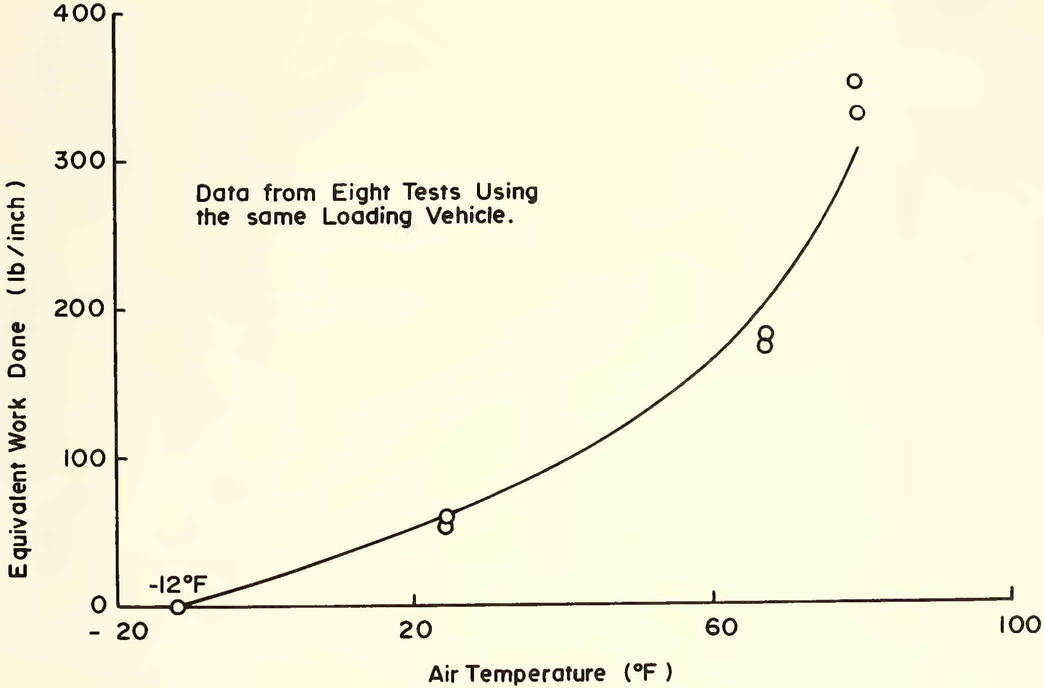

FIGURE 7.21 EQUIVALENT WORK Vs. AIR TEMPERATURE.

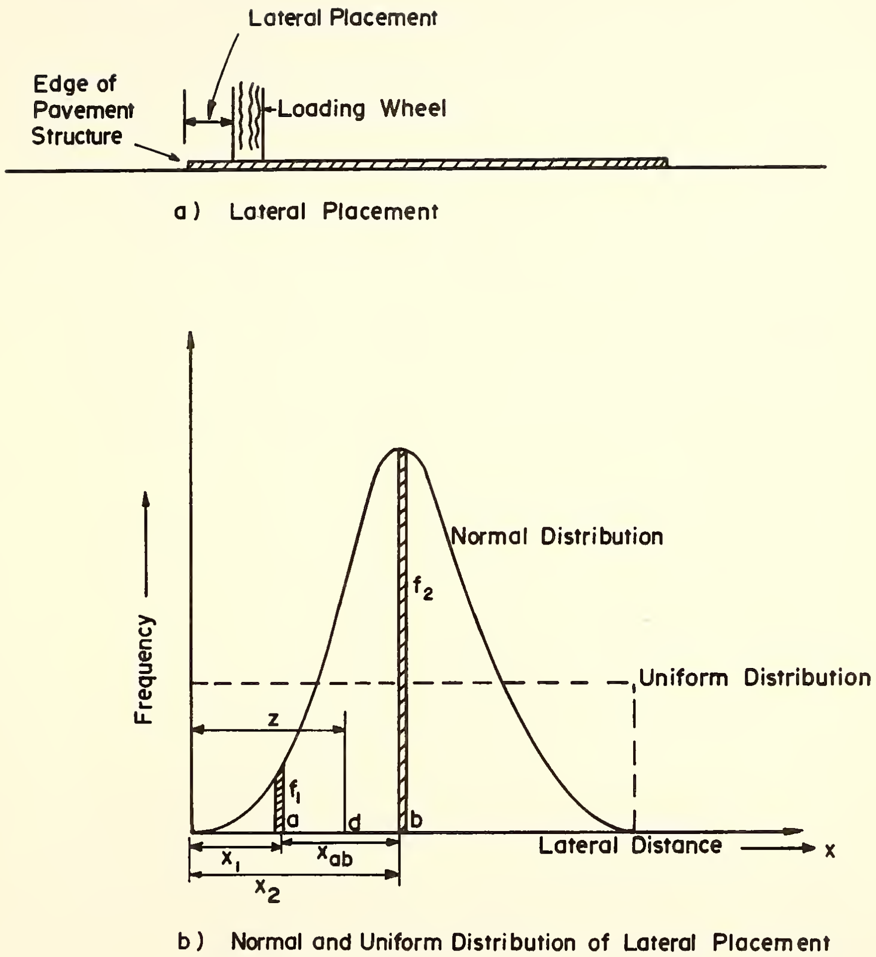

FIGURE 7.22 LATERAL PLACEMENT AND ITS DISTRIBUTIONS.

a highway depends upon the highway geometry, vehicle gear configuration, time of the day, ambient conditions, and pavement markings (11, 59, 60, 63).

In Figure (7.22b) is shown normal and uniform distributions of the lateral placement of vehicles. Suppose that two vehicles designated by subcripts (1 and 2) travel along the pavement. Their corresponding frequencies and distances from the edge of the pavement are denoted by f_1, f_2 and x_1, x_2.

Using equation (4.1), due to the passage of vehicles 1 and 2 at points a and b, point d on the surface of the pavement at a distance z from the edge (Figure 7.22b) will experience a cumulative total peak deflection given by

$$y(z) = y_1 \exp\left[-\frac{1}{B}(|z-x_1|)^N\right] + y_2 \exp\left[-\frac{1}{B}(|z-x_2|^N\right] \quad (7.4)$$

where y_1 = total peak deflection of the signature at point a due to the passage of the front, intermediate and rear tires for vehicle 1.

y_2 = same as above for point b and vehicle 2.

x_1, x_2 = lateral distance

For (P) passing vehicles equation (7.4) becomes

$$y(z) = \sum_{i=1}^{P} y_i \exp\left[-\frac{1}{B}(|z-x_i|)^N\right] \quad ; i = 1, 2, 3 \ldots P \quad (7.5)$$

For a width of the traffic area (R), a width of tire print (W), the total number of segments (J) is given by, Figure(7.23).

$$J = \frac{R}{W}$$

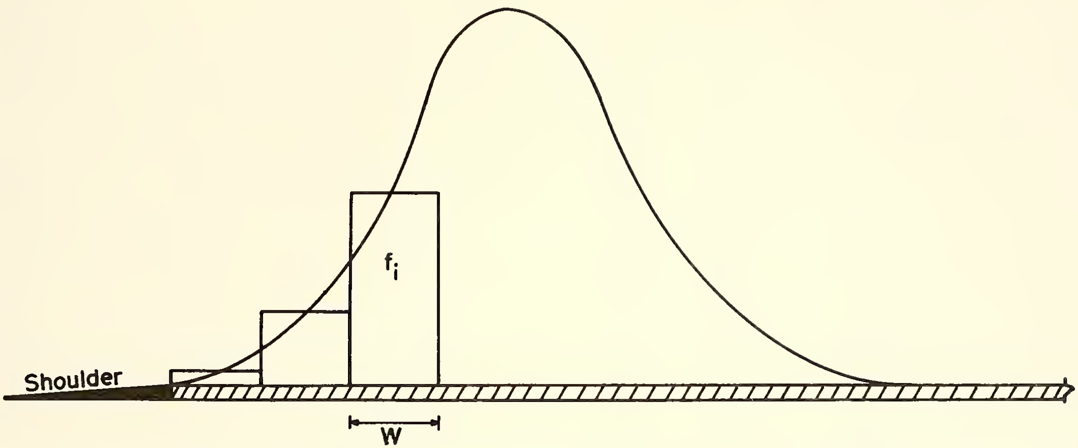

FIGURE 7.23 DISCRETE FREQUENCY OVER A TIRE WIDTH.

The number of passes of a loading vehicle over segment (i) (its center is located at a lateral distance of (x_i) from the edge of the pavement) is given by Pf_i, where (P) is the total number of passes over the pavement section and f_i is the frequency of the vehicle passing over the i^{th} segment. For (P) passes over the (J) segments, with each segment having a frequency of f_i, equation (7.5) gives for the cumulative total peak deflection at a lateral distance z from the edge of the pavement.

$$y(z) = P \sum_{i=1}^{J} f_i \, y_i \exp \left[- \frac{1}{B} (|z-x_i|)^N\right] \tag{7.6}$$

A somewhat similar expression was given by Deacon (63) and Yoder and Witczak (11)

$$n_e = \max \sum_{j=1}^{J} P_j \, f_{jx} \, F_j \tag{7.7}$$

where n_e = equivalent repetitions of a standard vehicle* producing a unit of damage ,

P_j = number of passes within time interval "t",

f_{jx} = frequency,

F_j = equivalent wheel load factor, and

j = total number of passes at a specific distance

It should be noted that for $x_i = z$, equations (7.7) and (7.6)

---

* Any vehicle can be defined as a standard if the pavement deflection it produces is assigned unity. Pavement deflections due to any other vehicles can then be scaled relative to the standard.

are identical. However, equation (7.7) does not account for the lateral position of the vehicle.

To explore the significance of the differences between equations (7.6) and (7.7), consider points d and b, Figure (7.22b), located 25 and 28 inches from the edge of the pavement. If it is assumed that each was passed over 100 times by a standard vehicle* [$F_j = 1$ in equation (7.7), f_i and f_{jx} will be equal to 0.5 in both equations]. Taking $y_i = F_j$ as a unit of damage, the cumulative damage at point d, given by equation (7.7) will be

$$n_e = \sum_{j=1}^{1} 200\ (0.5)\ (1) = 100 \text{ units of damage}$$

Equation (7.6) will produce

$$y(z) = 200\ (0.5)\ (1) + 200\ (0.5)\ (1) \exp\left[-\frac{1}{B}\left(|25-28|\right)^N\right]$$

For interstate 64, site 6, N = 0.87 and B = 6.87 (see Table 6.1); hence y(z) = 100 + 68 = 168 units of damage. These results indicate that equation (7.7) would underestimate the damage by about 60% for the considered case.

c) Passes and Equivalent Coverages

Equivalent coverages (C_e) is defined herein as the ratio of the cumulative total peak deflection [y(z)] at a point on the pavement to the total peak deflection (Δ) caused by one pass of a standard loading vehicle* at that point. The equivalent

* See previous footnote.

coverages to passes ratio (C_e/P) is defined as the ratio of equivalent coverages at a point of interest to the total number of passes of a standard vehicle along a pavement section. From these two definitions it can be seen that

$$C_e = \frac{y(z)}{\Delta}$$

$$\frac{C_e}{P} = \frac{y(z)}{P\Delta} \tag{7.8}$$

The term $P\Delta$ in equation (7.8) may be thought of as the cumulative total peak deflection at a point due to P passes of a standard vehicle at that point. The ratio C_e/P in equation (7.8) represents the percentage of the total energy of the stream of vehicles available to do work at a point on the pavement surface.

d) Peak Deflections and Vehicular speed

Highter and Harr (56) found peak delfections to be dependent upon the horizontal velocity of loading vehicles, Figure (7.24). Observations indicate that at speeds above 35 mph the number of peak deflections of multi-wheeled vehicles are reduced. For example, at creep speeds, a tandum truck will produces three distinct peak deflections per pass, Figure (7.25a). The same vehicle will produce two (Figure 7.25b) or even one peak deflection (Figure 7.25c) at higher speeds. This is a consequence of the inertia and damping of the pavement. That is, at high speed, the pavement will not have

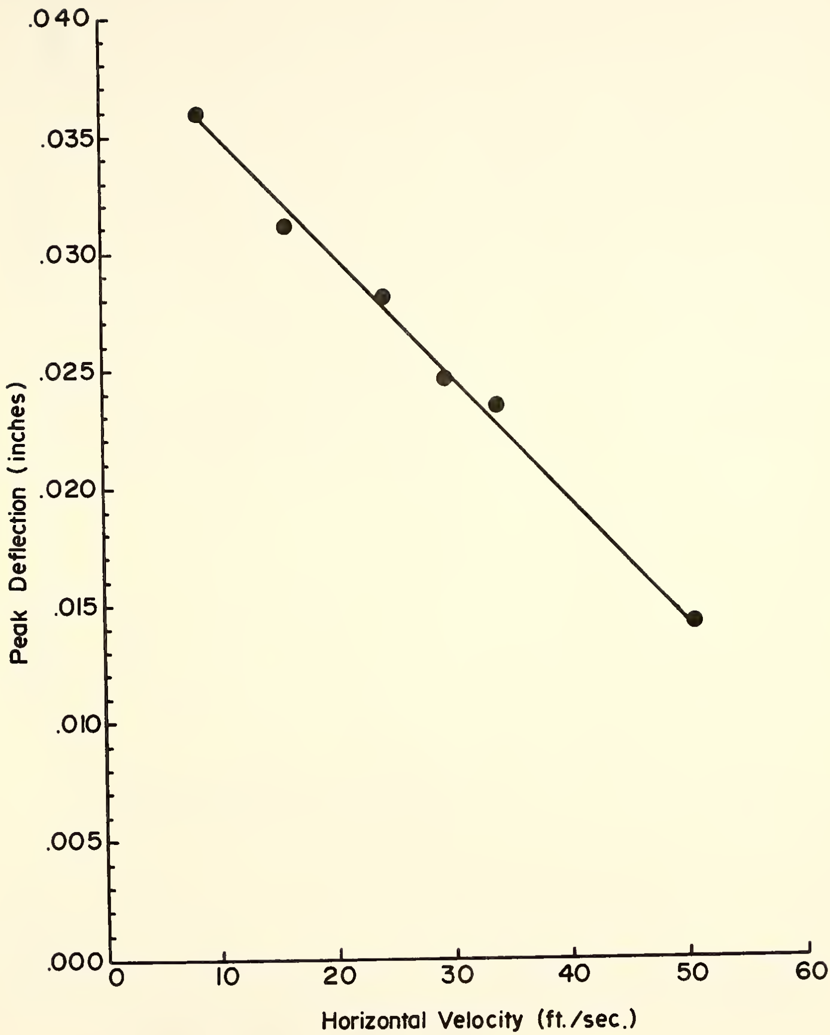

FIGURE 7.24 PEAK PAVEMENT DEFLECTION Vs. HORIZONTAL VELOCITY FOR P-2 FIRE TRUCK(56)

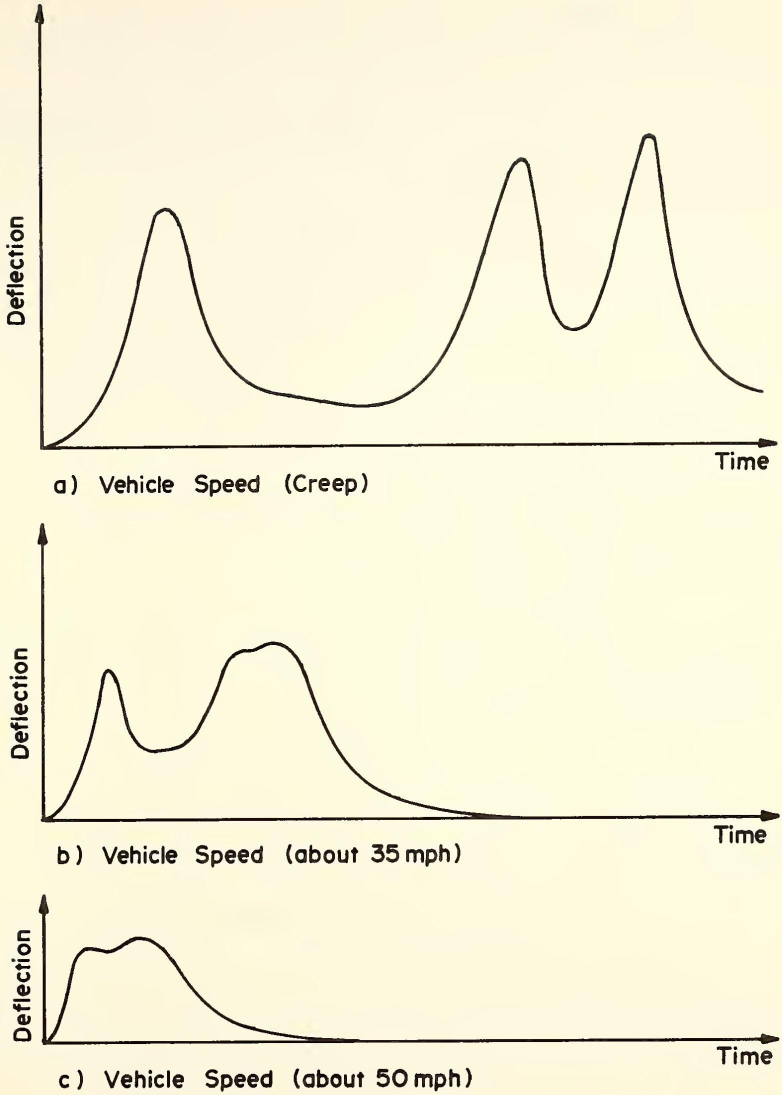

FIGURE 7.25 SCHEMATIC REPRESENTATIONS OF THE INFLUENCE OF THE SPEED OF A TANDEM TRUCK ON THE NUMBER OF PEAK DEFLECTIONS OF A POINT ON THE PAVEMENT SURFACE.

enough time to rebound under one set of wheels before the other set passes over the point.

V. Simplified Pavement Evaluation

Simplified procedures have been developed which will permit one to obtain approximations to parameters of a pavement without recourse to computer program PPP in Appendix C. The procedures will also be illustrated below by examples.

a) N and B parameters

The N and B parameters can be approximated using Figures (7.26) -obtained from Equation (4.1), page 28 - and (7.27).

1. Pavement deflections at various lateral distances from the edge of a tire are measured (using the LVDT beam) and plotted as a function of these distances, Figure(7.27).
2. Deflections at lateral distances of 6, 9 and 15 inches are then obtained from Figure(7.27). These are designated as y_6, y_9, and y_{15}, respectively.
3. The ratio* $\ln(y_{15}/y_6)/\ln(y_9 / y_6)$ is then calculated and located on the left ordinate axis of Figure(7.26). The value of the N parameter can then be determined as shown in the figure. The N values are located on the abscissa axis.
4. Having the N parameter, the corresponding value of $N' = 9^N - 6^N$ can then be obtained on the indicated right ordinate axes.
5. B value can then be calculated from the expression.

$$B = N' / |\ln(y_9 / y_6)|$$

* Natural logarithm

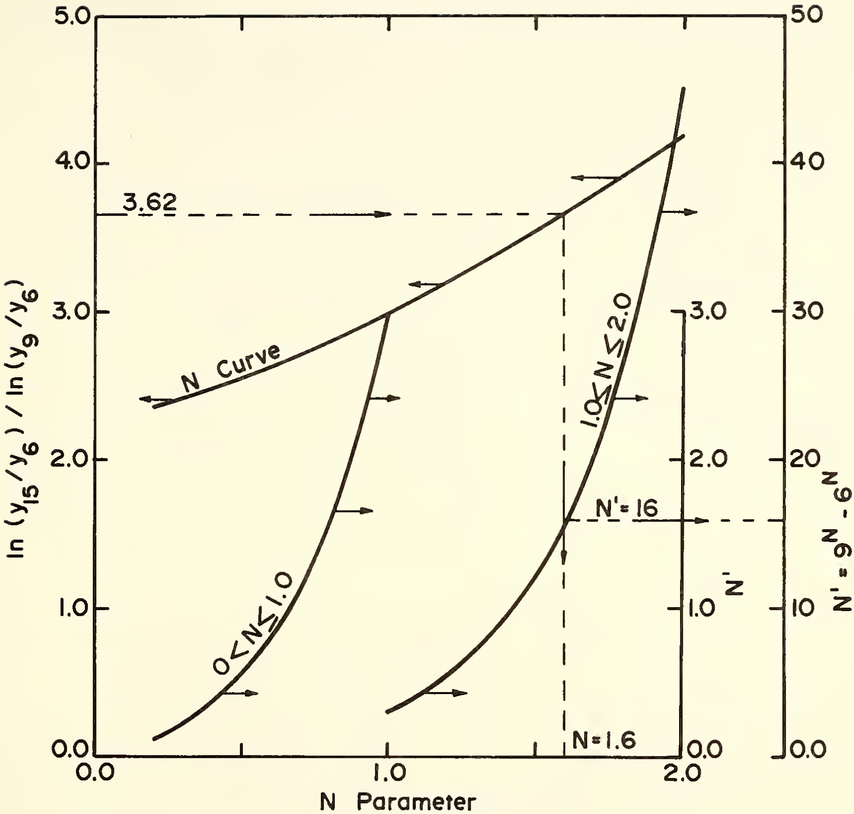

FIGURE 7.26 SIMPLIFIED PROCEDURE FOR OBTAINING N VALUES.

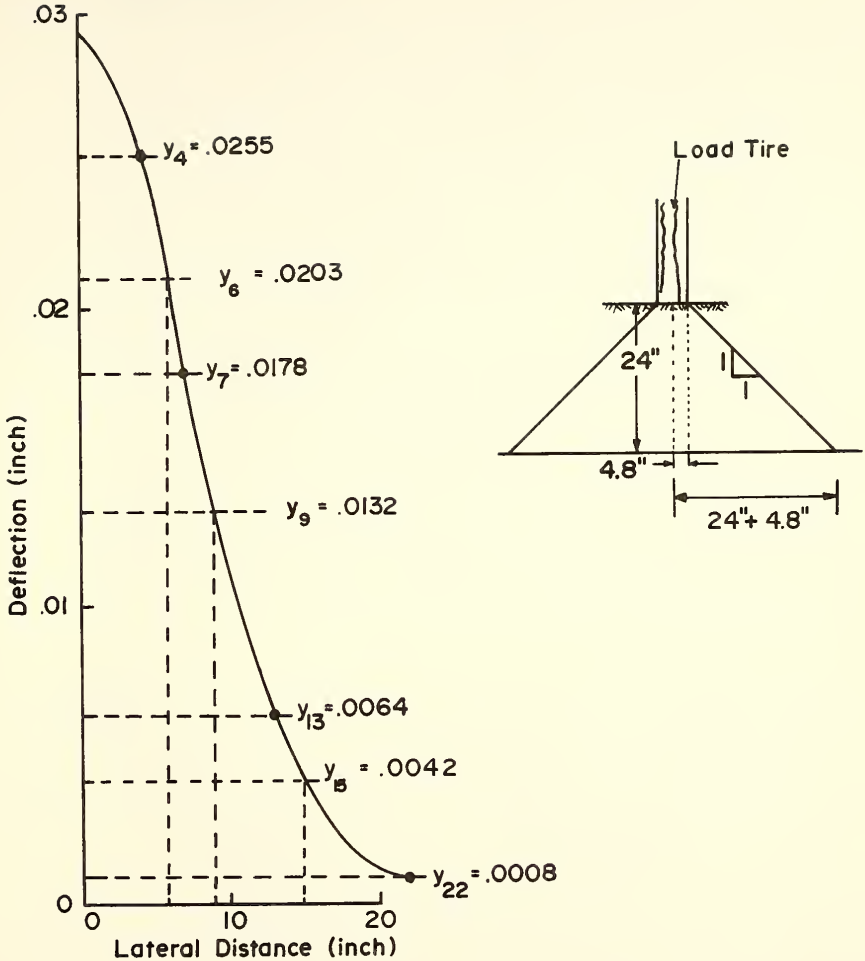

FIGURE 7.27 CASE STUDY.

b) Subgrade Evaluation

The peak deflection under the edge of a load tire can be calculated using N and B parameters and the measured deflections from above. The modulus of subgrade reaction (k_s), California bearing ratio (CBR), soil support value (SSV), and the elastic modulus (E) can then be estimated following the procedure outlined in previous sections.

c) Structural Evaluation

Having N and B and the peak deflection (Figure 7.24 may be used to estimate the deflections at other speeds), the cumulative total peak deflection can be calculated (for any number of load repetitions). The condition of the pavement section may then be estimated using either Figure (2.1) or (7.17).

VI. Case Study

A pavement evaluation test was performed on site 3 using the LVDT beam. The following peak pavement deflection data were obtained.

Deflection (inch)	Lateral distance (inch)
y_4 = .0255	4
y_7 = .0178	7
y_{13} = .0064	13
y_{22} = .0008	22

The vehicle speed was 2.25 mph,

the tire pressure was 83 psi and the tire load was 6003 pounds

a) N and B parameters

1. The data are plotted in Figure(7.27) as a function of lateral distance. The desired values of y_6, y_9, and y_{15} are then determined to be .0203, .0132, and .0042 inches, respectively.

2. The deflection ratios are formed

$$y_9/\ y_6 = .65, \qquad y_{15}/\ y_6 = .21$$

$$\ln(y_{15}/\ y_6)\ /\ \ln(y_9/\ y_6) = 3.62$$

3. Using Figure(7.26):

$$N = 1.6, \quad N' = 16, \quad B \simeq 37$$

b) Subgrade Evaluation (see Figure 7.12)

1. The peak deflection under the edge of tire is calculated using equation (4.1)

$$y_P = .0255 \exp(+\frac{1}{37}(4)^{1.6}) = .0327 \text{ inches}$$

using this value of y_P and equation (4.1) as a chek,

$$y_4 = .0255,\ y_6 = .0203,\ y_7 = .0178,\ y_9 = .0132,\ y_{15} = .0042$$

2. Equivalent spring constant:

$$k = Q/y_P = 6003/.0327 = 183574 \text{ lb/in}$$

3. The contact area:

$$a = Q\ /\ p = 6003\ /\ 83 = 72 \text{ in}^2$$

4. Radius of contact area:

$$r = \sqrt{a\ /\pi} = 4.8 \text{ in}$$

5. Equivalent area 24 inches below (T=24) the surface

$$a_e = (r + T)^2\pi = 2602 \text{ in}^2$$

6. Modulus of subgrade reaction:

$$k_s = k \;/ a_e = 183574 \;/\; 2606 = 70 \text{ pci}$$

7. California bearing ratio:

from Figure (7.13). $CBR_k = 2.0$

8. Soil support value:

from Figure (7.14). SSV = 3.0

c) Cumulative Peak Deflection (Structural Evaluation)

1. From Figure (7.24)(extrapolating linearly) the ratio of peak deflection at speed of 2.25 mph to that at 55 mph:

   $.0385 \;/\; .015 = 2.6$

   Expected deflection at the site for loading vehicle speed of 55 mph:

   $.0327/\; 2.6 = .0126$ in

2. From Table (4.5) the traffic per year was found to be:

   30,000 trucks, 60,000 pickup(s), 210,000 cars

   Taking the deflections of an automobile to be (1/5)* that of a truck and of pickup to be (1/3) of a truck.

   The cumulative total peak deflection per year is found to be:

   $.0126\;(30{,}000 + 60{,}000/3 + 210{,}000/5)/12 = 97$ feet/year

3. To account for freezing and subfreezing temperatures a factor of .6† is recommended for the state of Indiana; hence the estimated cumulative total peak deflections are:

   $97\;(.6) = 58$ feet/year

---

* The factors 1/3 and 1/5 are dependent upon the wheel load of each vehicle, the presented ratios were obtained from Table (6.1) and deflection data on site 1.

† Based on average temperature in Tippecanoe County, Indiana (70).

4. Present serviceability index (PSI)

Using the equation on Figure (7.17), for a PSI = 2

$$2 = .031 + .383\,(3.02) + .077(6) + .071\,(3.02)\,(6) - .0022D + 5.56 \times 10^{-7}\,D^2$$

from which

$$D^2 - 3957D + 1683453 = 0.0$$

$$D = 510 \text{ feet}$$

That is distress is estimated to occur for a cumulative total peak deflection of 510 feet. Given 58 feet/year it is estimated that the pavement can function under stated condition for 510 / 58 ≃ 9 years.

BLANK PAGE

CONCLUSIONS

On the basis of the results of this study, the following conclusions are made for the flexible highway pavements investigated:

1. A relationship was found to be valid which related the pavement deflection response function (output) and a vehicular input in the form of a time dependent transfer (TDT) function. The characteristics of the TDT function can be used as follows:
   a) as indicators of the performance and condition of a pavement system.
   b) to indicate the effects of ambient conditions.
   c) to obtain the shape of the peak deflection curves consequent to the passage of a wide range of vehicles.
   d) to assess the lateral attenuation of energy following the passage of a vehicle.
   e) to predict the time response of a pavement system.
2. The results obtained from the LVDT beam (linear variable differential transducers) were found to be in extremely close agreement with the embedded LVDT gages.
3. The lateral extent of the deflection basin was found, in all cases, to be less than fifty inches from the edge of the tire of the loading vehicle.
4. The deflection basin extending laterally from the edge of a tire of a loading vehicle was found to follow the equation

$$y(x,t) = y(0,t) \exp\left(-\frac{1}{B} x^{N}\right)$$

The N and B parameters in the above expression, for a particular site, were found to be independent of the gear configuration or wheel loads of the loading vehicle. They did depend on the number of load repetitions. It was found that they provide a measure of lateral attenuation of induced energy. In particular the B parameter was found to be a good indicator of the rate of dissipation of the applied vehicular loading.

5. The parameters contained within the TDT function were shown to be properties of a given pavement section. As such, changes in their characteristics were found to reflect corresponding changes in pavement conditions. As had been found to be the case in previous studies by Highter, Boyer and Harr (56), the TDT function can be used to predict the deflection basin for a wide range of vehicles, gear configurations and loadings. It was demonstrated that predicted deflections could even be made for an automobile from the TDT function obtained from a standard highway truck.

   It was found that the parameters of the TDT function; in particular, the spring constant (k) might be related to many current design parameters used in highways; CBR, and modulus of subgrade reaction, as well as the stiffness modulus of the pavement.

6. Results have been simplified and approximate procedures are presented whereby computations can be performed using developed nomographs to

provide information as to the performance of highway pavements. In this regard, an evaluation procedure is offered that can provide a measure of the number of years for which a pavement can be expected to perform adequately.

SUGGESTIONS FOR FUTURE RESEARCH

The results of this investigation have deomonstrated the ability to evaluate pavements and to determine when remedial measures might be required. Four sites were tested in the vicinity of West Lafayette, Indiana. No knowledge was available of when these pavements had been built or the degree to which they had been rehabilitated. Consequently, it is advisable that a study be undertaken to examine newly constructed pavements to assess the general validity of the evaluation prodedure. The new section of Interstate 64 represents one such point in time: a start has been made. It is recommended that studies be continued so that the changes in the transfer function can be assessed periodically.

The development of the LVDT beam offers a nondestructive rapid test whereby the evaluations noted above might be made. However, the recent findings using a newly developed noncontact LED beam (light emitting diodes) suggest far greater speed of testing for that device. It is recommended that efforts be expended to employ this apparatus in the nondestructive testing and evaluation of highway pavements.

BIBLIOGRAPHY

BIBLIOGRAPHY

1. Crafton, P. A., Shock and Vibration in Linear Systems, Harper and Brothers, Inc., New York, 1961.

2. Harrison, H. L., and Bollinger, J. G., Introduction to Automatic Controls, International Textbooks Company, Inc., Scranton, 1963.

3. Tsien, H. S., Engineering Cybernetics, McGraw Hill Book Company, Inc., New York, 1954.

4. Harr, M. E., Application of Mathematics for Engineers and Scientists, Unpublished Notes, Purdue University, 1969.

5. Wylie, C. R., Jr., Advanced Engineering Mathematics, McGraw Hill Book Company, Inc., New York, 1960.

6. Swami, S. A., Goetz, W. H., Harr, M. E., "Time and Load Independent Properties of Bituminous Mixtures", Highway Research Board, Record Number 313, 1970.

7. __________ "Deteriorating Airport Pavements Spur Effort to Head Off Crisis", Engineering News Record, November 4, 1971.

8. __________ "Development of CBR Flexible Pavement Design Methods for Airfields," Symposium, Transactions, American Society of Civil Engineering, Vol. 115, 1950.

9. Highter, W. H., "The Application of Energy Concepts to Pavements", Joint Highway Research Project, Purdue University and Indiana State Highway Commission, November 1972 - No. 38.

10. __________ Soils Manual for Design of Asphalt Pavement Stuctures. The Asphalt Institute, Second Edition, April 1963, Third Printing, February 1969, Manual Series No. 10 (SM-10).

11. Yoder, E. J. and Witczak, M. W., Principle of Pavement Design, John Wiley and Sons, Inc., New York, 1975.

12 Boyer, R. E., Predicting Pavement Performance Using Time-Dependent Transfer Functions, Joint Highway Research Project, Purdue University and Indiana State Highway Commission, September 1972, No. 32.

13. Horonjeff, B., Planning and Design of Airports, McGraw Hill Book Company, Inc., New York 1962.

14. Boussinesq, J. W., "Application des Potentials à L'étude de L'équilibrium et du Mouvement des Solids Elastiques", Paris, Bauthier - Villiers, 1885.

15. Ali, G.A.,"A Laboratory Investigation of the Application of Transfer Functions to Flexible Pavements", Ph.D. Thesis, Purdue University, August 1972.

16. Harr, M. E., Foundations of Theoretical Soil Mechanics, McGraw Hill Book Company, Inc., New York, 1966.

17. Westergard, H. M., "Stresses in Concrete Pavements Computed by Theorotical Analysis", Journal of Public Roads, Vol. 7, No. 2, 1926.

18. Westergard, H. M., "Theory of Concrete Pavement Design", Proceedings, Highway Research Board, 1927.

19. Westergard,H. M., "Stresses in Concrete Runways of Airports", Proceedings, Highway Research Board, 1939.

20. Hogg, A. H. A., "Equilibrium of a Thin Plate, Symmetrically Loaded, Resting on an Elastic Foundation of Infinite Depth", Philosophical Magazine, Vol. 25, 1928.

21. Harr, M. E. and Leonards, G. A., "Analysis of Concrete Slab on Ground", Journal of the Soil Mechanics and Foundation Division, Proceedings of the ASCE, Vol. 85, No. SM3, June 1959.

22. Burmister, D. M., "The Theory of Stresses and Displacements in Layered Systems and Applications to the Design of Airport Runways", Proceedings of the Highway Research Board, Vol. 23, 1943.

23. Burmister, D. M., "The General Theory of Stresses and Displacements in Layered Soil Systems", Journal of Applied Physics, Vol. 16, 1945.

24. Burmister, D. M., "Evaluation of Pavement Systems of the WASHO Road Test by Layered System Methods", Highway Research Board, Bulletin 177, 1958.

25. Barksdale, R. D. and Leonards, G. A., "Predicting Performance of Bituminous Surfaced Pavements", Proceedings of the Second International Conference on the Structural Design of Asphalt Pavements, University of Michigan, Ann Arbor, 1968.

26. Witczak, M. W., Structural Evaluation and Overlay Design Methodology for Airfield Pavements: State of the Art, Report No. FHWA, RD. 74-60, Transportation Research Board, Washington, D. C., June 1970.

27. Hall, J. W., Jr., Non-destructive Testing of Flexible Pavements A Literature Review, Technical Report, AFWL-TR-68-147, Kirtland Air Force Base, New Mexico, May 1970.

28. Green, J. L. and Hall, J. W., Non-Destructive Vibratory Testing of Evaluation Methodology and Procedure, Volume 1, Report No. FAA-RD-73-205-1, U. S. Department of Transportation, FAA, Washington, D. C., September 1975.

29. Haas, R., Surface Evaluation of Pavements: State of the Art Report No. FHWA-RD-74-60, Transportation Research Board, Washington, D. C., June 1970.

30. Norman, P. J., Snowdon, R. A., and Jacobs, J. C. Pavement Deflection Measurements and their Application to Structural Maintenance and Overlay Design, Transport and Road Research Laboratory, Department of the Environment, TRRL Report LR 571, 1973.

31. __________ Pavement Rehabilitation: Proceedings of a Workshop, Transportation Research Board, Report No. FHWA-RD-74-60, June 1974.

32. Henkelom, W. and Foster, C. R., Dynamic Testing of Pavements, Journal Soil Mechanics and Foundations Division, American Society of Civil Engineers, Vol. 86, Number SM 1, Part 1, February 1960, pp. 1-28.

33. Maxwell, A. A., Nondestructive Testing of Pavements, U.S. Army Engineer Waterways Experiment Station, CE, Vicksburg, Mississippi, Miscellaneous Paper Number 4-373, January 1960.

34. __________ Nondestructive Testing of Pavements: Tests on Multiple-Wheel Heavy Gear Load Sections at Eglin and Hurlburt Airfields, Air Force Weapons Laboratory, Albuquerque, New Mexico, Technical Report # AFWL-TR-71-64, March 1972.

35. Kaplan, W., Advanced Calculus, Second Edition, Addison-Wesley Publishing Company, 1973.

36. Lago, G., and Benningfield, L. M., Control System Theory, The Ronald Press Company, New York, 1962.

37. Swami, S. A., "The Response of Bituminous Mixtures to Dynamic and Static Loads Using Transfer Functions", Ph.D. Thesis, Submitted to Purdue University, 1969.

38. Nixon, Floyed E., "Handbook of Laplace Transformation: Tables and Examples", Prentice-Hall, Inc., Englewood Cliffs, New Jersey, 1960.

39. Harr, M. E., "Ground Water and Seepage", McGraw Hill Book Company, New York, 1962.

40. Richart, F. E., Jr., Hall, J. R., Jr., and Woods, R. D. Vibrations of Soils and Foundations, Prentice-Hall, Inc., Englewood Cliffs, New Jersey, 1970.

41. Kinariwalla B., Kuo F. F., and Tsao N. K. "Linear Circuit and Computation" John Wiley and Sons Inc., New York, 1973.

42. ________ "Light Beam Oscillograph Mark 2300" Clevite Corporation, 37th and Perkins, Cleveland, Ohio, 7-22-68.

43. ________ " Medium Gain Amplifiers Low Gain Amplifiers" Clevite Corporation, 37th and Perkins, Cleveland, Ohio, 7-22-68.

44. ________ "SMS/GPM/LVDT Signal Conditioning Module" Schaevitz Engineering, Instruction Manual Number 7201.

45. Harr, M. E., "Influence of Vehicle Speed on Pavement Deflections" Highway Research Board Proceedings, Vol. 4, pp. 77-82, 1962

46. Cannon, R. H. Jr., "Dynamics of Phisical Systems" MeGraw Hill Book Company, 1967.

47. Ng-A-Qui, N. T., "Noncontact Nondestructive Evaluation of Flexible Pavements Using Prototype Loads" Ph.D. Thesis, Purdue University, December 1976.

48. Vantil, C. J. and Vallerga, B. A., "Application of a Theoretical Procedure to Airfield Pavement Evaluation and Overlay Design" Proceedings, Third International Conference, Structural Design of Asphalt Pavements, London, 1972.

49. Voss, D. A., and Terrel, R. L., "Structural Evaluation of Pavement for Overlay Design", HRB Special Report 116, 1971.

50. Wiseman, G., "The Interpretation of Surface Deflection Measurements Using the Model of an Infinite Plate on an Elastic Foundation", Symposium on Nondestructive Test and Evaluation of Airport Pavements, Vicksburg, Mississippi, November 1975.

51. Weiss, R. A., "Nondestructive Vibratory Testing of Airport Pavements", Vol. II, Report No. FAA-RD-73-205-II, U. S. D.T-FAA, Washington, D. C., April, 1975.

52. Guillemin, R. and Gramsammer, J.C., "Dynamic Nondestructive Testing of Pavements in France", Proceedings Third International Conference on the Structural Design of Asphalt Pavements, London, 1972.

53. Daugherty, R. L., Franzini, J. B., "Fluid Mechanics with Engineering Applications", Sixth Edition, McGraw Hill Book Company, New York, 1965

54. _________ "The Design of Concrete Pavements for City Streets" Portland Cement Association Publication 1963.

55. Boyer, R. E. and Harr, M. E., "Predicting Pavement Performance", Journal of Transportation Engineering, ASCE, May, 1974.

56. Highter, W. H. and Harr, M. E., "Cumulative Deflection and Pavement Performance", Journal of Transportation Engineering, ASCE, August, 1975.

57. _________ "AASHO Interim Guide for Design of Pavement Structures", Published by the Americal Association of State Highway Officials.

58. Yoder, E. J., " Principles of Pavement Design", John Wiley and Sons, Inc., New York, 1955.

59. Rosenfield, D. "Lateral Placement of Vehicles Under Specified Conditions", MSCE. Thesis, Purdue University, 1956.

60. Weckesser, P. M. "The Effect of Pavement Type and Edge Lines on Lateral Placement". Joint Highway Research Project, Purdue University, 1957.

61. Huekelom, W., and Foster, C. R., "Dynamic Testing of Pavements" Proceedings, ASCE, Vol. 86, 1960.

62. Seed, H. B., Chan, C. K., and Lee, C. E., "Resilient Characteristics of Subgrade Soils and Their Relation to Fatique in Asphalt Pavements" Proceedings of the International Conference on the Structural Design of Asphalt Pavements, 1963, University of Michigan, Ann Arbor, Michigan.

63. Deacon, J. A., "Equivalent Passages of Aircraft with Respect to Fatique Distress of Flexible Airfield Pavements", Proceedings, AAPT, Vol. 40, 1971.

64. Hosang, V. A., "Field Survey and Analysis of Aircraft Distribution on Airport Pavements" U. S. Department of Transportation, Federal Aviation Administration, February 1975, Final Report.

65. Wylie, C. R., Jr., Advanced Engineering Mathematics, McGraw-Hill Book Company, Inc., NY, 1960

66. Crafton, P.A., Shock and Vibration in Linear Systems, Harper and Brothers, NY, 1961.

67. Raven, F.H., Automatic Control Engineering, McGraw-Hill Book Company, Inc., NY, 1968.

68. Senant, C.J., Jr., Fundamentals of the Lapalce Transformation, McGraw-Hill Book Company, Inc., NY, 1962.

69. Senant, C.J., Jr., Control System Design, McGraw-Hill Book Company, Inc., NY, 1964.

70. __________ "Soil Survey, Tippecanoe County Indiana", United States Department of Agriculture, Soil Conservation Service in Cooperation with Purdue University, Agricultural Experiment Station. Series 1940. No. 22. Issued January, 1959.

NOTICE

The following Appendices listed in the Table of Contents of this Report have not been included in this copy of the Report.

Appendix	Title	Pages
A	Instrumentation and Test Procedure	160-179
B	Convolution	180-194
C	Computer Program for Predicting Pavement Performance and an Output Sample	195-256
D	Measured Deflection Response Data	257-341

A recipient of the Report may secure a copy of the Appendix desired upon request to:

Joint Highway Research Project
Civil Engineering Building
Purdue University
West Lafayette, Indiana 47907

COVER DESIGN BY ALDO GIORGINI